Study on Energy-Efficiency Enhancement Techniques for 5G Cellular Networks

March 2024

Arif Dataesatu

Study on Energy-Efficiency Enhancement Techniques for 5G Cellular Networks

by

Arif Dataesatu, B.Eng., M.Eng.

Submitted in fulfillment of the requirements
for the Degree of Doctor of Engineering

Supervisor: Professor Kazuo Mori

Division of Systems Engineering
Graduate School of Engineering
Mie University
March 2024

I hereby declare that the contents of this thesis have not been previously submitted for a degree or diploma at the University or any other academic institution, except for the inclusion of background information that has been duly acknowledged in the thesis. Furthermore, I confirm that, to the best of my knowledge and belief, this thesis does not include any previously published or authored material by another individual, unless proper acknowledgment has been provided within the text of the thesis.

Signed: _____

Arif Dataesatu

Date: _____

Signed: _____

Arif Dataesatu

Date: _____

Abstract

5G New Radio (NR) cellular network is expected to provide three major services including enhanced Mobile Broadband (eMBB), Ultra-Reliable Low Latency Communications (URLLC), and massive Machine Type Communication (mMTC). eMBB applications aim to achieve extremely high data rates. URLLC supports low-latency transmissions of small payloads with very high reliability. Meanwhile, mMTC targets to support the connectivity of billions of Internet of Things (IoT) devices. Importantly, this thesis focuses on achieving eMBB and URLLC services from the viewpoint of system-level solution.

As the world adopts greener technologies and reduces energy waste, energy efficiency in wireless networks has become more important than ever. The 5G NR network is designed to improve energy efficiency, making research and network design a crucial component. 5G NR network is expected to meet the requirements for eMBB and URLLC. Several technologies are being integrated into 5G networks to meet the diverse needs of users. Such a complex network design will increase energy consumption. Consequently, energy efficiency becomes of the highest importance.

Considering that 5G NR cellular networks need to achieve eMBB services while ensuring seamless integration with all existing and emerging technologies, one of the most promising strategies for addressing these challenges involves the densification of base station (BS) deployments through the use of heterogeneous cellular networks (HetNets). HetNets consist of various tiers of base stations, which include both macro base stations (MBSs) and small base stations (SBSs). Typically, the SBS tier overlays on the MBS tier within HetNets. Consequently, the deployment of a HetNet, which combines MBSs and SBSs, can significantly improve the performance of 5G eMBB by increasing capacity, coverage, spectral efficiency, and overall user experience. Nevertheless, the dense implementation of SBSs within the MBS coverage results in a negative impact, such as an increase in energy consumption due to the inclusion of several SBSs, which can result in a decrease in energy efficiency on the network side. Therefore, various techniques for reducing energy consumption and enhancing energy efficiency in 5G NR cellular networks have been suggested. Despite the fact that these techniques can reduce energy consumption and improve energy efficiency, they may lead to a degradation in system throughput when compared to the no-sleep control system.

5G NR also provides URLLC services that satisfy the stringent latency and reliability requirements for one-way latency of 1 ms with 99.999% reliability. To satisfy URLLC requirements, grant-free (GF) transmissions with the K-repetition transmission (K-Rep)

have been introduced. Due to its repeated operation, the K-Rep scheme significantly increases the number of packet transmissions. Consequently, an excessive increase in packet transmissions causes severe interference at the receiving BS, resulting in degraded reliability. Moreover, the increase in packet transmissions on the K-Rep scheme results in a significant increase in energy consumption, leading to the early depletion of the battery and a decrease in energy efficiency on the user equipment (UE) side.

To address the first problem, this thesis proposes an enhanced algorithm for SBS sleep control based on energy efficiency as a decision criterion for SBS operating state, with a primary focus on supporting eMBB services. Using energy efficiency as a decision criterion, the proposed sleep control algorithm aims to achieve a balance between reducing power consumption and maintaining system performance. The proposed algorithm employs a 2-phase control procedure, where the first phase selects tentative sleep SBSs based on their energy efficiency and the second phase activates additional SBSs from the sleep state to improve energy efficiency while maintaining system throughput. The results of computer simulation evaluation indicate that the proposed sleep control scheme can provide improved performance for both energy efficiency and system throughput simultaneously. In other words, it effectively enhances energy efficiency while maintaining practically the same system throughput as the no-sleep control system.

To overcome the second problem of severe interference and reduced energy efficiency on the UE side resulting from an increase in packet transmissions in GF URLLC, this thesis proposes two innovative adaptive K-Rep control schemes. These schemes employ site diversity reception with the primary objective of reducing the number of packet transmissions. The first of these adaptive K-Rep control schemes, presented as adaptive K-Rep control scheme I, assigns a different number of associated cells to each UE. Meanwhile, the second scheme, known as adaptive K-Rep control scheme II, assigns a constant number of associated cells for all UEs. In adaptive K-Rep control scheme I, the number of packet transmissions for each UE is dynamically adjusted based on the specific number of associated cells for all UEs, whereas in adaptive K-Rep control scheme II, the dynamic adjustment of packet transmissions based on the variation in the reference signal received power (RSRP) levels. The performance evaluation demonstrates that the proposed adaptive K-Rep control schemes significantly improve communication reliability and reduce transmission energy consumption compared with the conventional K-Rep scheme, thereby satisfying the URLLC requirements while reducing energy consumption and enhancing energy efficiency at the UE side.

From the numerous computer simulation results at the system level evaluation, it is confirmed that the proposed schemes present in this thesis can be employed as solutions to enhance energy efficiency for eMBB services at the network side and for URLLC services at the UE side within the context of a 5G NR cellular network.

Acknowledgement

الحمد لله على كل حال All praise and thanks are only for the Lord in all circumstances.

Firstly, I would like to express my appreciation for the enthusiastic supervision of my Ph.D. studies and thesis by Professor Dr. Kazuo Mori. During the entirety of my studies at the Communications Laboratory, Division of Electrical and Electronics Engineering, Graduate School of Engineering, Mie University, I am profoundly grateful to him for his patience, support, encouragement, and extensive knowledge. For my Ph.D. studies, I could not have imagined a better advisor and mentor. The influence of his excellent personality and literate knowledge helped me to succeed in the research.

An expression of appreciation is extended to Associate Professor Dr. Hiroyuki Hatano. His invaluable advice motivates me to overcome any challenges I have encountered in my studies and research. Additional appreciation is extended to Assistant Professor Dr. Kosuke Sanada for his insightful remarks and suggestions made during the discussions of the research results. I would also like to thank Mr. Yoshihiro Yamamoto for his continual willingness to assist with technical issues.

I am grateful to Associate Professor Dr. Pisit Boonsrimuang from the Broadband Wireless Access Research Laboratory of the Department of Telecommunications Engineering, King Mongkut's Institute of Technology Ladkrabang (KMITL), Thailand, for his invaluable assistance, support, and encouragement throughout the study.

I am greatly indebted to the Japanese Government Monbukagakusho (MEXT) Scholarship for providing me with the extraordinary opportunity to study at Mie University and for its generous support.

My heartfelt thanks to the communications laboratory students and all my friends at Mie University – Thai, international, and Japanese. Your friendship and support have meant the world to me.

Finally, I am deeply thankful to my parents and my brothers for their unwavering support and encouragement throughout the journey of completing this thesis paper. Your love and belief in me have been my greatest source of inspiration.

Contents

List of Figures

List of Tables

Chapter 1

Introduction

This chapter presents an overview of the research topic that begins with Section 1.1 where the background of research is highlighted. Challenges are presented in Section 1.2. Section 1.3 describes the main research objectives are explained. The organization of the thesis is described in Section 1.4.

1.1 Research Background

Cellular Networks and 5G Services

From 1G to 5G, cellular networks have gone through five generations. The evolution of cellular network is shown in Figure 1.1. 1G marked the beginning of cellular networks that allowed for mobile voice calls. Text messaging via SMS became possible with the introduction of 2G. 3G was the first generation of mobile web browsing, and when 4G was released, data speed and capacity increased significantly, leading the way for mobile video streaming. Finally, 5G brings an extensive number of new features, such as improved network connectivity and lower latency. It enables new use case opportunities and more connected devices, which were previously impossible. The International Telecommunication Union (ITU) recommendations report [1] provides the vision for the next generation system for 5G New Radio (NR) defined as International Mobile Telecommunications for 2020 and beyond (IMT-2020). It describes three main services, including enhanced Mobile Broadband (eMBB), Ultra-Reliable and Low Latency Communications (URLLC), and massive Machine-Type Communications (mMTC), as illustrated in Figure 1.1 [1, 2].

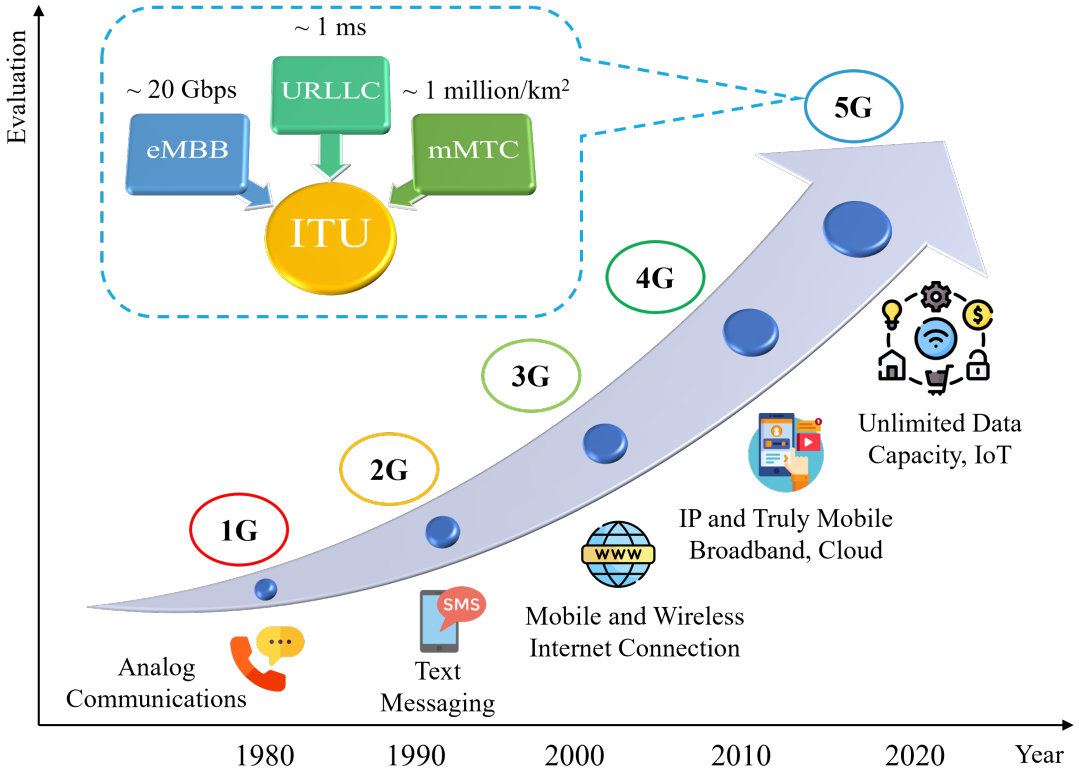

Figure 1.1: Evolution of cellular wireless networks.

Each of these services is associated with specific performance indicators; for instance, eMBB service drives high capacity, high data rates, and better coverage. URLLC service ensures extremely high reliability with very low latency. mMTC service provides a plat-

form that can handle a huge number of devices simultaneously [3]. Extensive descriptions of various use cases, including their enabling services and features, are provided below [4]:

eMBB service provides faster data rates for a better user experience while also aiming to provide the required QoS. eMBB also allows for improved broadband access in areas with high populations such as malls, stadiums, offices, and conference centers. The advent of eMBB is facilitating a range of services, including virtual reality (VR), augmented reality (AR), mixed reality (MR), immersive video conferencing, 360-degree video streaming, and high-definition screen display. eMBB service supports several features, including a peak data rate of 20 Gb/s for DL and 10 Gb/s for UL, the user experienced a data rate of 100 Mb/s for DL and 50 Mb/s for UL, and increasing energy efficiency by 100 times.

URLLC service guarantees very low latency and extremely high reliability, typically achieving less than 1ms per packet with 99.999% of reliability. For example the devices of industry 4.0, cooperative robots, and V2V communication. URLLC must meet several key requirements, including achieving a user plane latency of 1 ms, ensuring a reliability rate of 99.999% success probability, maintaining a control plane latency of 10-20 ms, and limiting mobility interruption time to under 1 ms.

mMTC is one of the primary services of 5G NR for communication between these massive numbers of connected devices. Health monitoring, autonomous driving, factory automation, fleet and logistics management, and smart metering will all be applications of mMTC. mMTC service can enable the high connection density of 1 million devices/km^2, wider coverage, and low-cost IoT.

Energy Efficiency

One of the primary concerns is the increasing energy demands of Information and Communications Technology (ICT) as a result of its rapid evolution and transformation. The electricity consumed by ICT networks increased by 31% between 2010 and 2015. During the same period, operational carbon emissions increased by 17%. According to KTH Centre for Sustainable Communications report [5], total annual operational carbon emissions from ICT networks in 2015 are estimated to be 169 Mtonnes CO_2. This corresponds to 0.53% of global energy-related carbon emissions (about 32 Gtonnes) or 0.34% of total carbon emissions (about 50 Gtonnes). The expansion of cellular networks is the main factor causing the approximately linear annual increase in operational CO_2 emissions and energy consumption.

It is expected that by the end of 2024, 5G will have reached more than 40% of the world's population. Total mobile data traffic is expected to increase by a factor of 5 between 2018 and 2024, with 5G networks carrying 25% of mobile traffic by the end of the period [6]. The base stations in cellular networks consume the most power, accounting

for roughly 60% of total energy consumption, as shown in Figure 1.2 [7, 8]. The majority of power optimization can thus be done in base stations. It not only reduces the environmental footprint by lowering energy consumption, but it also lowers the operational energy costs for the network operators. To reduce the energy consumption of base stations in cellular networks, designing an energy-efficient base station is an optimization issue that attempts to minimize network energy consumption while maintaining the specified quality of service (QoS) for 5G services. As a result, it is critical to consider the relationship between energy consumption metrics and other performance indicators for QoS.

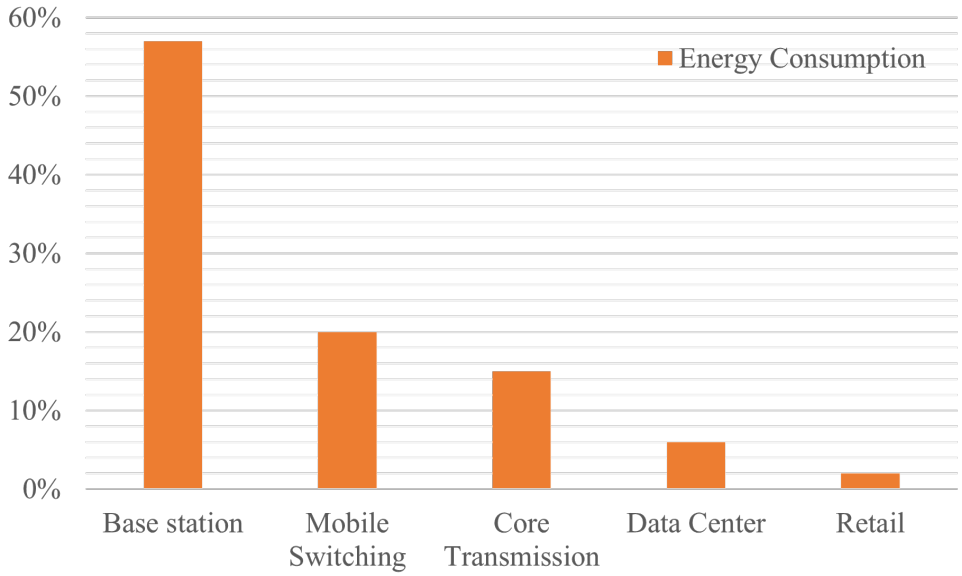

Figure 1.2: Energy consumption of a wireless cellular network.

On the other hand, user equipment (UE) is a term used in cellular networks to describe a device, such as a smartphone, IoT device, or other type of wireless device that is used to access the network. Recently, UEs have become common in all aspects of our lives. Consequently, they will consume a massive amount of electricity, which will substantially increase the carbon footprint and have a significant impact on global warming. The implementation of green principles and efficient power management and energy-saving techniques for UE batteries could significantly contribute to the sustainability of UE usage. [9, 10].

At the same time, energy efficiency has emerged as a critical performance metric in 5G New NR networks, which aim to support a variety of services, such as eMBB, URLLC, and mMTC [11, 12]. Energy efficiency requires careful trade-offs with other critical performance factors, such as throughput, latency, and reliability. This factor is essential for both the perspectives of UE and base station (BS) or network.

HetNets for eMBB

In order to meet the increasing demand for mobile broadband traffic and eMBB services in 5G NR cellular networks, the deployment of multiple tiers of BSs, also known as heterogeneous cellular networks (HetNets), has emerged as a promising solution [13]. HetNets employ different types of BSs, including macro base stations (MBSs) and small base stations (SBSs) as shown in Figure 1.3. MBSs provide low-frequency carriers and high-transmission power to ensure wide coverage with a range of over a kilometer. In contrast, SBSs employ high-frequency carriers and low-power radio access, covering shorter distances, typically ranging from tens to a few hundred meters such as a shopping mall, residential areas, a hotel, or a train station. These SBSs are further classified into femtocells, picocells, and microcells, with femtocells being the smallest and microcells being the largest [14]. Therefore, HetNets deployment allows significant capacity enhancements and better coverage conditions that can be particularly beneficial for supporting eMBB services in 5G NR network.

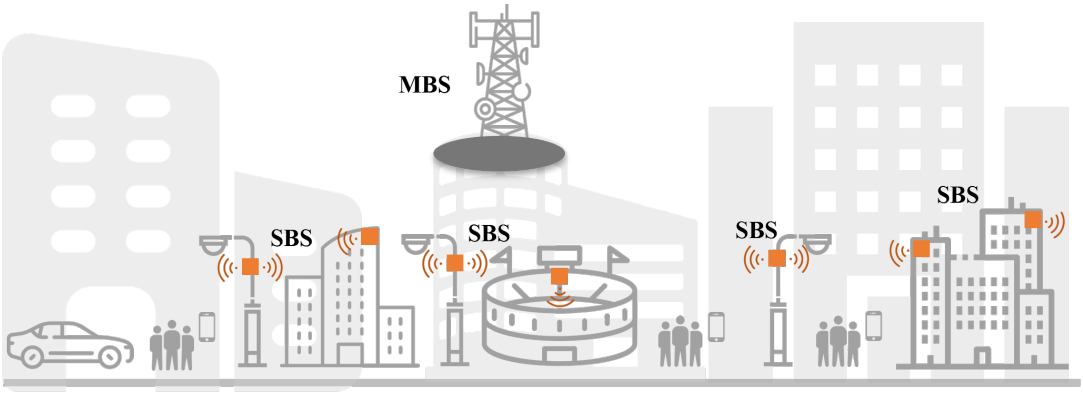

Figure 1.3: A typical heterogeneous cellular network deployment.

K-Repetition for URLLC

The 3rd Generation Partnership Project (3GPP) has established stringent requirements for URLLC, with a particular focus on achieving 1 ms user-plane latency and 10^{-5} communication reliability. URLLC has become essential for real-time applications, such as telemedicine, smart grids, industrial automation, and traffic control. To address these requirements, 3GPP introduced Grant-Free (GF) transmission to support URLLC UE by eliminating scheduling requests and grants. While this reduces access latency, it can result in a high collision probability when multiple URLLC UEs transmit simultaneously. To mitigate this issue, the concept of K-Repetition transmission (K-Rep) has been introduced as one of the transmission schemes for 5G URLLC. In this scheme, the UE is configured to autonomously transmit the same packet K times [15, 16], and then the BS performs soft combining of these repetitions to enhance signal quality.

1.2 Challenges

From an energy-efficient perspective, two key challenges arise:

- Energy consumption in HetNets for eMBB: The dense deployment of SBSs within MBS coverage areas of HetNets can lead to increased energy consumption, which has an impact on energy efficiency and operational costs [17]. An in-depth analysis of the energy consumption of cellular networks demonstrates that approximately 60% of the energy is consumed on the BS side [18]. Introducing sleep control into SBSs is one of the most promising schemes for reducing energy consumption and enhancing energy efficiency [19, 20]. These sleep control schemes offer reduced energy consumption and improved energy efficiency compared to systems with no sleep control. However, it is important to note that these sleep control schemes can result in decreased system throughput compared to the systems without sleep control, which may not support eMBB services [21, 22].

- Energy consumption in K-Repetition Transmission for URLLC: The K-Rep transmission approach significantly increases the number of packet transmissions, resulting in severe interference and a substantial increase in energy consumption, which negatively impacts energy efficiency on the UE side [23]. Furthermore, UEs have energy constraints due to limited battery life, especially in the case of IoT devices [24, 25]. Therefore, the increased packet transmissions in the K-Rep scheme can result in early battery depletion.

This research background provides a comprehensive overview of the key elements and challenges associated with 5G networks, energy efficiency, and the specific areas of concern related to HetNets for eMBB and K-Repetition transmission for URLLC. The importance of addressing energy efficiency in the context of diverse 5G services is highlighted by these challenges.

1.3 Research Objectives

The overall objective is to enhance energy efficiency in 5G NR cellular network, focusing on eMBB and URLLC services, while ensuring that energy efficiency improvements do not degrade system performance. This evaluation is conducted at the system level simulation, aiming to evaluate the performance of a whole network comprising a substantial number of BSs and UEs [26]. The signals received from the serving as well as the propagation attenuation are modeled. The primary focus of system level simulations is on the aspects related to both BSs and UEs, specifically the evaluation of key parameters such as energy efficiency, system throughput, latency, and communication reliability.

The objectives of this thesis are to achieve the following challenges:

- Enhanced energy efficiency for eMBB services: To develop and propose an advanced algorithm for SBS sleep control in HetNets, with a primary focus on energy efficiency as the decision criterion. The main objective is to enhance overall energy efficiency, particularly on the network side, while nearly maintaining the same system throughput as the systems without sleep control to support eMBB services.

- Enhanced energy efficiency for URLLC services: To develop and propose innovative adaptive K-Rep control schemes that utilize site diversity reception to address the problems of severe interference and reduced energy efficiency on the UE side resulting from increased packet transmissions. The primary objective is to reduce energy consumption and improve energy efficiency in URLLC services. Site diversity reception is employed to enhance the reliability of communication by combining signals received from multiple cell sites, potentially improving the signal quality at the BS. By combining signals received at multiple cell sites, site diversity reception can potentially reduce the number of packet repetitions in the K-Rep scheme, as the combined signal quality may be sufficient to meet the reliability requirement with fewer repetitions while improving energy efficiency on the UE side.

By addressing these problems and objectives, the thesis aims to contribute to the efficient design and operation of 5G NR cellular networks, aligning with the global trend towards greener technologies and reduced energy waste.

1.4 Thesis Structure

The structure of this thesis is designed to address the significant energy efficiency challenges faced by eMBB and URLLC in 5G NR. Figure 1.4 depicts the importance of energy efficiency in HetNets for eMBB services in Chapter 3 and K-Repetition for URLLC services in Chapter 4. The relation between each chapter can be summarized as follows:

Chapter 2 presents a comprehensive overview of 5G NR cellular networks in Section 2.1. In Section 2.2, we briefly explain the concept of HetNets for eMBB services. We also introduce grant-free access and K-Repetition transmission for URLLC services in Section 2.3. Section 2.4 presents channel model, site diversity reception, and power control as related techniques and fundamental concepts employed in this thesis. In Section 2.5, we discuss existing schemes that aim to reduce energy consumption and enhance energy efficiency, including sleep control for SBSs in HetNets and the adaptive repetition control approach for K-Repetition transmission. The final section of this chapter focuses on the critical aspect of energy efficiency in 5G networks, addressing both network and UE perspectives in Section 2.6.

Chapter 3 presents the proposed system performance enhancement with energy efficiency-based sleep control for 5G HetNets, as illustrated in Figure 1.4. Section 3.2 reviews prior research on sleep control for SBS and provides a detailed description of both conventional cell throughput-based sleep control and adaptive SBS sleep control. The proposed energy efficiency-based sleep control scheme is described in Section 3.3. The system model for performance evaluation is outlined in Section 3.4, and the results of the performance evaluation, contributing to the objective of improving energy efficiency in eMBB services, are presented in Section 3.5. Finally, the conclusions drawn from this study are summarized in Section 3.6.

Chapter 4 continues the discussion on energy efficiency but focuses on grant-free URLLC in 5G NR. It presents the proposed adaptive K-repetition transmission with site diversity reception for energy-efficient in 5G NR URLLC, as displayed in Figure 1.4. Section 4.2 provides related work on the adaptive K-Rep control scheme and site diversity reception. Section 4.3 presents the proposed adaptive K-Rep control schemes employing site diversity reception. Section 4.4 describes the evaluation methodology and simulation assumptions for performance evaluation. Section 4.5 presents the simulation results, along with a thorough performance evaluation and discussion by addressing energy efficiency for URLLC services. Finally, in Section 4.6, we summarize the key conclusions derived from this chapter.

The overall conclusion of the thesis is provided in Chapter 5. This chapter summarizes the key findings and contributions from both Chapter 3 and Chapter 4, highlighting how the proposed solutions address the challenges of energy efficiency for eMBB and URLLC

services in 5G NR.

In summary, the thesis is structured to first introduce the necessary background and concepts, followed by two main chapters that address specific challenges in energy efficiency.

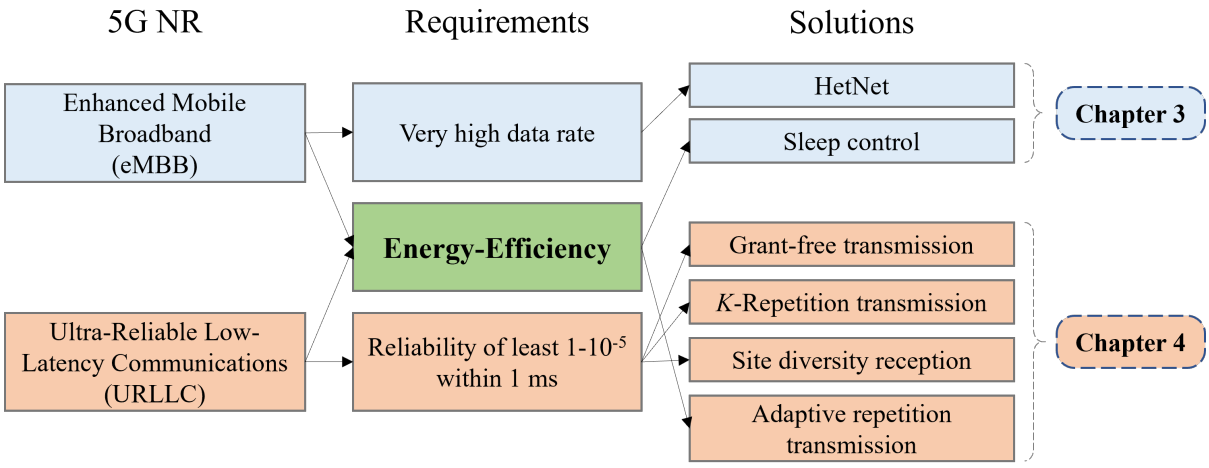

Figure 1.4: Mapping from 5G service requirements to potential solutions.

Chapter 2

Overview of 5G NR Cellular Networks and Energy Efficiency

This chapter presents an overview of 5G NR (New Radio) cellular networks in Section 2.1. In Section 2.2, the concept of heterogeneous cellular networks (HetNets) is briefly explained, encompassing both macro base stations (MBSs) and small base stations (SBSs) that facilitate enhanced Mobile Broadband (eMBB) services. Section 2.3 introduces the concept of grant-free access and K-Repetition transmission for ultra-reliable low-latency communications (URLLC) services. The related techniques and fundamental concepts are described in Section 2.4. In Section 2.5, we discuss existing schemes aimed at addressing energy consumption and energy efficiency challenges, such as sleep control for SBSs in HetNets, as well as the adaptive repetition control approach for K-Repetition transmission. The final section of the chapter focuses on the critical aspect of energy efficiency in 5G networks from both network and UE perspectives.

2.1 Overview of 5G NR

2.1.1 Basic Cellular Networks

A cellular network, also known as a cellular network, is a telecommunications network that uses a series of interconnected base stations (BSs) to provide wireless communication services over a wide geographic area, as seen in Figure 2.1. The network is referred to as "cellular" because the coverage area is divided into smaller geographic regions known as "cells." Key components of a cellular network include a variety of elements:

- **Base Station (BS)**: Also referred to as Macro Base Stations (MBS), these are physical structures equipped with antennas and radio equipment distributed across the coverage area. They provide the means for wireless communication, with each base station covering a specific cell or geographic area.
- **User Equipment (UE)**: These are the devices used by consumers, such as smartphones, tablets, or devices, which can connect to the cellular network. They are equipped with transceivers that communicate with nearby the BS.

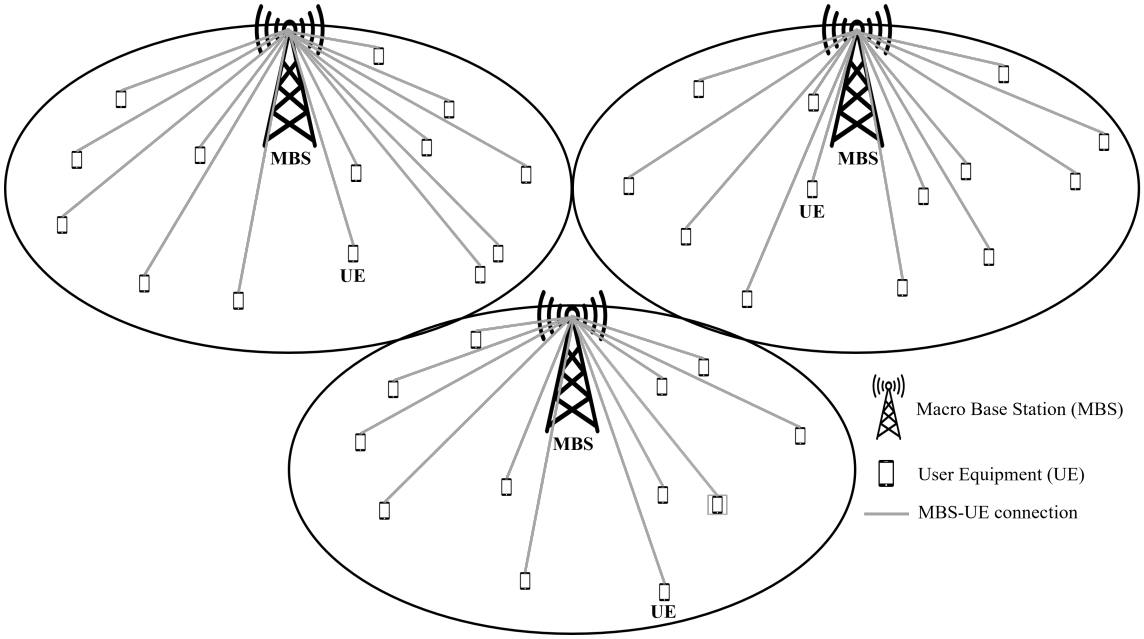

Figure 2.1: Homogeneous cellular network.

The development of cellular networks is required to support the growing number of users, mobility, higher coverage, data rate, and spectral efficiency, among other factors [2,27]. In the 1980s, 1G was released to provide analog signals for voice calls. In the 1990s, 2G started providing digital signals for voice services. SMS functionality is supported by 2G networks. Email and web browsing began with 2.5G. 3G initiated video telephony,

mobile television, and video conferences in the 2000s. The introduction of smartphones and mobile broadband occurs. 1G and 2G technologies use circuit switching, whereas 2.5G and 3G technologies use both circuit and packet switching. In the 2010s, 4G enables high-data-rate applications, such as HD television, cloud computing, and video gaming. In the 2020s, 5G deployment began, enabling Internet of Things (IoT), smart city, massive broadband, virtual reality (VR), augmented reality (AR), device-to-device communication, vehicular, and other applications. In 4G and 5G, only packet switching is used. There is a need for 1G to 5G speeds. 1G, 2G, 3G, 4G, and 5G support data transfer rates of 2.4 kbps, 64 kbps, 5 Mbps, 100 Mbps, and over 1 Gbps, respectively.

This thesis primarily focuses on the 5G NR cellular network, which needs to support multimedia applications with a wide variety of requirements, including higher peak and user data rates, reduced latency, enhanced indoor coverage, improved energy efficiency, and so on. The primary technologies and approaches to address the requirements for 5G systems can be classified in the next Section 2.1.2.

2.1.2 Major Service for 5G NR

The International Mobile Telecommunications for 2020 and Beyond (IMT-2020) [1,28] establishes the goals for fifth generation (5G) cellular networks as the future vision for cellular networks. The vision includes support for heterogeneous services; enhanced Mobile Broadband (eMBB) with high average data rate and very high peak data rate, Ultra-Reliable Low-Latency Communications (URLLC) which requires a substantial reduction in one-way latency and high reliability, and massive Machine Type Communication (mMTC) which requires a dramatic increase in connection density. Figure 2.2 depicts the three primary service scenarios and highlights IMT-2020 requirements, which are summarized as follows:

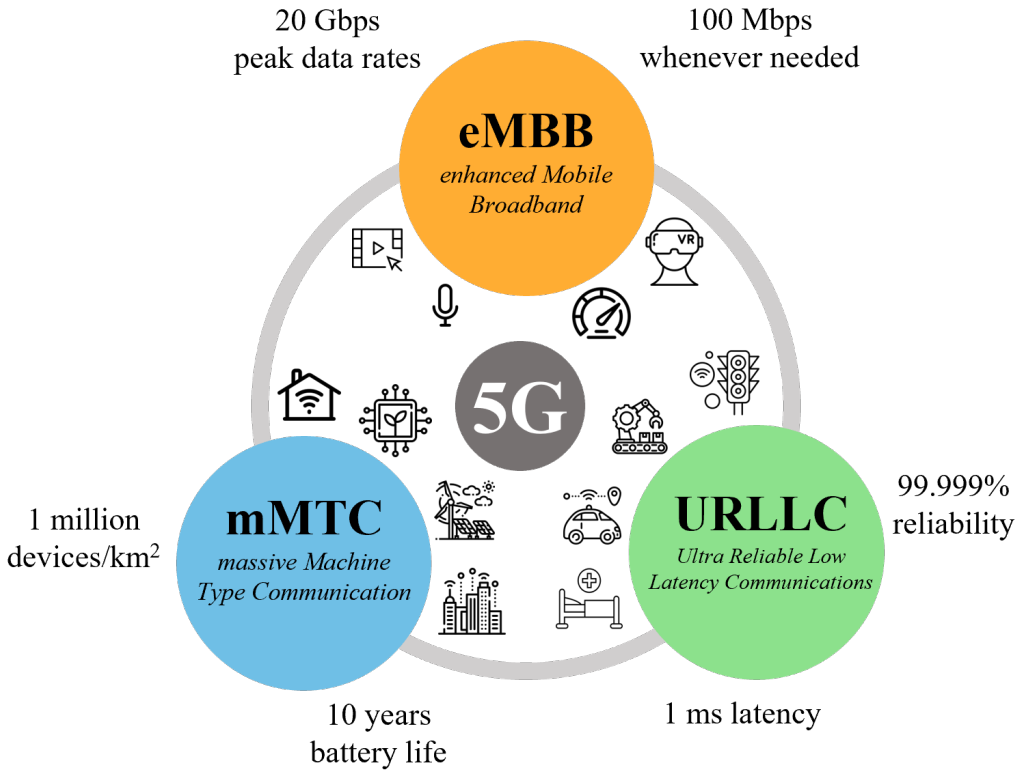

Figure 2.2: Overview of the 5G services and their requirements.

- **enhanced Mobile Broadband (eMBB)**: This usage scenario extends current broadband services to serve to evolved human-centric use cases such as multimedia streaming and high-speed internet services. To meet the increasing demands for data rates, capacity, and mobility, an improved network efficiency is required. The primary requirements for eMBB are peak data rates of 20 Gbps in the downlink and 10 Gbps in the uplink, respectively. The user's experienced data rate should be 100 Mbps in the downlink and 50 Mbps in the uplink.

- **Ultra-Reliable Low-Latency Communications (URLLC)**: URLLC focuses on new services related to mission-critical applications, requiring very stringent requirements for low end-to-end latency and a high degree of reliability. This is applicable in areas such as wireless industry automation, remote tactile control, and teleprotection. The defined reliability requirement for the URLLC radio interface is a success probability of 10^{-5} for transmitting a packet of 32 bytes within a 1 ms latency.

- **massive Machine Type Communication (mMTC)**: This can be viewed as an extension of Internet of Things (IoT) technologies like Enhanced Machine Type Communication (eMTC) and Narrowband IoT (NB-IoT). It addresses use cases involving a large number of IoT devices, such as in smart city applications, which

typically transmit small data volumes sporadically. The network should meet the extreme requirements of low cost and low energy consumption for these devices. It should support a connection density of at least 1 million devices per square kilometer and ensure a battery life of over 10 years.

2.2 Heterogeneous Cellular Networks

Cellular networks have traditionally consisted of a homogeneous deployment comprising only macro base stations (MBSs), as depicted in Figure 2.1, in a planned design to provide the required network coverage and capacity. However, due to the increase in data traffic demand and the high energy consumption associated with installing more macro BSs, such networks are no longer economically or ecologically feasible.

Moreover, eMBB is one of the primary services for 5G networks and is focused on providing significantly faster data rates and enhanced mobile internet experiences. Heterogeneous cellular networks (HetNets) for eMBB are designed to provide high-speed, high-capacity wireless connectivity to meet the demands of data-intensive applications and services, such as streaming high-definition video, online gaming, and augmented/virtual reality. HetNets consist of multiple tiers of base stations, including macro base stations (MBSs) and small base stations (SBSs) [13, 29], as shown in Figure 3.1. In the context of eMBB, HetNets with MBSs and SBSs function as follows:

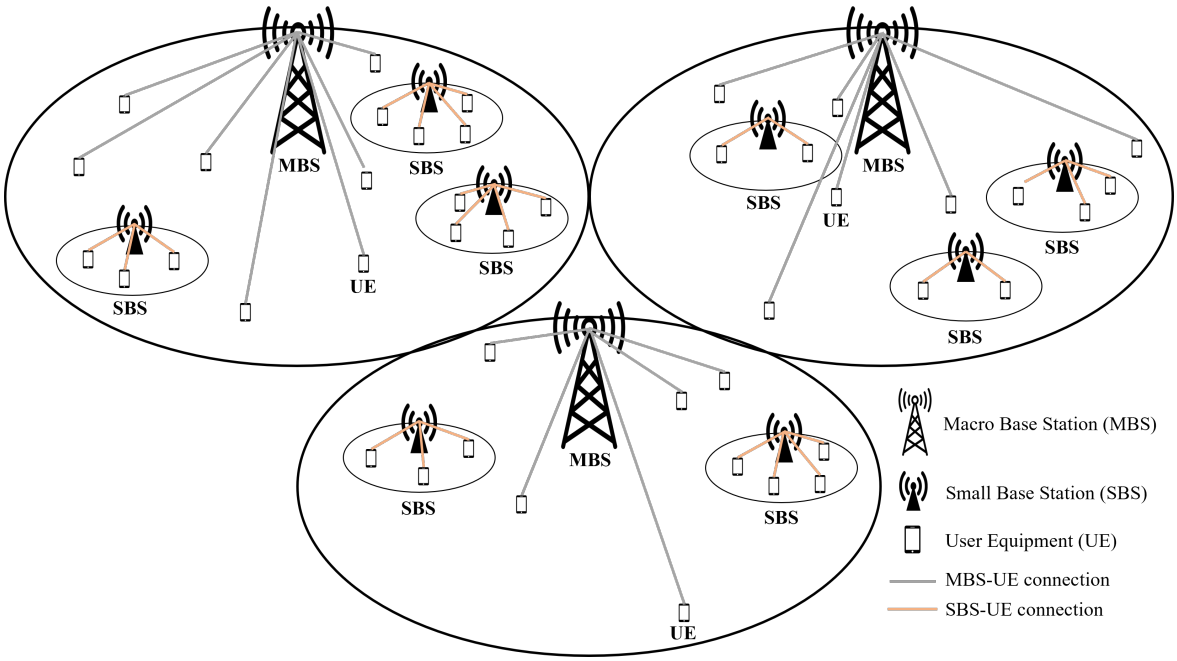

Figure 2.3: Deployment of heterogeneous networks with MBS and SBS.

- **Macro base stations (MBSs)**: MBSs provide low frequency carrier and high transmission power as the backbone of the network, providing the foundational coverage for wide geographic areas, including urban and suburban regions. They ensure that even in areas with lower population density, users can access basic mobile services.

- **Small base stations (SBSs)**: SBSs provide high frequency carrier and low power.

SBSs are also deployed to increase network capacity and deliver high data rates in congested or high-demand areas. SBSs provide localized coverage for usually ten to a few hundred meters of coverage and help ensure that users in crowded places have access to high-speed data services.

While HetNets offers several advantages, including improved capacity and coverage for eMBB services, they can also introduce challenges that may lead to increased energy consumption and reduced energy efficiency [30].

2.3 Grant-Free with *K*-Repetition Transmission

The uplink transmission, where UEs transmit data to the BS, is a fundamental component of cellular communication systems. Grant-based (GB) access is a well-established method used in cellular networks as specified in [31]. In this approach, UEs must request and obtain a resource allocation grant, named scheduling procedure, from the BS before initiating packet transmission. As shown in Figure 2.4(a), the UE transmits a scheduling request (SR) to the BS. Then, BS grants resources to the UE with scheduling grant (SG). Lastly, UE transmits packet transmission to allocated resources. This can reduce contention between UEs, resulting in lower collision rates and improved reliability. However, the scheduling procedure increases latency, making it difficult to satisfy URLLC latency requirements.

Grant-Free (GF) transmission has been introduced by 3GPP to support URLLC [15, 16]. GF transmission schemes are also well-known solutions for rapid uplink access, as they eliminate the phases of scheduling request and scheduling grant, as illustrated in Figure 2.4(b). With grant configuration, the BS can configure the UE to have pre-allocated radio resources available for packet transmissions. While this approach can significantly reduce latency, it also introduces a challenge related to a high collision probability if multiple UEs transmit simultaneously over the same resource, which degrades reliability performance [32].

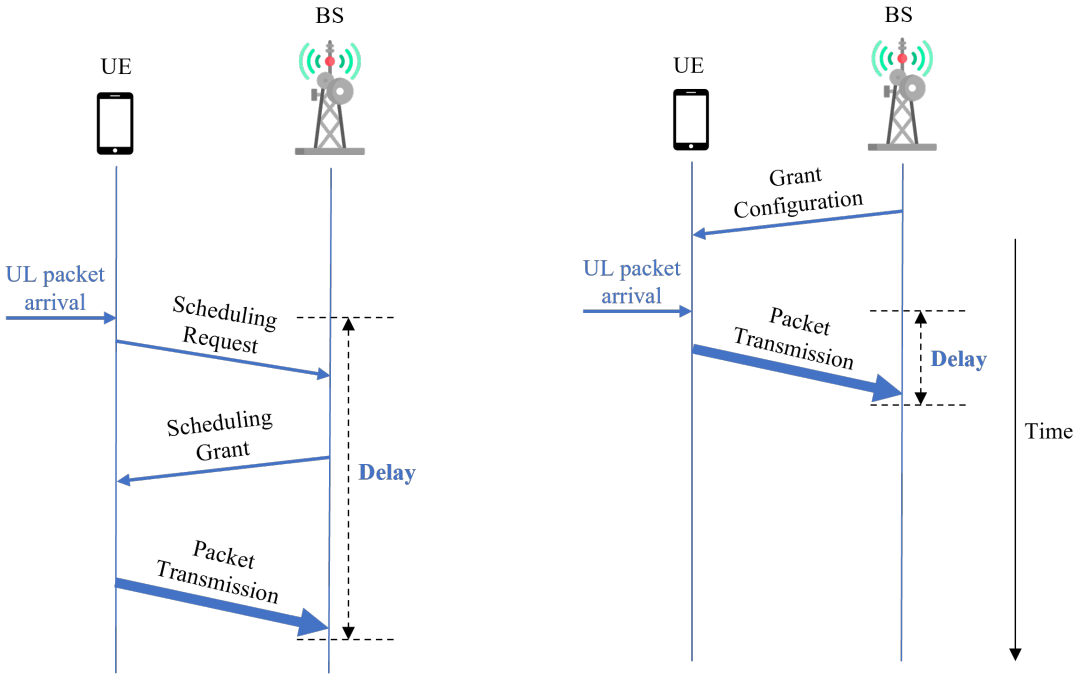

(a) Grant-Based transmission (b) Grant-Free transmission

Figure 2.4: Uplink transmission access.

K-Repetition (K-Rep) transmission is a specific strategy within grant-free URLLC that focuses on enhancing the reliability of transmissions by using transmission repetition [15, 16]. The "K" in K-Rep represents the number of times a UE transmits the same data packet. In this transmission technique, a UE transmits the same data packet K times.

The main idea behind K-Rep transmission is to exploit time diversity gain. By transmitting the same data packet multiple times, the probability of at least one of these transmissions being successfully received by the BS is increased. This repetition helps to minimize the negative effects of fading, interference, and other channel conditions. At the BS side, maximal ratio combining (MRC) can be used to process the K received transmissions [33]. This technique aims to maximize the probability of successfully transmitted data. K-Rep enhances the reliability of URLLC communication. The more times a UE transmits the same data, the higher the chance that at least one of these transmissions will be successfully received, even in challenging channel conditions.

However, the increased number of repetitions can result in increased interference among UEs, which has a direct impact on signal quality degradation [23]. Moreover, the increase in packet transmissions on the K-Rep scheme results in a significant increase in energy consumption, leading to an early battery depletion on the UE side [24].

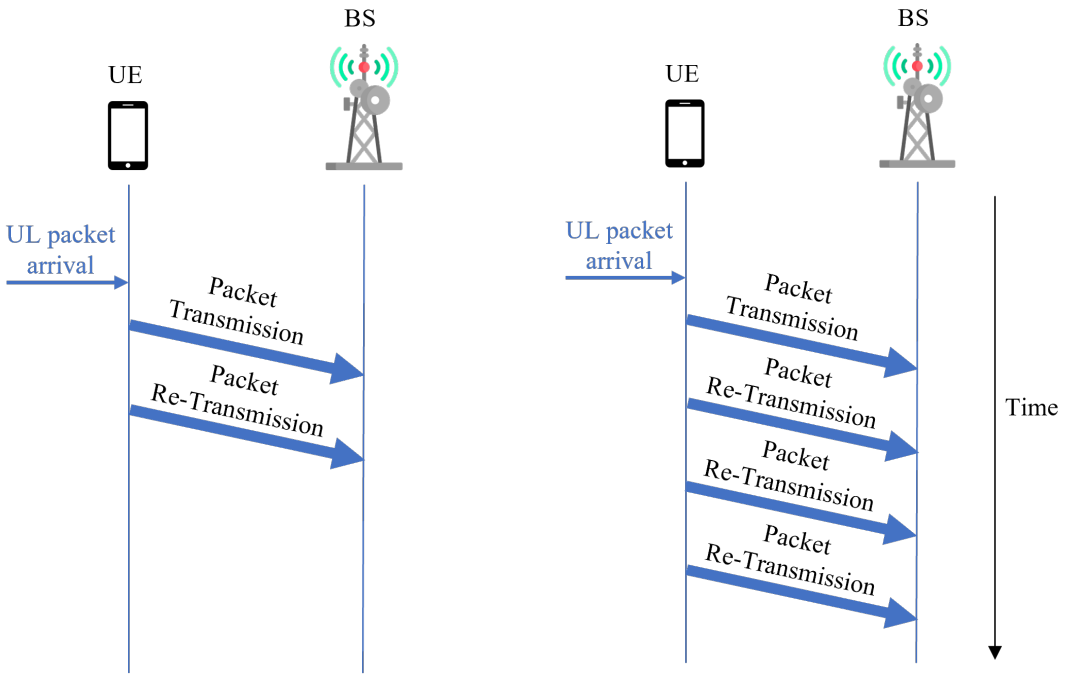

(a) Two number of repetitions ($K = 2$) (b) Four number of repetitions ($K = 4$)

Figure 2.5: K-Repetition transmission.

2.4 Related techniques

2.4.1 Channel Model

In the context of HetNets in 5G eMBB services, the signal propagation assumes path loss due to the distance attenuation and log-normal shadow fading. The path loss characteristics are specifically defined in the 3GPP specification TR 38.901 [34] for the carrier frequencies employed in 5G networks. Notably, the MBS tier employs the 3GPP 3D UMa model, while the SBS utilizes the 3GPP 3D UMi model.

Regarding K-Rep in 5G URLLC services, signal propagation within the radio channel relies on the 3GPP 3D UMa model as a foundational component for the path loss model, as referenced in [35]. It is important to note that an independent fading coefficient is assumed between consecutive transmission repetitions, following an exponential distribution, to account for Rayleigh fading fluctuations.

2.4.2 Site Diversity Reception

In 5G wireless communication systems, site diversity reception is a technique used to improve the reliability and performance of uplink communication, especially in scenarios with challenging propagation conditions. Site diversity reception, also known as multiple cell combining, is a more advanced technique compared to single-cell reception.

In single-cell reception, a UE connects with only one cell or BS at a time. The UE selects the strongest signal strength cell to connect, which can be illustrated in Figure 2.6(a). Single-cell reception may suffer from fading and interference issues, especially in challenging radio environments.

Site diversity reception involves the UE simultaneously connecting with multiple cell sites (BSs) and combining their received signals to improve the overall signal quality and reliability [36, 37]. In this approach, the UE is allowed to transmit its data to several neighboring cells. These received signals are then combined at the baseband unit (BBU), as shown in Figure 2.6(b). By using multiple cells for reception, the network can combine and process signals received from these cells in a way that mitigates the impact of fading and interference, enhances signal quality, and improves the overall reliability of the uplink communication.

In summary, site diversity reception (multiple cell combining) in 5G uplink is a more advanced technique compared to single-cell reception. It involves the simultaneous use of multiple cells to receive and combine signals from a UE, aiming to improve reliability, data rates, and overall network performance, especially in challenging radio environments.

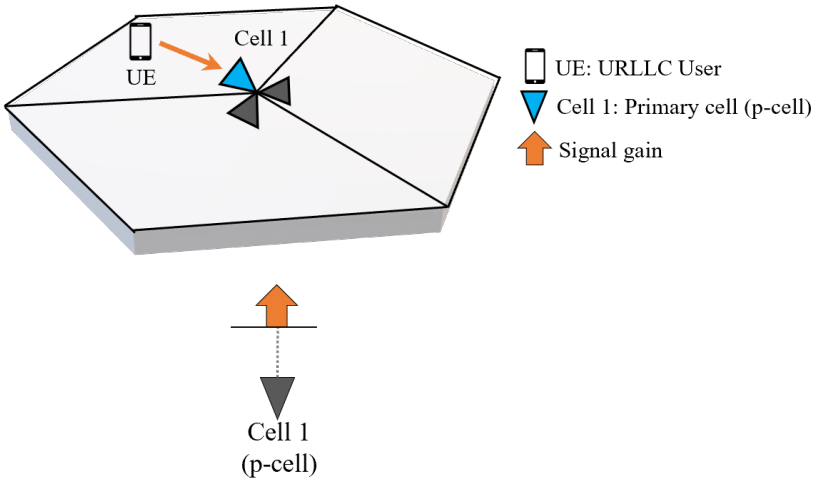

(a) Single cell reception

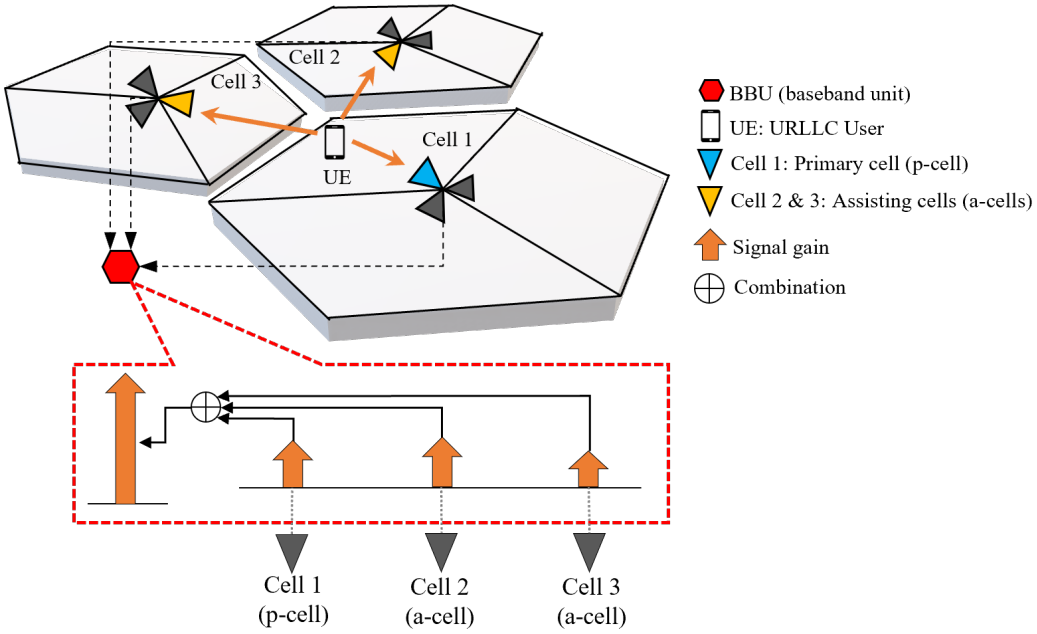

(b) Site diversity reception

Figure 2.6: Difference between single cell reception and site diversity reception.

2.4.3 Power Control

Power control is an important function in cellular wireless networks and refers to setting the output power levels of transmitters. There are two distinct mechanisms for uplink power control [38]: Open Loop Power Control (OLPC) and Closed Loop Power Control (CLPC). In uplink OLPC, UE performs power control using parameters and measurements acquired from signals transmitted by the BS, which can effectively compensate for long-term channel variations such as path loss and shadowing. In this scenario, there is no need for the UE to receive feedback regarding the transmission

power it should use. While the uplink CLPC mechanism aims to enhance power control performance by compensating for rapid channel variations caused by multi-path fading. In CLPC, the BS sends Transmit Power Control (TPC) commands to the UE to adjust its transmit power.

This thesis focuses on an OLPC scheme. 3GPP defines standard power control in [39] as fractional power control (FPC). FPC combines OLPC with fractional path-loss compensation. It allows a reduction in the transmit power of cell-edge UES, thereby reducing their interference on neighboring cells [40].

2.5 Existing Schemes

2.5.1 Sleep Control

HetNets, characterized by the dense and random deployment of multiple SBSs within the coverage area of a MBS as described in Section 2.2, result in increased energy consumption and reduced energy efficiency [30].

The recently finalized 5G NR 3GPP Rel-15 standard is designed to enable very low energy consumption. As such, new features for energy savings are introduced. Several techniques for reducing the energy consumption of cellular networks have been proposed. Integration of sleep control into SBSs is one of the most promising schemes for reducing energy consumption and enhancing energy efficiency [19, 20].

In [41], an analytical model has been proposed to determine the number of SBSs that can be switched off with vertical traffic offloading using two sleeping schemes (random and repulsive). In the random scheme, all SBSs have an equal chance of being turned off, whereas in the repulsive scheme, only the SBSs nearest to the MBS are turned off as shown in Figure 2.7. In a prior study [21], a sleep control scheme has implemented on SBSs within the downlink communications network, as shown in Figure 2.8. The conventional sleep control scheme focuses mainly on the number of UEs that are connected to the SBS. In other words, the number of UEs connected to the SBS is used as the decision criteria for setting the SBS into a sleep state. According to the defined decision criteria, the SBSs must be switched into a sleep state when the number of UEs connected to them is less than or equal to a specified sleep threshold. In contrast, the SBSs maintain an active state even when a large number of UEs are connected.

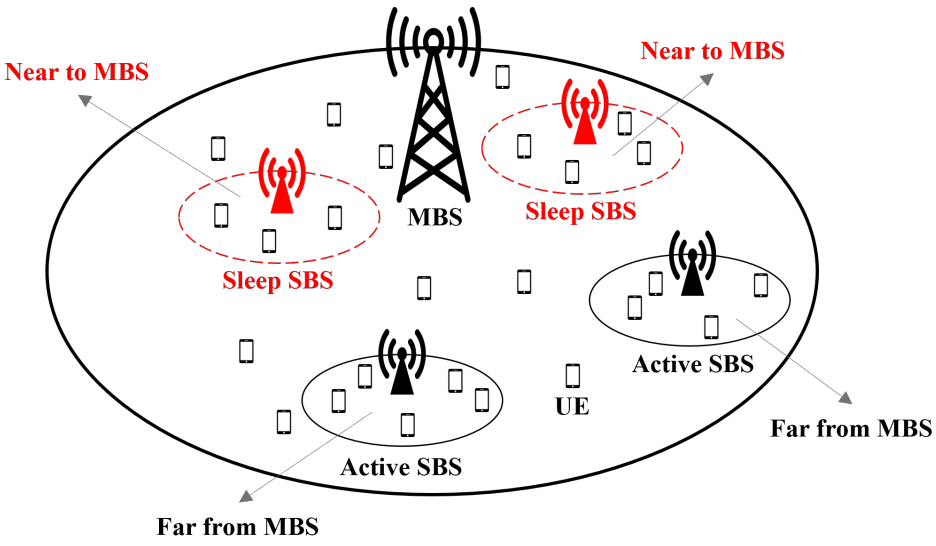

Figure 2.7: Sleep control scheme based on SBSs near to the MBS.

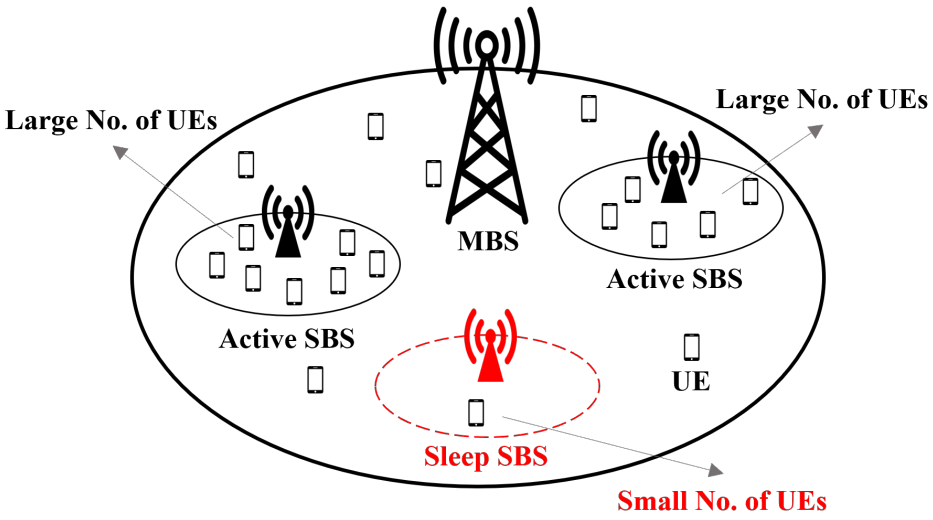

Figure 2.8: Sleep control scheme based on the number of UEs connected to the SBS.

In [42], the authors have presented a decentralized ON/OFF algorithm for opportunistically switching the BSs ON/OFF in wireless SBSs as a trade-off between energy consumption and load. In [43], the authors have highlighted the energy consumption behavior of SBS deployments and emphasized sleep mode solutions for reducing network energy consumption. The authors have also investigated three distinct sleep mode strategies by heuristic algorithm that result in energy savings between 10 to 60%. In [44], analytical models have been developed to determine the optimal fixed SBS switch-off times based on the daily traffic pattern. A centralized and decentralized Q-learning algorithm has been developed in [45] to optimize traffic offloading and SBS switch-off.

In addition, a prior study in [22] has proposed a sleep control scheme that is based on traffic load. Regarding their sleeping procedure, activated SBSs frequently monitor the served traffic load. When the measured traffic load over a specified period is low, the SBS enters a sleep state in order to minimize energy consumption.

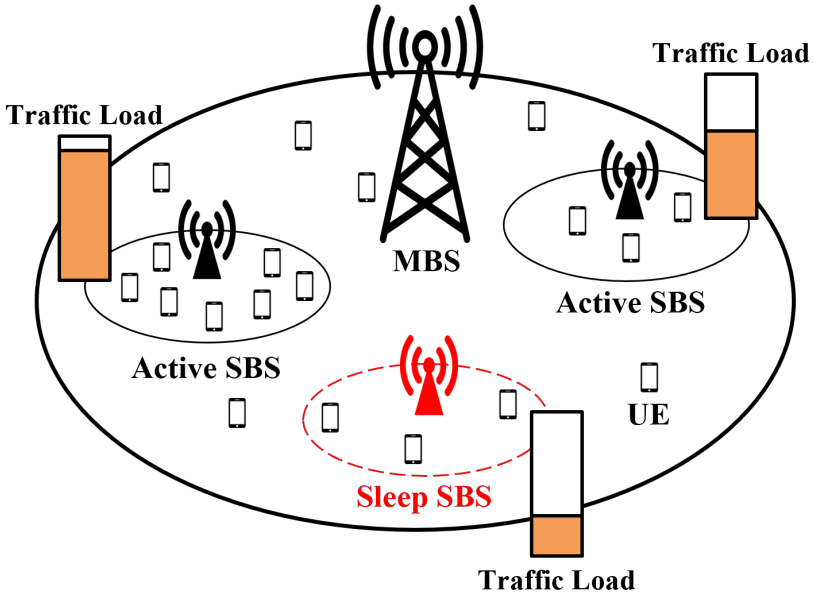

Figure 2.9: Sleep control scheme based on traffic load.

By implementing these control procedures, sleep control schemes offer reduced energy consumption and enhanced energy efficiency when compared to no-sleep control system. Nevertheless, these sleep control schemes can lead to a decrease in system throughput compared to no-sleep control system [21, 22], which may not meet the requirements of eMBB scenarios. As a result, we introduce an enhanced scheme in Chapter 3 that improves energy efficiency while nearly maintaining the same system throughput as the no-sleep control system.

2.5.2 Adaptive Repetition Control

In the conventional K-Rep scheme [15, 16], all the UEs employ the same number of repetitions referred to as constant K-Rep scheme as illustrated in Figure 2.10(a). However, the K-Rep essentially increases the number of packet transmissions [23], consequently increasing energy consumption at the UE side and thereby reducing energy efficiency. Furthermore, it is not imperative for all UEs to transmit the same number of repetitions to meet the URLLC requirements.

To reduce the number of repetitions, numerous studies have concentrated on the development of adaptive K-Rep control schemes. These techniques dynamically adjust the number of repetitions based on specific conditions, as illustrated in Figure 2.10(b). It is evident that each UE has a varying number of repetitions, effectively decreasing the overall number of repetitions. Consequently, these techniques enhance transmission energy efficiency while meeting URLLC requirements.

In [46], the authors have proposed an adaptive repetition control technique using terminal mobility to mitigate packet collision in uplink GF URLLC. This scheme determines

the necessary number of repetitions for K-Rep based on fading correlation obtained from terminal speed, thereby reducing repetitions in scenarios with low fading correlation while simultaneously enhancing reliability and energy efficiency.

The paper in [47] has proposed an optimized repetition scheme for URLLC, which aims to improve energy efficiency and decrease collision probability by optimizing the number of repetitions for K-Rep based on diverse reliability requirements and active probabilities of different UEs. Their simulation results explain that the proposed scheme can reduce uplink transmission energy consumption by 10-30% compared to the conventional K-Rep scheme.

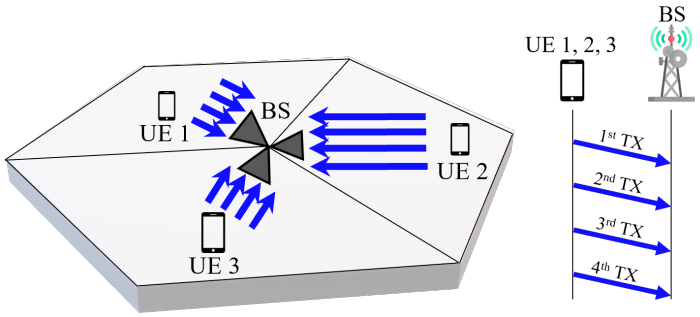

(a) Conventional K-repetition ($K = 3$)

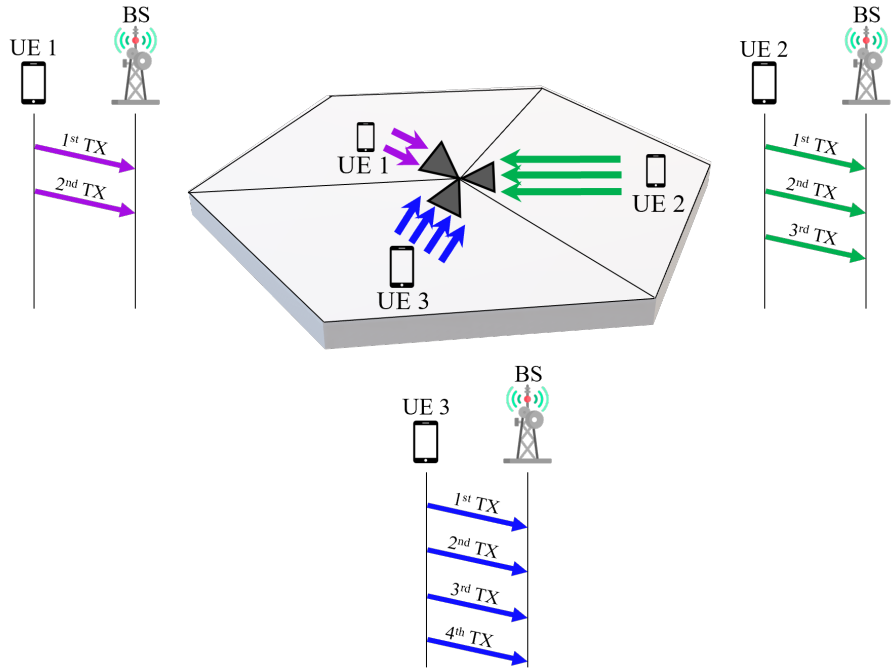

(b) Adaptive K-repetition control

Figure 2.10: Conventional K-repetition and adaptive repetition control scheme.

2.6 Energy Efficiency

Energy efficiency in cellular networks is becoming a critical requirement for network operators seeking to reduce operative expenditure (OPEX) and reduce the environmental impact of Information and Communication Technologies (ICT). ICT costs and greenhouse gas emissions have grown in recent years due to increased traffic demand from mobile devices such as smartphones and tablets. Global mobile data traffic increased by 63% in 2016 [48], and cloud-based and Internet of Things services are expected to worsen this trend further. In fact, mobile traffic will grow by seven times between 2016 and 2021, at a compound annual growth rate (CAGR) of 47%, reaching 49.0 exabytes per month by 2021. As a result, it is widely assumed that the 5G NR networks will support 1,000 times more capacity per unit area than 4G. According to a recent report by Digital Power Group [49], the world's ICT ecosystem already consumes about 1500 TWh of electric energy annually, accounting for close to 10% of global electricity generation and 2% of human activity's carbon footprint. For example, ICT energy consumption contributes to 25% of global car emissions and is equal to all global airplane emissions. Telecom operators consume 254 TWh per year (77% of global ICT electricity consumption), with an annual growth rate higher than 10% [50].

Energy efficiency is one of the key performance indicators in 5G NR networks targeted to support diversified services including eMBB, URLLC, and mMTC [11, 12]. Trade-offs have to be carefully considered between energy efficiency and other performance aspects such as throughput, latency, and reliability. Energy efficiency is important for both UE side and BS or network side.

On the network side, the implementation of an efficient network is important from both an environmental and an operational cost perspective. To meet diverse requirements and trade-offs, the 5G NR standard is designed with an elevated level of network operation mode flexibility. Figure 2.11 illustrates an example of employing HetNets for eMBB services, which increase energy consumption as well as decrease energy efficiency on the network side.

On the UE side, the battery life of a UE has a significant impact on the overall UE experience. It is challenging to enhance the UE experience in other performance aspects without adversely affecting the battery life of 5G handsets. Figure 2.12 shows an example of implementing K-Rep for URLLC services, which results in increased energy consumption, decreased energy efficiency, and consequently affects the battery life on the UE side.

Several studies investigate the approaches to reduce energy consumption and improve energy efficiency in the face of the problems mentioned above, while maintaining their Quality of Service (QoS):

- **Sleep control for HetNets - Energy efficiency on the network side**: As

explained in Section 2.5.1, incorporating sleep control into SBSs stands out as a promising approach for enhancing energy efficiency and reducing energy consumption. In [41], an analytical model determines the number of SBSs that can be turned off using random and repulsive sleeping schemes for vertical traffic offloading. The random scheme uniformly selects SBSs for shutdown, while the repulsive scheme targets only the SBSs closest to the Macro Base Station (MBS), as shown in Figure 2.7. In a previous study [21], a sleep control scheme has applied to SBSs. This scheme primarily considers the number of UEs connected to an SBS as the criterion for switching it into sleep mode, with a specified threshold. In contrast, SBSs remain active even with a high number of connected UEs. Additionally, [42] presents a decentralized ON/OFF algorithm for energy-efficient switching of SBSs, balancing energy consumption and load. [43] discusses energy consumption patterns in SBS deployments and proposes heuristic algorithms for sleep mode strategies. [44] develops analytical models to determine optimal fixed SBS switch-off times based on daily traffic patterns. Finally, [45] introduces centralized and decentralized Q-learning algorithms to optimize traffic offloading and SBS switch-off.

- **Adaptive repetition control - Energy efficiency on the UE side**: As explained in Section 2.5.2, all UEs use a fixed number of repetitions in the traditional K-Rep scheme, which increases energy consumption and reduces energy efficiency. Adaptive K-Rep control schemes dynamically adjust repetitions based on specific conditions, enhancing energy efficiency while meeting URLLC requirements. An adaptive approach [46] uses terminal mobility to determine repetitions, reducing them in scenarios with low fading correlation and improving reliability and energy efficiency. Another optimized scheme [47] optimizes repetitions based on reliability requirements and UE probabilities, reducing uplink energy consumption by 10-30% compared to the conventional K-Rep scheme.

In conclusion, energy saving is a key factor for sustainable energy-efficient 5G network deployment. This thesis focuses on improving energy efficiency by reducing network and UE energy consumption.

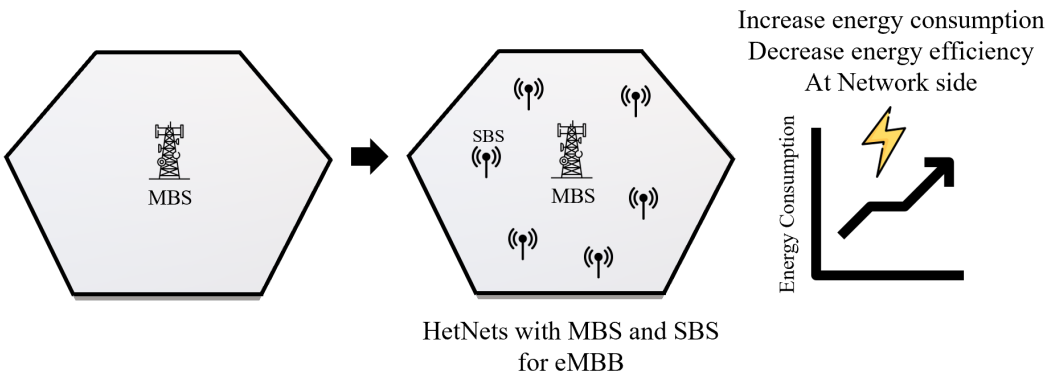

Figure 2.11: Problem of energy efficiency at network side by employing HetNets for eMBB services.

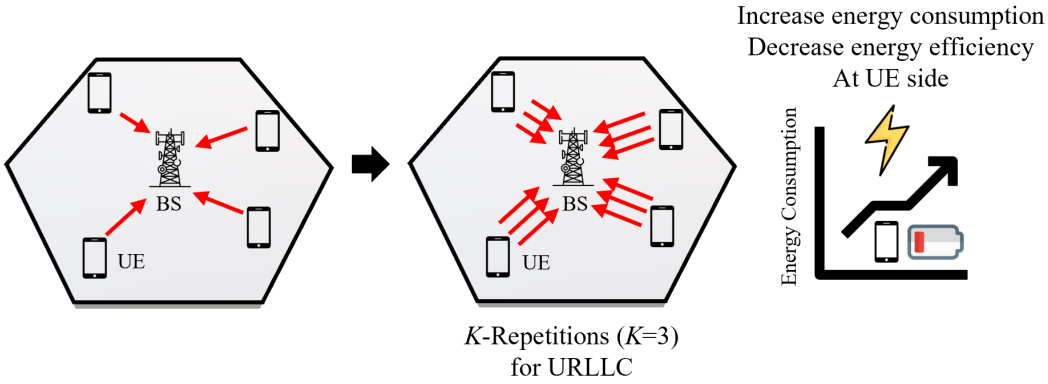

Figure 2.12: Problem of energy efficiency at UE side by employing K-Rep for URLLC services.

Chapter 3

System Performance Enhancement with Energy Efficiency Based Sleep Control for 5G Heterogeneous Cellular Networks

This chapter presents an improved sleep control algorithm for small base stations (SBSs) in 5G New Radio (NR) heterogeneous cellular networks (HetNets), with a focus on enhancing performance for enhanced Mobile Broadband (eMBB) services. HetNets consist of various base station tiers, including macro base stations (MBSs) and small base stations (SBSs), and have been suggested as a promising solution to enhance wireless coverage and eMBB services, employing many SBSs into the MBS coverage. However, power consumption increases significantly as a result of an increase in the number of SBSs, which can lead to lower energy efficiency at the network side. To address this problem, SBS sleep control has been proposed as a way to reduce power consumption for SBSs and improve energy efficiency. However, this method leads to decreased system throughput compared to the no-sleep control system, potentially degrading the quality of service (QoS) at user equipment (UEs). This chapter proposes an enhanced algorithm for SBS sleep control based on energy efficiency as a decision criterion for SBS operating state, specifically designed to support eMBB services. From the evaluation results through computer simulation, the proposed scheme can provide improved performance for both energy efficiency and system throughput simultaneously, that is it can improve energy efficiency while maintaining almost the same system throughput as the no-sleep control system. Concretely, the proposed scheme has the 14.89% improvement in energy efficiency while providing almost the same system throughput of over 99%, compared with no-sleep control system.

3.1 Introduction

The three majors of use cases for the fifth-generation new radio (5G NR) mobile networks include enhanced mobile broadband (eMBB), massive machine type communications (mMTC), and ultra-reliable and low latency communications (URLLC) [3]. There are different key performance indicators for different use cases. The user-experienced data rate is essential for eMBB, whereas mMTC is mainly concerned with the density of connections and the main parameters for URLLC are latency and reliability.

Considering that 5G NR mobile networks need to achieve eMBB services and should be capable of interconnecting with all existing and emerging technologies, one of the most promising solutions for overcoming these challenges is attempting densification of base station (BS) deployment through heterogeneous cellular networks (HetNets), which include different tiers of BSs, macro base stations (MBSs) and small base stations (SBSs), as shown in Figure 3.1 [13,29,51]. MBSs provide low-frequency carrier and high-transmission power to achieve wider coverage with a range of over one kilometer. In contrast, SBSs provide high-frequency carrier and low-power radio access for usually ten to a few hundred meters of coverage. They are classified as femtocells, picocells, and microcells with the smallest being femtocells and the largest being microcells [3]. The SBS tier generally overlays on the MBS tier in the HetNets. It is necessary to balance service quality and cost efficiency while planning and deploying HetNets. Low cost covers power consumption cost, as well as network planning and operating charges. The implementation of SBSs can achieve both better user quality of service (QoS) and lower operating costs [51].

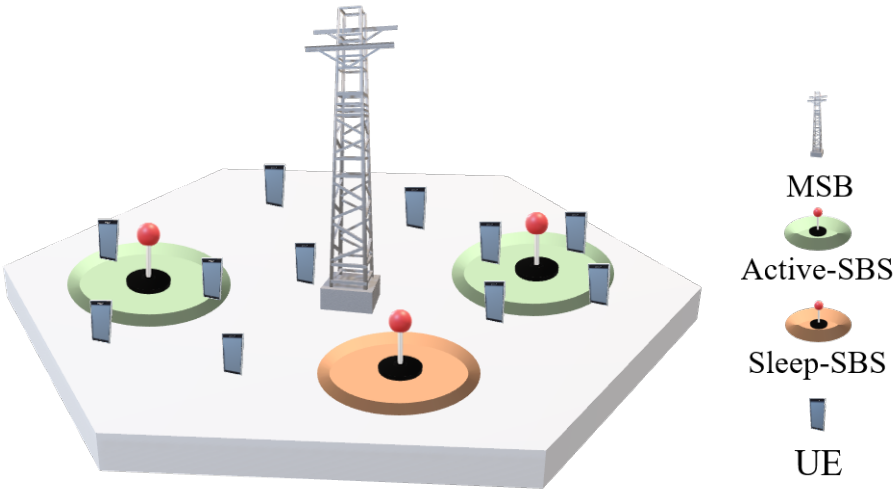

Figure 3.1: Example of cell deployment for 5G NR heterogeneous cellular networks.

However, dense and random implementation of SBSs inside the MBS coverage leads to various negative impacts, including a rise in power consumption due to the inclusion of many SBSs [30]. Therefore, various techniques for reducing power consumption in

cellular networks have been proposed [7, 52]. One of the most attractive techniques for reducing power consumption and increasing energy efficiency is to integrate sleep control into SBSs. The existing schemes for SBS sleep control have been proposed, for example: random and repulsive schemes [41], distance-sensitive repulsive sleeping strategy [53], traffic based sleep control scheme [22], cell throughput based sleep control scheme [54], and adaptive SBS sleep control scheme [55]. Although these schemes can reduce power consumption and improve energy efficiency, they could degrade system throughput when compared with the no-sleep control system.

This chapter proposes an enhanced SBS sleep control scheme for downlink communications in 5G HetNets to simultaneously improve energy efficiency and system throughput. Specifically, it aims to enhance energy efficiency while maintaining almost the same system throughput as the no-sleep control system at the system level evaluation. To achieve these objectives, this chapter proposes an enhanced algorithm for the SBS sleep control, which activates more SBSs while providing the improved energy efficiency. However, increasing the number of active SBSs could lead to increased power consumption and then decreased energy efficiency. Based on this perspective, the proposed scheme employs energy efficiency as the decision criteria for SBS sleeping in order to provide the improved energy efficiency.

The remainder of this chapter is structured as follows: Section 3.2 presents related work to the SBS sleep control and then provides detailed description on the conventional cell throughput based sleep control and adaptive SBS sleep control. The proposed energy efficiency based sleep control scheme is described in Section 3.3. Section 3.4 describes the system model for performance evaluation. The results of the performance evaluation are presented in Section 3.5. Finally, the conclusions are given in Section 3.6.

3.2 Related Work

3.2.1 Sleep Control for SBSs in HetNets

Several SBS sleep control schemes have been proposed, for example, random and repulsive schemes are studied in [41]. Under the random scheme, SBSs are put in the sleep state with a certain probability, whereas the repulsive scheme inactivates only the SBSs within the sleeping radius of the MBS. However, these sleep controls could degrade the QoS performance of user equipment (UEs) and bring coverage holes incurred by the SBS sleeping. To solve the problems, Distance-Sensitive Distributed Repulsive Sleeping Strategy (DSDRSS) has been proposed in [53]. The DSDRSS scheme inactivates all the SBSs within the certain area with a light traffic load. These SBSs are then merged to form a sleeping cluster. To guarantee UE coverage in that area, the DSDRSS will activate one SBS for this sleeping cluster. While DSDRSS achieves a maximum power savings of 50% by sleeping the SBSs, system throughput is also drastically decreased when compared with the no-sleep control system. In [22], a sleep control scheme based on traffic load during a certain period of time has been proposed. In terms of its sleeping procedure, the activated SBSs monitor the served traffic on a regular basis. If the traffic load measured over a specified period is low, the SBS is put to sleep state to reduce power consumption. However, this technique also reduces system throughput in comparison to the no-sleep control system.

3.2.2 Conventional Cell Throughput Based Sleep Control

The conventional cell throughput based sleep control [54] is a simple but effective scheme applied for the SBS sleeping. The cell capacity ratio, which is a ratio of currently achieved cell throughput to maximum achievable cell throughput, is introduced as decision criteria for making SBSs sleep, in order to find the SBSs with the waste of energy. It results in SBSs with small throughput are put into the sleep state, whereas those with large cell throughput remain in the active state. Then the conventional cell throughput based sleep control scheme can reduce power consumption, and then improve energy efficiency.

The cell capacity ratio R^i_{SBS} for the i-th SBS can be obtained from the currently achieved cell throughput S^i_{SBS} [bps] at the i-th SBS normalized by cell capacity C_{SBS} [bps], which is formulated by:

$$R^i_{\mathrm{SBS}} = \frac{S^i_{\mathrm{SBS}}}{C_{\mathrm{SBS}}} \quad , \tag{3.1}$$

where C_{SBS} represents the maximum cell throughput achievable when the SBS fully utilizes its allocated frequency bandwidth for communication services. The S^i_{SBS} can be obtained by summing the user throughput S^j_{UE} achieved at all the UEs connecting to the

i-th SBS, and S^i_{SBS} can be written as:

$$S^i_{\mathrm{SBS}} = \sum_{j=1}^{N^i_{\mathrm{con}}} S^j_{\mathrm{UE}} = \sum_{j=1}^{N^i_{\mathrm{con}}} \{B^j_{\mathrm{UE}} \log_2 (1 + SINR^j_{\mathrm{UE}})\} \quad , \tag{3.2}$$

where N^i_{con} is the number of UEs connecting to the i-th SBS, B^j_{UE} is the assigned frequency bandwidth to the j-th UE, and $SINR^j_{\mathrm{UE}}$ is the received signal to interference plus noise ratio (SINR) at the j-th UE.

The sleep control algorithm employed in the conventional cell throughput based sleep control is shown on the inside of the dashed rectangle in the upper part of Figure 3.2. The conventional cell throughput based sleep control algorithm employs a threshold-based control for the cell capacity ratio R^i_{SBS} to determine the operation state for every SBS. The following formula is used to determine the operating state OS^i at the i-th SBS:

$$OS^i = \begin{cases} \text{sleep} & ; \ R^i_{\mathrm{SBS}} \leq \alpha \\ \text{active} & ; \ \text{otherwise} \end{cases} \quad , \tag{3.3}$$

where α is a predefined threshold value for the cell capacity ratio. As shown in Eq. (3.3), when R^i_{SBS} is less than or equal to α, the SBSs enter the sleep state, otherwise, the SBSs remain in the active state.

Applying this control procedure, the conventional sleep control scheme provides reduced power consumption and then improved energy efficiency, compared with no-sleep control system. However, this conventional cell throughput based sleep control also causes degradation in system throughput in comparison to the no-sleep control system. This is because the conventional cell throughput based sleep control excessively inactivates SBSs with a lower cell capacity rate. Then, this system throughput degradation leads to a serious problem from the perspective of efficient frequency utilization.

3.2.3 Conventional Adaptive SBS Sleep Control

The conventional adaptive SBS sleep control [55] focuses on cell-level energy efficiency instead of system-level energy efficiency. This control proposes a sleeping technique to improve cell-level energy efficiency for active SBSs by determining and then inactivating the SBS with the minimum cell-level energy efficiency.

The conventional adaptive SBS sleep algorithm can be described as follows: after calculating the cell-level energy efficiency for all the active SBSs, the algorithm finds the SBS with minimum cell-level energy efficiency $EE^{\mathrm{min\_org}}_{\mathrm{SBS}}$. Then, the SBS with $EE^{\mathrm{min\_org}}_{\mathrm{SBS}}$ temporarily changes its operating state from active to tentative sleep state. After then, the cell-level energy efficiency for all the active SBSs is recalculated, and then the updated minimum cell-level energy efficiency $EE^{\mathrm{min\_upd}}_{\mathrm{SBS}}$ is derived. Finally, if the updated

minimum cell-level energy efficiency is greater than the original minimum cell-level energy efficiency ($EE_{\text{SBS}}^{\text{min\_upd}} > EE_{\text{SBS}}^{\text{min\_org}}$), the SBS with $EE_{\text{SBS}}^{\text{min\_org}}$ changes its operating state from tentative sleep to permanent sleep state.

By employing the above control procedure, this conventional adaptive SBS sleep control achieves lower power consumption and increased energy efficiency while maintaining almost the same system throughput as the no-sleep control system. However, as compared with the conventional cell throughput based sleep control [54], this conventional adaptive SBS sleep control [55] results in decreased energy efficiency, and thus it cannot provide satisfactory improvement in energy efficiency.

3.3 Proposed Energy Efficiency Based Sleep Control

To solve the problems with the conventional sleep control schemes, described in the previous section, this section proposes an enhanced SBS sleep control scheme as an energy efficiency based sleep control scheme to enhance both energy efficiency and system throughput simultaneously.

Since active SBSs contribute to gain in system throughput, it is necessary to increase the number of active SBSs in order to improve system throughput. On the other hand, however, increasing the number of active SBSs results in an increased power consumption, which leads to a decrease in energy efficiency. From these considerations, energy efficiency must be a key element for achievable system performance from the perspectives of both the efficiencies of frequency utilization and energy consumption. Under the condition of the energy efficiency maintained without any degradation, the system can activate additional SBSs to improve system throughput. Therefore, the proposed sleep control scheme employs energy efficiency as the decision criteria for SBS operating state.

The sleep control algorithm for the proposed scheme consists of 2 phases: pre-decision phase and final-decision phase, which is shown in Figure 3.2 and can be described as follows:

Pre-decision phase: The operation in this phase is applied throughout all the SBSs and is a similar operation to the conventional cell throughput based sleep control [54].

For the SBSs with cell capacity ratio R^i_{SBS} up to a predefined threshold α, they will be temporarily considered in a "tentative sleep" state, which is a different decision from the conventional cell throughput based sleep control [54], otherwise, they remain in the active state, as shown in Eq. (3.4):

$$OS^i = \begin{cases} \text{tentative sleep} & ;\ R^i_{\mathrm{SBS}} \leq \alpha \\ \text{active} & ;\ \text{otherwise} \end{cases} . \tag{3.4}$$

Final-decision phase: This operation is applied to the tentative sleep SBSs, which will be considered to be activated in this phase.

At the first step in this phase, the temporal energy efficiency EE^k_{sys} [bps/W] is calculated supposing that all the tentative sleep SBSs operate in the sleep state, where EE^k_{sys} is defined as the ratio of temporal achievable system throughput S^k_{sys} [bps] to temporal power consumption P^k_{sys} [W], which can be written as:

$$EE^k_{\mathrm{sys}} = \frac{S^k_{\mathrm{sys}}}{P^k_{\mathrm{sys}}} , \tag{3.5}$$

where S^k_{sys} is defined as the summation of the achievable cell throughputs S^l_{MBS} [bps] at all the MBSs and those S^l_{SBS} [bps] at all the SBSs, which can be given by Eqs. (3.6) and (3.7), and P^k_{sys} can be expressed as Eq. (3.8):

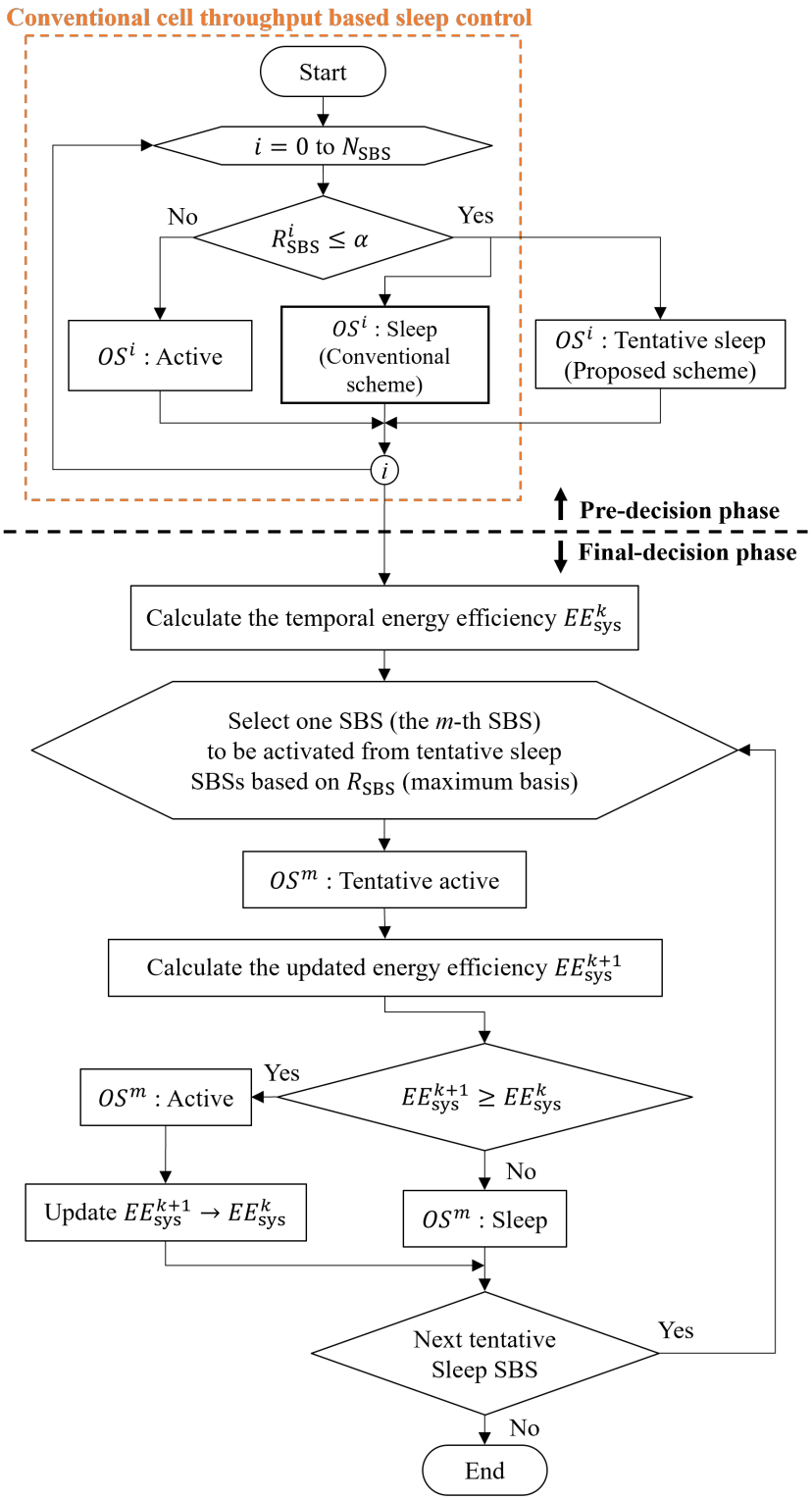

Figure 3.2: The flowchart for the proposed sleep control algorithm.

$$S^k_{\text{sys}} = \sum_{l=1}^{N_{\text{MBS}}} S^l_{\text{MBS}} + \sum_{i=1}^{N_{\text{SBS}}} S^i_{\text{SBS}} \quad , \tag{3.6}$$

$$S^l_{\text{MBS}} = \sum_{j=1}^{N^l_{con}} S^j_{\text{UE}} = \sum_{j=1}^{N^l_{con}} \{B^j_{\text{UE}} \log_2 (1 + SINR^j_{\text{UE}})\} \quad , \tag{3.7}$$

$$P^k_{\text{sys}} = P_{\text{MBS}} + P^k_{\text{Active}} + P^k_{\text{Sleep}} \ , \tag{3.8}$$

where N^l_{con} is the number of UEs connected to the l-th MBS. Note that the detailed definition of P^k_{sys} will be provided in Sect. 3.4.

Then, one SBS is chosen from the tentative sleep SBSs on the basis of the maximum cell capacity ratio R_{SBS}, and the chosen SBS with the maximum R_{SBS}, saying the m-th SBS, is changed the operating state from the tentative sleep to the active state. After then the updated energy efficiency EE^{k+1}_{sys} is calculated supporting the operating state OS^m of the chosen SBS is active.

Finally, if the updated energy efficiency EE^{k+1}_{sys} is greater than or equal to the temporal energy efficiency EE^k_{sys}, which indicates no degradation in energy efficiency, the chosen SBS will eventually change the operating state OS^m from the tentative sleep to the active state. Otherwise, the OS^m changes to the sleep state, as defined in Eq. (3.9):

$$OS^m = \begin{cases} \text{active} & ; \ EE^{k+1}_{\text{sys}} \geq EE^k_{\text{sys}} \\ \text{sleep} & ; \ \text{otherwise} \end{cases} \quad . \tag{3.9}$$

This operation is repeated for the subsequent tentative sleep SBS until all the tentative sleep SBSs are chosen.

Through the above control procedure, the proposed sleep control scheme has the potential to simultaneously provide improved energy efficiency and almost the same system throughput as the no-sleep control system, which cannot be provided by the conventional sleep control schemes.

Note that the activation of SBSs following sleep periods will occur at regular intervals. The proposed sleep control scheme will be implemented immediately after activation, and this process will repeat periodically. MBS will manage these control schemes as MBS and SBSs consistently communicate through wired connections.

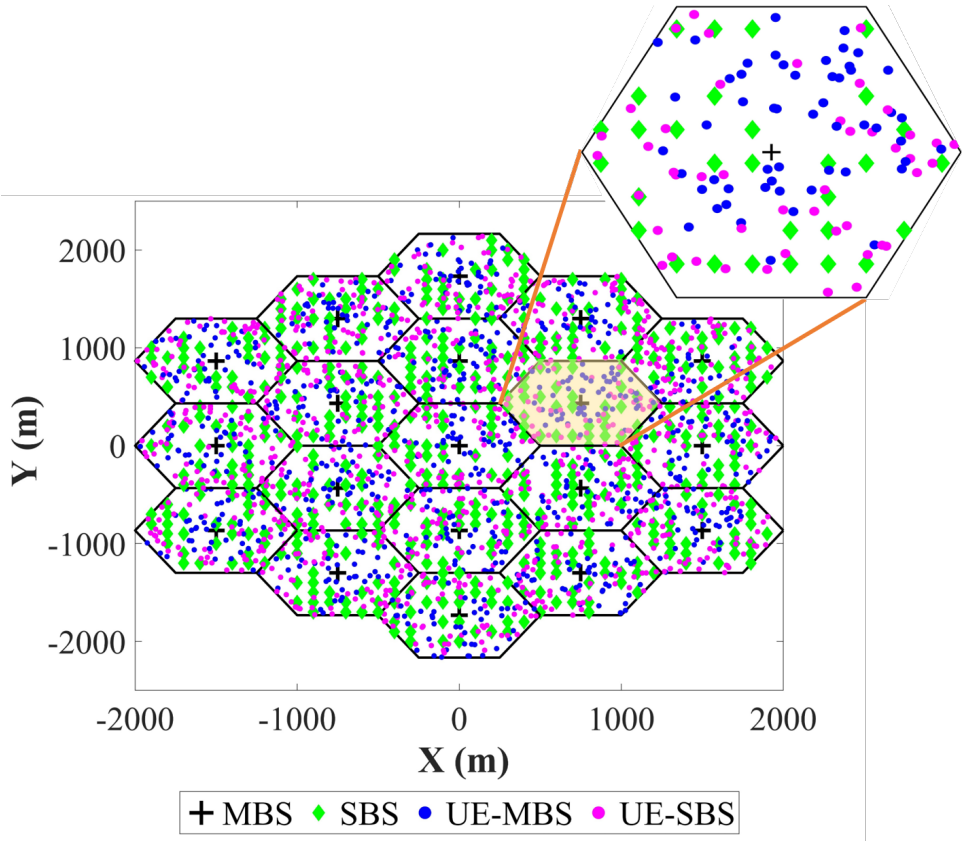

Figure 3.3: BS and UE configuration under consideration.

3.4 System Model for Performance Evaluation

This section describes the system model assumed in performance evaluations, evaluation metrics, and the schemes for performance comparison.

3.4.1 System Model

The HetNet for the performance evaluation consists of two tiers of base stations: MBS tier and SBS tier. The cell layout of the MBS tier is a 2-ring structure composed of 19 cells, each with a hexagonal coverage area, as shown in Figure 3.3. The MBS is located at the center of the hexagonal coverage area, and the distance between MBSs is d_{cell} [m]. The N_{SBS} SBSs and N_{UE} UEs are distributed uniformly within a hexagonal coverage area of every MBS. The UEs are connected to either the MBS or SBS based on the maximum received signal power from them.

The network employs orthogonal frequency division multiple access (OFDMA) for radio channel access, in which the MBS or SBS allocates the same amount of the frequency bandwidth to each connecting UE by equally dividing its total frequency bandwidth B_{MBS} [Hz] or B_{SBS} [Hz], respectively.

The signal propagation assumes path loss due to the distance attenuation and log-

normal shadow fading. Thus, the received signal power $P_{\text{rx}}^{i,j}$ [dB] at the j-th UE for the signal from the i-th base station can be written as:

$$P_{\text{rx}}^{i,j} = P_{\text{tx}}^{i} - (PL^{i,j} + \psi^{i,j}) \quad , \tag{3.10}$$

where P_{tx}^{i} [dB] and $PL^{i,j}$ [dB] denote transmission power at the i-th base station (MBS or SBS), and the distance attenuation in the signal propagation path respectively. $\psi^{i,j}$ [dB] denotes its shadow fading attenuation which follows a log-normal distribution with zero mean and standard deviation of σ_{MBS} or σ_{SBS} [dB] for MBS or SBS tier. The path loss $PL^{i,j}$ is specified in the 3GPP specification TR 38.901 [34] for the carrier frequencies in 5G networks. For the MBS tier, the path loss $PL_{\text{MBS}}^{i,j}$ [dB] can be found as Eq. (3.11):

$$PL_{\text{MBS}}^{i,j} = 13.54 + 39.08 \log_{10}(d_{\text{3D}}^{i,j}) + 20 \log_{10}(f_c^{\text{MBS}}) - 0.6(h_{\text{UE}} - 1.5) \quad , \tag{3.11}$$

where $d_{\text{3D}}^{i,j}$ [m] denotes the 3-dimension distance between from the i-th MBS to the j-th UE, f_c^{MBS} [Hz] is a carrier frequency used in the MBS tier, and h_{UE} [m] is an antenna height for UEs. The path loss $PL_{\text{SBS}}^{i,j}$ [dB] for the SBS tier is defined in Eq. (3.12), where f_c^{SBS} [Hz] defines a carrier frequency for the SBS tier:

$$PL_{\text{SBS}}^{i,j} = 22.4 + 35.3 \log_{10}(d_{\text{3D}}^{i,j}) + 21.3 \log_{10}(f_c^{\text{SBS}}) - 0.3(h_{\text{UE}} - 1.5) \quad . \tag{3.12}$$

The network employs the different carrier frequency bands f_c^{MBS} and f_c^{SBS} between the MBS and SBS tiers. The network does not employ frequency reuse technique for both the MBS and SBS tiers. Therefore, the co-channel interference at the UE is caused by the arriving signals from all the BSs except its own connected BS in the same tier as shown in Figure 3.4.

As for the SINR $SINR_{\text{MBS}}^{j}$ at the j-th UE connecting to the i-th MBS and that $SINR_{\text{SBS}}^{j}$ at the j-th UE connecting to the i-th SBS can be expressed by [56]:

$$SINR_{\text{MBS}}^{j} = \frac{P_{\text{rx}}^{i,j}}{I_{\text{MBS}}^{j} + N_0 B_{\text{MBS}}^{j}} \quad , \tag{3.13}$$

$$SINR_{\text{SBS}}^{j} = \frac{P_{\text{rx}}^{i,j}}{I_{\text{SBS}}^{j} + N_0 B_{\text{SBS}}^{j}} \quad , \tag{3.14}$$

where N_0 [dBm/Hz] denotes noise power density, B_{MBS}^{j} and B_{SBS}^{j} [Hz] are the frequency bandwidth allocated to the j-th UE by the connected i-th MBS and SBS, respectively. The I_{MBS}^{j} and I_{SBS}^{j} denote the total co-channel interference at the j-th UE from other BSs in the same BS tier, except its own connected BS, which are defined by:

$$I_{\text{MBS}}^{j} = \sum_{i \in \emptyset_{\text{MBS}}^{j}} P_{\text{rx}}^{i,j} \quad , \tag{3.15}$$

$$I_{\text{SBS}}^{j} = \sum_{i \in \emptyset_{\text{SBS}}^{j}} P_{\text{rx}}^{i,j} \quad , \tag{3.16}$$

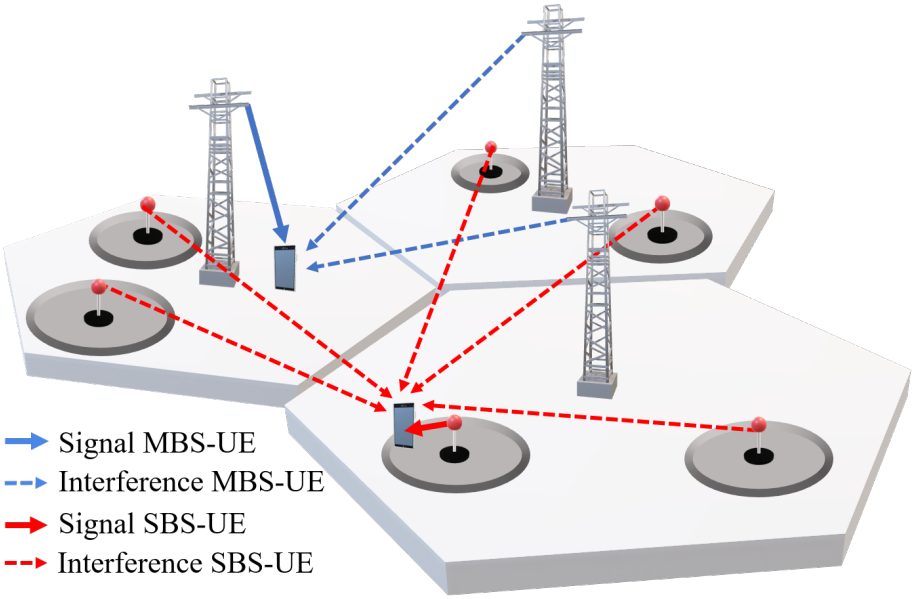

Figure 3.4: Signal and interference for two-tier heterogeneous network.

where $\emptyset^j_{\text{MBS}}$ and $\emptyset^j_{\text{SBS}}$ represent the set of BSs interfering to the j-th UE.

Only the downlink communication from BSs to UEs is assumed and its data traffic employs a full buffer model. Therefore, the UE throughput S^j_{UE} [bps] at the j-th UE can be derived by using Shannon's channel capacity theory in Eq. (3.17) [57]:

$$S^j_{\text{UE}} = B^j_{\text{UE}} \log_2 \left(1 + SINR^j_{\text{UE}}\right) \quad , \tag{3.17}$$

where B^j_{UE} is either of B^j_{MBS} or B^j_{SBS} depending on the BS tier connected by the j-th UE. $SINR^j_{\text{UE}}$ is also either of $SINR^j_{\text{MBS}}$ or $SINR^j_{\text{SBS}}$.

For the power consumption at each BS, this chapter focuses on the power consumption at the transceiver on the BSs, which typically consists of a power amplifier (PA) module, a radio frequency signal (RF) module, a baseband processing (BB) module, a DC-DC power supply (DCDC), an active cooling system (CO), and an AC-DC (main supply) unit (ACDC) [18,58]. For the power consumption at the SBS, we assume different states for SBS operations: active, idle, and sleep. The active state is defined as the state in which the SBS is fully operational, including the operation of the PA and RF modules with maximum power due to the provision of communication services to connected UE. In the idle state, the SBS is partially operational, which means the SBS does not operate especially the PA and RF modules due to no requirement of communication services to UEs under the case with no connected UEs, and consumes lower power than the active state. In the sleep state, the SBS does not operate major operating parts, however, to ensure that it could be activated, it should not be entirely powered off, and then may continue to consume some power.

Each operating state is assumed to consume the different power: P_{Active}, P_{Idle}, and

P_{Sleep} [W] for active, idle, and sleep state, respectively. For the power consumption at the MBS, all the MBSs always active, and then their power consumption P_{MBS} [W] is assumed to be constant.

3.4.2 Evaluation Metrics

In the performance evaluation, system throughput S_{sys}, system power consumption P_{sys}, and energy efficiency EE_{sys} are evaluated by computer simulation.

The system throughput S_{sys} [bps] is defined as the summation of the cell throughputs for all the MBSs and SBSs with their final operation state in the HetNets, which is calculated by applying Eqs. (3.2), (3.6), and (3.7).

The system power consumption P_{sys} [W] is defined as the total power consumed at all the base stations. Thus, P_{sys} can be expressed by:

$$P_{\text{sys}} = (P_{\text{MBS}} \cdot N_{\text{MBS}}) + (P_{\text{Active}} \cdot N_{\text{Active}}) + (P_{\text{Idle}} \cdot N_{\text{Idle}}) + (P_{\text{Sleep}} \cdot N_{\text{Sleep}}) \quad , \tag{3.18}$$

where N_{Active}, N_{Idle}, and N_{Sleep} are the number of SBSs under the final operating states of active, idle, and sleep, respectively.

The energy efficiency EE_{sys} [bps/W] is defined as an achieved system throughput S_{sys} normalized by the power consumption P_{sys}, which is calculated by applying Eq. (3.5) [59].

3.4.3 Schemes under Comparison

For the performance evaluation, this chapter compares the performances for four different schemes.

- no-sleep control system: All the SBSs remain in the active state, except for the SBSs with no UEs connected, which are under an idle state.
- The conventional cell throughput based sleep control [54], which employs the cell capacity ratio as a decision criteria, described in Sect. 3.2.2.
- The conventional adaptive SBS sleep control [55], which inactivates the SBS with the minimum cell-level energy efficiency, explained in Sect. 3.2.3.
- The proposed sleep control, described in Sect. 3.3.

3.5 Performance Evaluation

This section presents the computer simulation results for four different schemes. All simulations were conducted using MATLAB software and included Monte Carlo simulations for 105 trials to ensure statistically significant results. The system throughput S_{sys}, system power consumption P_{sys}, and energy efficiency EE_{sys} are shown while comparing between four schemes. The performances for the sleeping operation rate SOR_{SBS} also shown in this section.

3.5.1 Simulation Parameters and Their Settings

We use the parameter settings for the simulation parameters listed in Table 3.1 [34,54]. The total number of SBSs and UEs per MBS coverage is defined between 5 to 50 and 50 to 300, respectively. The frequency bandwidth is 20 MHz for both MBSs and SBSs. The carrier frequencies for MBS and SBS tiers are 0.8 GHz and 3.7 GHz, respectively [60]. The transmission power at MBSs and SBSs is 46 dBm and 30 dBm, respectively. The threshold α for cell capacity ratio is set as a constant value of 0.25, which is an optimum value for the energy efficiency in the conventional cell throughput based sleep control scheme and proposed sleep control scheme.

Table 3.1: Simulation parameter setting.

	Symbol	**Value**	
Distance between MBSs	d_{cell}	$500\sqrt{3}$	[m]
No. of MBS	N_{MBS}	19	
No. of SBS [/MBS]	N_{SBS}	5-50	
No. of UE [/MBS]	N_{UE}	50-300	
Bandwidth	$B_{\text{MBS}}, B_{\text{SBS}}$	20	[MHz]
Carrier frequency at MBS, SBS	$f_{\text{c}}^{\text{MBS}}, f_{\text{c}}^{\text{SBS}}$	0.8, 3.7	[GHz]
TX power at MBS, SBS	$P_{\text{tx}}^{\text{MBS}}, P_{\text{tx}}^{\text{SBS}}$	46, 30	[dBm]
Shadow fading std for MBS, SBS	$\sigma_{\text{MBS}}, \sigma_{\text{SBS}}$	6, 7.82	[dB]
Noise power density	N_0	-174	[dBm/Hz]
Cell capacity threshold	α	0.25	
Power consumption at MBS, Active, Idle, Sleep	P_{MBS}	150	[W]
	P_{Active}	30	
	P_{Idle}	25	
	P_{Sleep}	15	

3.5.2 System Throughput Performance

Figure 3.5(a) shows the system throughput S_{sys} for varying the number of SBSs per MBS for the number of UEs $N_{\text{UE}} = 100$. The proposed sleep control scheme improves system throughput S_{sys} over the conventional cell throughput based sleep control scheme [54] and achieves almost the same as no-sleep control system and the conventional adaptive sleep control scheme [55]. This is because the proposed one can activate more SBSs, compared with the cell throughput based scheme [54], and this activation contributes to an improvement in the system throughput. As can be observed in Figure 3.5(a), the proposed scheme achieves more improvement in the system throughput over the cell throughput based sleep control scheme, especially for the case with the larger number of SBSs N_{SBS} from 30 to 50. For example, at $N_{\text{SBS}} = 50$, the proposed scheme achieves only 0.6% degradation from the no-sleep control system, whereas the conventional cell throughput based sleep control scheme [54] shows 3.1% degradation.

The system throughput S_{sys} for varying the number of UEs per MBS is also shown in Figure 3.5(b) for the case of $N_{\text{SBS}} = 30$. The proposed sleep control scheme also provides almost the same system throughput as the no-sleep control system and the conventional adaptive sleep control scheme [55] for any number of UEs. The reason for this improvement is the same as that in Figure 3.5(a). Furthermore, the proposed scheme largely improves system throughput for the case with the smaller number of UEs N_{UE} from 50 to 150. This improvement under such the case, as well as the case with the larger number of SBSs in Figure 3.5(a), is caused by the fact that the network has the large number of candidate SBSs to be activated under such the cases, as can be found in Figure 3.6, which shows the sleeping operation rate under the same condition as Figure 3.5. We can find in Figure 3.6 that the sleeping operation rate is relatively high under such the cases, and then the network has more SBSs to be activated in the final decision phase by the proposed scheme, resulting in a larger improvement in the system throughput.

In addition, as illustrated in Figure 3.5, the proposed scheme shows the constant normalized system throughput, which is defined as a ratio of the achievable system throughput to that for the no-sleep control system, for any number of SBSs and UEs. In contrast to the proposed scheme, the normalized system throughput for the conventional cell throughput based sleep control scheme [54] depends on the number of SBSs and UEs, and then, the conventional scheme [54] cannot provide the constant normalized system throughput for all the system conditions.

3.5.3 Power Consumption Performance

Figure 3.7 shows the system power consumption P_{sys} under the same conditions as Figure 3.5. It is observed that the power consumption P_{sys} for all the sleep control schemes are less than that for the no-sleep control system. However, the conventional

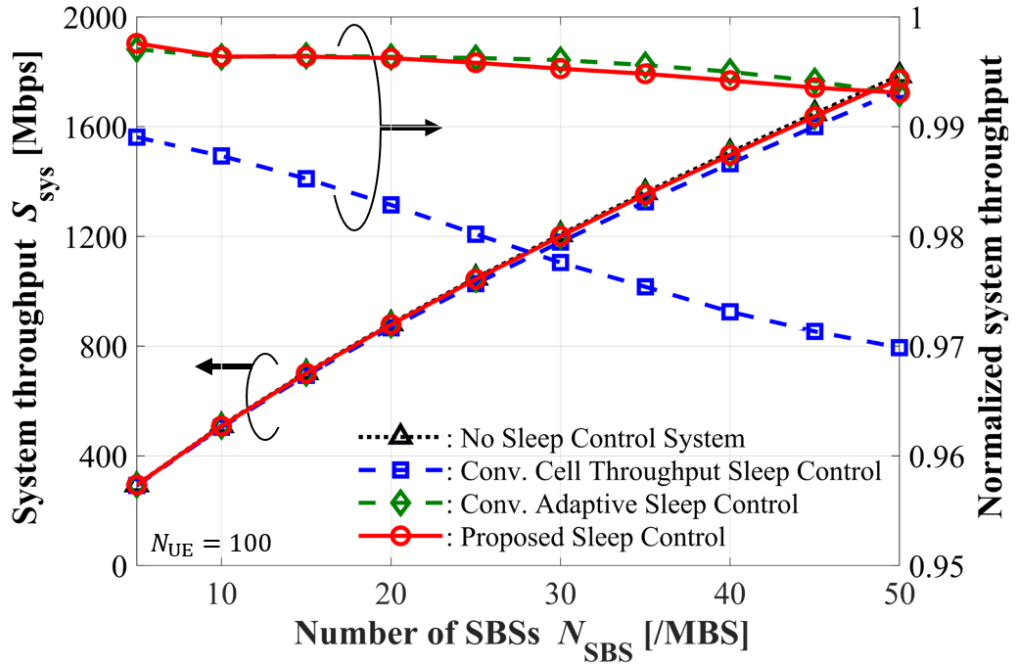

(a) SBSs N_{SBS}

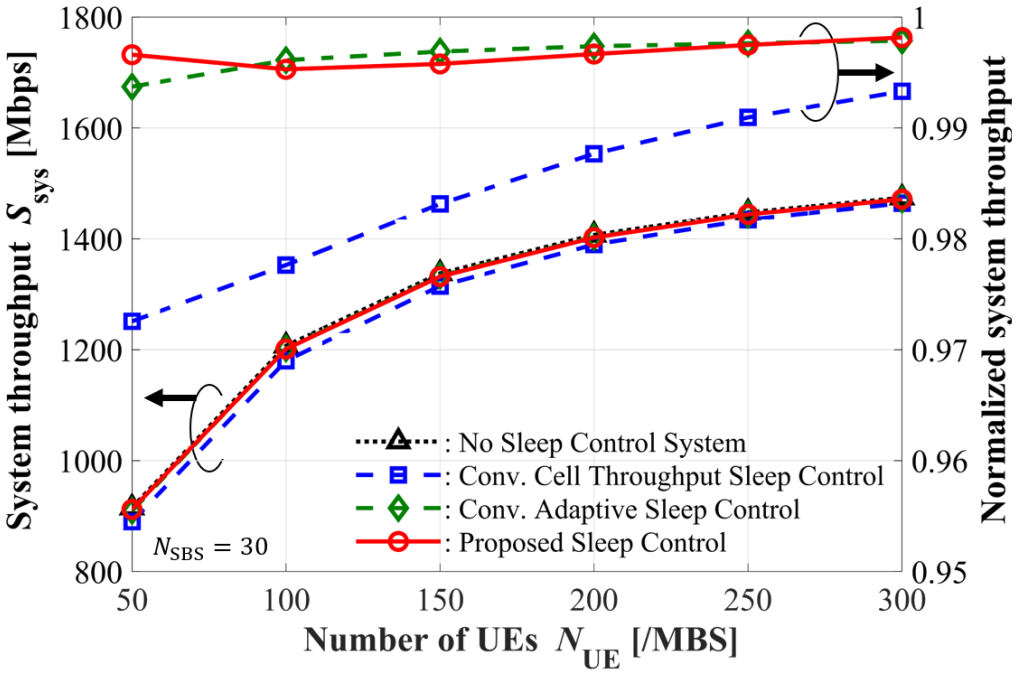

(b) UEs N_{UE}

Figure 3.5: The system throughput S_{sys}.

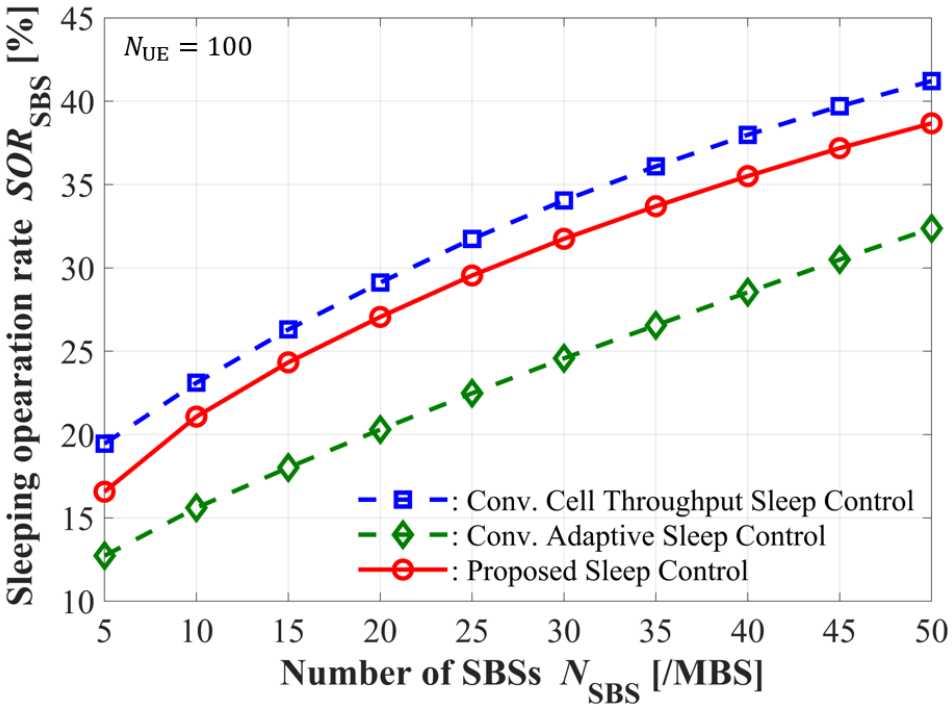

(a) SBSs N_{SBS}

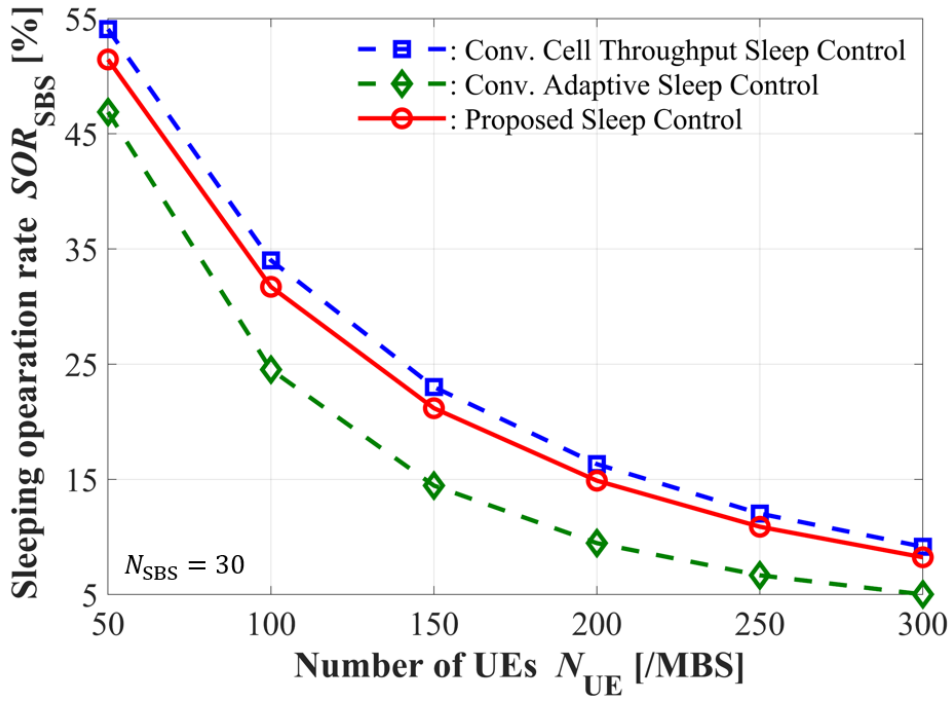

(b) UEs N_{UE}

Figure 3.6: The sleeping operation rate SOR_{SBS}.

adaptive sleep control scheme [55] consumes larger power than the proposed scheme and conventional cell throughput based sleep control scheme [54]. The proposed scheme achieves the smallest P_{sys} performance, however it shows slightly larger P_{sys} than the conventional cell throughput based sleep control scheme [54]. This is due to the fact that the proposed scheme activates additional SBSs from the tentative sleep SBSs in its final-decision phase. As a result, the proposed sleep control scheme activates a larger number of SBSs, leading to slightly larger power consumption.

Moreover, the proposed scheme shows slightly larger degradation in the power consumption for the cases with larger improvement in the system throughput, that is the cases with larger N_{SBS} or smaller N_{UE}. This means the proposed scheme provides throughput improvement with a cost of power consumption.

3.5.4 Energy Efficiency Performance

Figure 3.8 shows the energy efficiency EE_{sys} under the same conditions as Figure 3.5. The proposed scheme can achieve superior EE_{sys} performance to both the conventional sleep control schemes, particularly compared with the conventional adaptive sleep control scheme [55], which provides almost the same system throughput. This is because the proposed scheme employs energy efficiency as the criteria for the decision of the SBS operating state in its final-decision phase prior to activating additional SBSs for the purpose of improving system throughput. The performance gain in the energy efficiency by the proposed scheme gets larger for the cases with larger improvement in the system throughput. This fact shows the gain in the system throughput surpasses the cost in the energy consumption in the proposed scheme.

Table 3.2 compares the energy efficiency EE_{sys} achieved by different schemes for different numbers of SBSs N_{SBS}. We can find from Table 3.2 that the proposed sleep control scheme can provide the highest EE_{sys} of for example 1.304 [Mbps/W] at $N_{\text{SBS}} = 50$, which is a 14.89% improvement in comparison to the no-sleep control system, whereas the conventional cell throughput based scheme [54] and the conventional adaptive sleep control scheme [55] improve performance by only 13.83% and 11.01%, respectively.

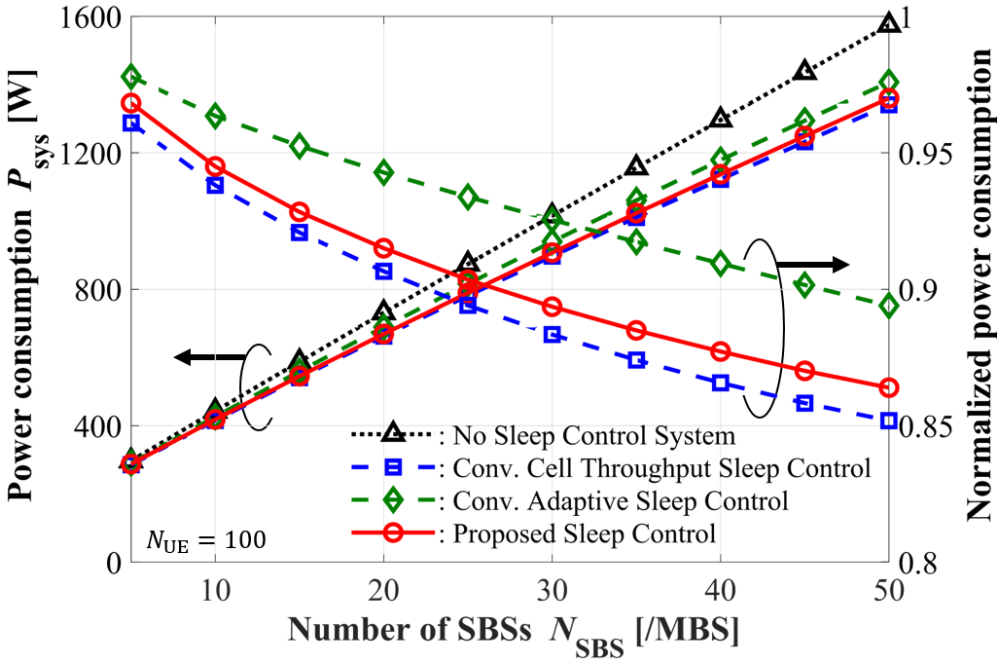

(a) SBSs N_{SBS}

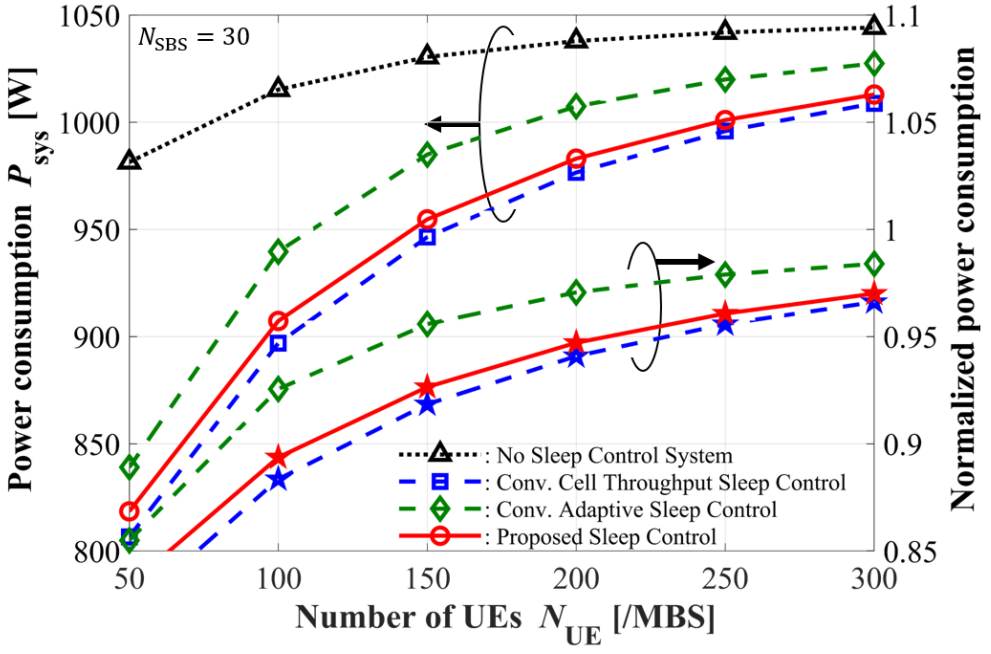

(b) UEs N_{UE}

Figure 3.7: The system power consumption P_{sys}.

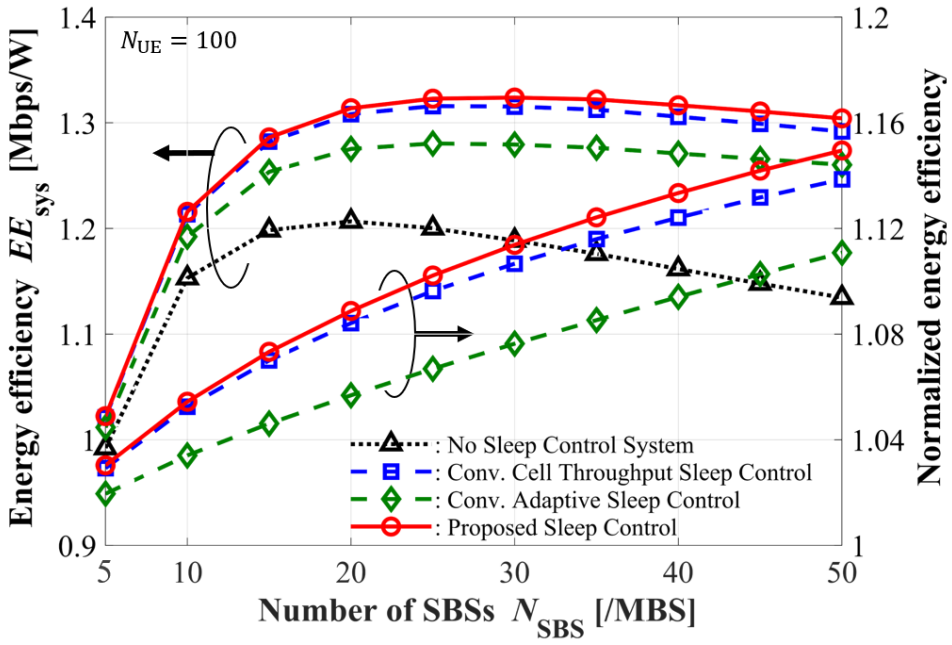

(a) SBSs N_{SBS}

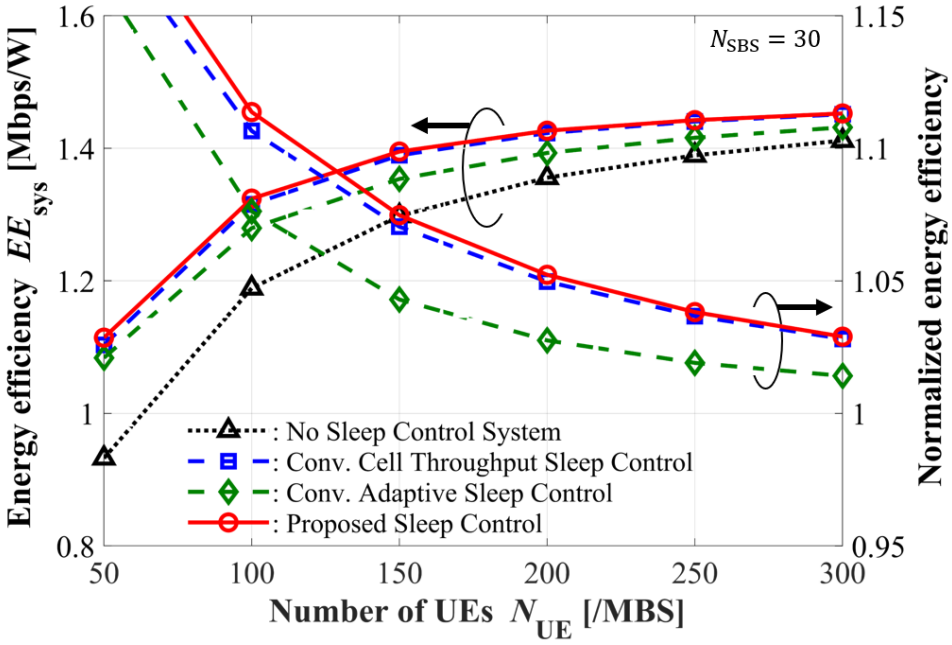

(b) UEs N_{UE}

Figure 3.8: The energy efficiency EE_{sys}.

Table 3.2: Comparison of energy efficiency EE_{sys} for different numbers of SBSs N_{SBS} and $N_{\text{UE}} = 100$.

Sleep Control Schemes	$N_{\mathbf{SBS}}$		
	30	**40**	**50**
no-sleep control system	1.189	1.162	1.135
Conv. cell throughput sleep control [54]	1.315	1.306	1.292
Conv. adaptive sleep control [55]	1.279	1.271	1.260
Proposed sleep control	1.324	1.317	1.304

3.6 Conclusions

This chapter discussed the sleep control applied for the SBSs in 5G HetNets. Aiming at improving energy efficiency and system throughput while considering the demands of eMBB services simultaneously, this chapter proposed the enhanced sleep control algorithm which employs energy efficiency as a decision criterion for switching the SBS state into active or sleep state. The proposed sleep control introduces a 2-phase control procedure and its second phase activates additional SBSs from the sleep SBSs to improve the energy efficiency while retaining the system throughput.

We evaluated the system throughput, power consumption, and energy efficiency for the proposed scheme and compared with the conventional schemes. The evaluation results through computer simulation at the system level performance demonstrate that, the proposed sleep control scheme achieves superior energy efficiency and system throughput simultaneously, indicating that it can improve energy efficiency while maintaining almost the same system throughput as no-sleep control system, which cannot be provided by the conventional sleep control schemes. Moreover, the proposed scheme improves energy efficiency by 14.89% while maintaining almost the same system throughput of over 99% when compared with the no-sleep control system. Consequently, the proposed scheme can contribute to providing high capacity green HetNets for eMBB services in 5G NR cellular networks.

In addition to the findings presented in this thesis, it is important to note that the activation scheme for SBSs has not been addressed in the current study. Future work will focus on the development and exploration of an SBSs activation scheme, with particular emphasis on accommodating dynamic behaviors such as UE mobility and traffic fluctuations within HetNets. This extension aims to further enhance the overall efficiency and adaptability of the proposed sleep control algorithm in diverse operational scenarios.

Chapter 4

Adaptive K-Repetition Transmission with Site Diversity Reception for Energy-Efficient Grant-Free URLLC in 5G NR

The fifth-generation (5G) new radio (NR) standard employs ultra-reliable and low-latency communication (URLLC) to provide real-time wireless interactive capability for the internet of things (IoT) applications. To satisfy the stringent latency and reliability demands of URLLC services, grant-free (GF) transmissions with the K-repetition transmission (K-Rep) have been introduced. However, fading fluctuations can negatively impact signal quality at the base station (BS), leading to an increase in the number of repetitions and raising concerns about interference and energy consumption for IoT user equipment (UE). To overcome these challenges, this chapter proposes novel adaptive K-Rep control schemes that employ site diversity reception to enhance signal quality and reduce energy consumption. The performance evaluation demonstrates that the proposed adaptive K-Rep control schemes significantly improve communication reliability and reduce transmission energy consumption compared with the conventional K-Rep scheme, and then satisfy the URLLC requirements while reducing energy consumption and enhancing energy efficiency at UE side.

4.1 Introduction

The fifth-generation (5G) new radio (NR) standard employs ultra-reliable and low-latency communication (URLLC) to provide real-time wireless interactive capability [3,61]. The 3rd generation partnership project (3GPP) has adopted the standard URLLC requirements with performance targets of 1 ms user-plane latency and 10^{-5} communication reliability [62–64]. The advent of the internet of things (IoT) has facilitated the shift towards wireless real-time interactive systems, empowering low-latency control applications like telemedicine, smart grids, industrial automation, and traffic control [65, 66]. The URLLC is an important type of communication for many IoT applications because it enables the reliable and timely transfer of data and commands, which is required for the systems to function properly [65, 67].

The 3GPP introduced the grant-free (GF) transmission to support URLLC user equipment (UE) by removing scheduling request and grant from the conventional grant-based (GB) transmission [31], which cannot satisfy the URLLC latency requirement. Due to no need to send scheduling request or wait for scheduling grant from base station (BS), GF transmission can reduce access latency to meet URLLC requirements [68]. However, GF transmission allows URLLC UEs to randomly access shared sub-channels without the scheduling grant, resulting in a high collision probability if multiple URLLC UEs transmit simultaneously over the same sub-channel, thereby degrading reliability performance [32].

For reliability improvement, K-Repetition transmission (K-Rep) is one of the transmission schemes that have been investigated for 5G URLLC. In this scheme, the UE is configured to autonomously transmit the same packet K times without waiting for the feedback [15, 16, 69], and then the BS performs soft combining of these repetitions to improve the signal quality. However, the work in [23] indicates that the K-Rep scheme significantly increases the number of packet transmissions due to its repeated operation. As a result, an excessive increase in packet transmissions causes severe interference at the receiving BS, resulting in a degradation in reliability.

In addition, the majority of IoT UEs, including those designed for URLLC operation, have energy constraints due to limited battery lifetime [24]. These IoT URLLC UEs are regularly required to operate for extended periods on a single battery charge, and therefore, energy efficiency is a critical design consideration [25]. Nevertheless, the increase in packet transmissions on the K-Rep scheme causes a significant increase in energy consumption, resulting in the early battery depletion in IoT URLLC UEs.

By the way, site diversity reception is a technique that utilizes multiple-cell reception to improve signal quality [36, 37, 70, 71]. Multi-cell reception involves joint reception and combining of signals from multiple BSs in the network. In the context of URLLC in 5G NR systems, multi-cell reception can be used to enhance the reliability of GF transmis-

sions. This is achieved by combining the signals from multiple BSs to effectively improve the signal quality against severe interference caused by the additional repetitions and enhance the reliability performance in the K-Rep scheme for the GF URLLC. However, site diversity reception has not been investigated for the K-Rep scheme so far.

This chapter applies site diversity reception to the K-Rep scheme for uplink GF URLLC and proposes its adaptive K-Rep control schemes in order to handle two problems; severe interference and high energy consumption due to an increase in the number of repetitions. By adopting site diversity reception, the K-Rep scheme has the potential to decrease the number of repetitions. Therefore, the proposed adaptive K-Rep control schemes dynamically adjust the number of repetitions based on the situation of the UE in the K-Rep scheme. The performance evaluation through computer simulation demonstrates that the proposed schemes exhibit superior performance compared to the conventional scheme.

This chapter extends our previous conference chapter [72] by proposing an additional adaptive control mechanism for the K-Rep scheme and providing a more comprehensive analysis of the adaptive K-Rep control scheme. In contrast to [72], this chapter delves deeply into the benefits of utilizing site diversity reception, which has the potential to significantly enhance diversity gain and improve signal quality. As a result, this chapter shows that this approach can lead to a substantial improvement in overall transmission performance at the system level evaluation.

The subsequent sections of the chapter are organized as follows: Section 4.2 provides related work of the adaptive K-Rep control scheme and site diversity reception. Section 4.3 presents the proposed adaptive K-Rep control schemes employing site diversity reception. Section 4.4 describes the evaluation methodology and simulation assumptions for performance evaluation, followed by Section 4.5 which presents the simulation results, along with a thorough performance evaluation and discussion. Finally, Section 4.6 draws the key conclusions from this chapter.

4.2 Related Work

This section provides an overview of the existing work on uplink GF URLLC, focusing specifically on K-Rep scheme, adaptive K-Rep control, and site diversity reception.

4.2.1 *K*-Repetition and Adaptive *K*-Repetition Control

The K-repetition transmission (K-Rep) scheme is a technique used in wireless communication to improve the reliability of data transmission from UE to the BS [15,16,69]. In K-Rep, each UE transmits repeatedly the same packet K times, with the BS combining the received packets to improve the reliability of the transmission. The number of repetitions required for each UE is typically fixed [15, 16]. However, the K-Rep essentially increases the number of packet transmissions [23], leading to an increase in the interference at the BS side and energy consumption at the UE side.

Some studies have focused on developing adaptive K-Rep control schemes, which adjust the number of repetitions dynamically based on specific conditions, to improve transmission energy efficiency while maintaining reliability. Prior work, as referenced in [47], proposes an adaptive K-Rep control scheme that minimizes uplink transmission energy consumption while satisfying URLLC requirements for varying traffic conditions and reliability demands. In this scheme, each UE is initially configured with a single repetition ($K = 1$), and additional repetitions are added to UEs whose packet loss probability fails to meet their reliability requirements. The scheme delivers significant energy savings and improved reliability performance. However, the scheme does not consider the potential advantages of site diversity reception, which can improve the reliability of communication by combining signals received from multiple cell sites, potentially providing a more effective solution.

4.2.2 Site diversity reception

Site diversity reception can be achieved by employing the technique of multiple-cell combining [36, 37, 70]. This technique involves the combination of signals received at multiple cell sites in order to enhance the signal-to-interference plus noise ratio (SINR) at the BS, potentially enhancing the communication reliability in the context of 5G NR URLLC. For site diversity reception, multiple cell sites are typically deployed at different locations, with the signals from these cell sites being combined at the BS using a combining technique.

The site diversity reception has been applied to the reactive scheme in GF transmission [71] in order to improve the reliability in 5G URLLC scenarios. According to this research results, site diversity reception system can improve URLLC spectrum efficiency while meeting URLLC requirements when compared to single-cell reception one.

We believe that site diversity reception can be applied to the K-Rep scheme to enhance communication reliability by combining signals received at multiple cell sites. This can potentially reduce the number of packet transmissions in the K-Rep scheme, as the combined signal quality may be sufficient to meet the reliability requirement with fewer repetitions.

4.2.3 Problems with existing works

The adaptive K-Rep control scheme [47] adjusts the number of packet repetitions dynamically based on specific conditions to improve transmission energy efficiency while maintaining reliability. However, it does not take into account the potential benefits of site diversity reception, which can enhance the reliability of communication by combining signals received from multiple cell sites. Since this conventional scheme simply increases the number of repetitions for the UEs with poor channel conditions and high packet loss rates, site diversity reception may be a better approach to enhance the signal quality and improve the reliability of communication for such UEs, rather than simply increasing the number of packet repetitions under single site reception.

However, none of the existing studies have implemented site diversity reception into the K-Rep scheme for the GF URLLC. Therefore, we propose the integration of site diversity reception into the K-Rep scheme and examine its effectiveness in improving the received SINR and enhancing reliability.

4.3 Adaptive *K*-Repetition Transmission with Site Diversity Reception

This section introduces site diversity reception into the K-Rep scheme and proposes two adaptive K-Rep control schemes with the objective of reducing the number of repetitions required in the GF K-Rep system.

4.3.1 Site diversity reception for *K*-Repetition transmission

The implementation of site diversity reception requires the establishment of a set of associated cells for each UE. The UEs initially monitor the reference signal received power (RSRP) from their neighboring cells in the network. Based on the monitored RSRP values, they determine a primary cell (p-cell) with the highest RSRP and establish a connection to it. Subsequently, they select assisting cells (a-cells) based on two distinct proposed schemes, which will be described in detail in the following sections 4.3.2 and 4.3.2.

The baseband unit (BBU) is responsible for combining signals from the associated cells, including p-cell and a-cells, via the optical fiber fronthaul in cloud radio access network (C-RAN) architecture [73]. Assuming perfect combining using chase combining (CC) with maximum ratio combining (MRC) [74], the MRC can employ a linear summation approach to combine the signals. The received SINR $\psi_{i,j}^{k}$ at the j-th associated cell of the i-th UE during its k-th repeated transmission in the K-Rep can be written as:

$$\psi_{i,j}^{k} = \frac{P_{i,j}^{k}}{I_{j}^{k} + \sigma_{j}^{2}} \quad , \tag{4.1}$$

where $P_{i,j}^{k}$ donates the received power at the j-th associated cell from the i-th UE at the k-th repeated transmission, I_{j}^{k} donates the total interference at the j-th associated cell, and σ_{j}^{2} is the total noise power received by the j-th associated cell. The SINR γ_{i}^{k} ($k > 1$) achieved after combining during the k-th transmission for the i-th UE can be mathematically expressed as:

$$\gamma_{i}^{k} = \gamma_{i}^{k-1} + \sum_{j=1}^{N_{\text{ac\_cell}}^{i}} \psi_{i,j}^{k} \quad , \tag{4.2}$$

where $N_{\text{ac\_cell}}^{i}$ denotes the number of associated cells of the i-th UE, while $\gamma_{i}^{0} = 0$. The combined SINR γ_{i}^{k} at the k-th repeated transmission for the i-th UE encompasses the combined SINR γ_{i}^{k-1} obtained from the previous repeated transmission.

Figure 4.1 depicts the site diversity reception system employed in the K-Rep scheme. In this scheme, the UE 1 transmits the packet to its associated cells for K consecutive repetitions ($K = 2$ in Figure 4.1), and the signals received at each of these cells being

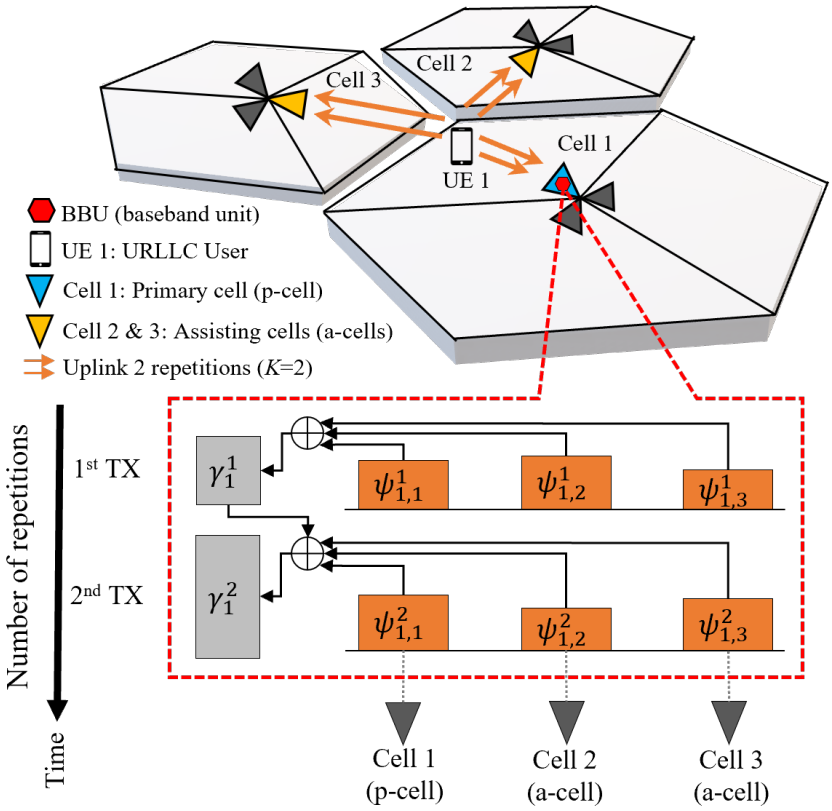

Figure 4.1: Site diversity reception applied to K-Repetition scheme.

combined after each repetition. The signal combining of the signals received at multiple cells enhances the SINR compared to single-cell reception, thereby increasing the reliability of packet transmissions. This advantage of multi-cell reception results in a significant improvement in the overall performance of the system.

4.3.2 Adaptive *K*-Repetition control schemes

In the normal K-Rep scheme, all the UEs employ the same number of repetitions, even though they may not necessarily transmit packets with the same number of repetitions to satisfy the URLLC requirements in the system with the site diversity reception. To achieve the reduction in the number of packet transmissions, we propose two adaptive K-Rep control schemes, specifically referred to as adaptive K-Rep control schemes I and II. The two schemes are differentiated by their selection mechanism for the associated cells and the definition of thresholds for selecting the number of repetitions for each UE, which will be explained in detail in the following section.

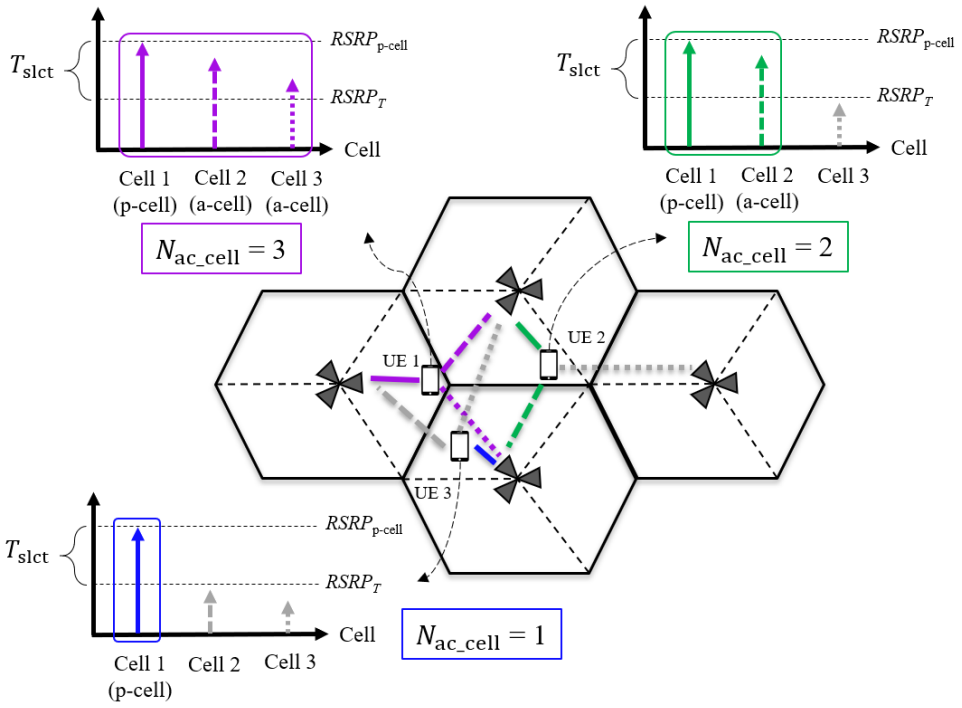

Figure 4.2: Associated cells for the proposed adaptive K-Repetition control scheme I.

Adaptive K-Repetition control scheme I

We propose an adaptive K-Rep control scheme I, which adjusts the number of repetitions based on the number of the associated cells $N_{\text{ac\_cell}}$ for the UE.

In the proposed adaptive K-Rep control scheme I, the UEs select assisting cells (a-cells) whose RSRP is not less than T_{slct} [dB] below that of the p-cell. T_{slct} is defined as the threshold for selecting assisting cells, referred to as the selection threshold. Under this selection mechanism for the associated cells, the number of associated cells $N_{\text{ac\_cell}}$ for each UE varies depending on its location and the selection threshold T_{slct}.

As illustrated in Figure 4.2, the UEs located near the cell edge have a large $N_{\text{ac\_cell}}$ as it has many surrounding cells that provide almost the same RSRP level and satisfy the selection threshold T_{slct} to become an assisting cell. Conversely, the UEs located near the cell center have a small $N_{\text{ac\_cell}}$ due to the surrounding cells with low RSRP that cannot meet the T_{slct} threshold. The different $N_{\text{ac\_cell}}$ depending on UE location results in different diversity gains under site diversity reception. For example, UEs with larger $N_{\text{ac\_cell}}$ and higher diversity gains can improve signal quality through site diversity reception and require fewer repetitions. However, UEs with a single associated cell and no diversity gain require more repetitions to ensure the requirement for reliability. As a result, the proposed adaptive K-Rep control scheme I varies the number of repetitions for each UE depending on its $N_{\text{ac\_cell}}$.

Table 4.1: Number of repetitions for adaptive K-Repetition control scheme I.

Number of associated cells $N_{\mathbf{ac\_cell}}$	>3	2	1
Site diversity gain	Large	Small	No
Number of repetitions $K_{\mathbf{adp}}$	2	3	4

Table 4.1 summarizes the number of repetitions K_{adp} assigned to UEs with different $N_{\text{ac\_cell}}$ under the proposed scheme I. For example, the UE with $N_{\text{ac\_cell}}$ of 3 (UE 1 in Figure 4.2), which obtains a large site diversity gain, is assigned 2 repetitions, while the UE with $N_{\text{ac\_cell}}$ of 2 (UE 2 in Figure 4.2) and a small site diversity gain, is set to 3 repetitions. In contrast, for UEs with only a p-cell and no site diversity gain ($N_{\text{ac\_cell}} = 1$; UE 3 in Figure 4.2), the number of repetitions K_{adp} is set to 4 to achieve significant diversity gain through repeated transmission.

Figure 4.3 illustrates the adaptive K-Rep control scheme I, which adjusts the number of repetitions depending on the $N_{\text{ac\_cell}}$. The UE 1 (where $N_{\text{ac\_cell}} = 3$ and $K_{\text{adp}} = 2$) obtains the combined SINR from 6 distinct signals, including 3 signals from 3 associated cells in the 1st repetition and 3 additional signals from the 2nd repetition. On the other hand, for the UE 3 with $N_{\text{ac\_cell}} = 1$ and $K_{\text{adp}} = 4$, the combined SINR comes from 4 different signals, including 1 signal from a single associated cell for each repetition of 4 repetitions.

Adaptive *K*-Repetition control scheme II

In this section, we additionally propose an adaptive K-Rep control scheme II that utilizes the advantages of site diversity reception for a fixed number of associated cells (constant $N_{\text{ac\_cell}}$) for all UEs. As opposed to the proposed scheme I in the previous section which each UE has a different $N_{\text{ac\_cell}}$, the proposed adaptive K-Rep control scheme II offers greater potential to increase diversity gain and enhance signal quality, leading to improvement of the overall transmission performance. Figure 4.4 illustrates that all UEs are assigned a fixed number of associated cells ($N_{\text{ac\_cell}} = 3$ in Figure 4.4).

For adaptive K-Rep control, adjusting the number of repetitions based on $N_{\text{ac\_cell}}$ cannot be employed with the proposed adaptive K-Rep control scheme II due to its constant $N_{\text{ac\_cell}}$. Consequently, the variation in the RSRP levels received at the UEs from the associated cells is introduced to adjust the number of repetitions in the proposed scheme II. The variation in the RSRP levels for the i-th UE is defined as the level difference between the RSRP of its p-cell and those of its a-cells, which is shown as d_u^i in

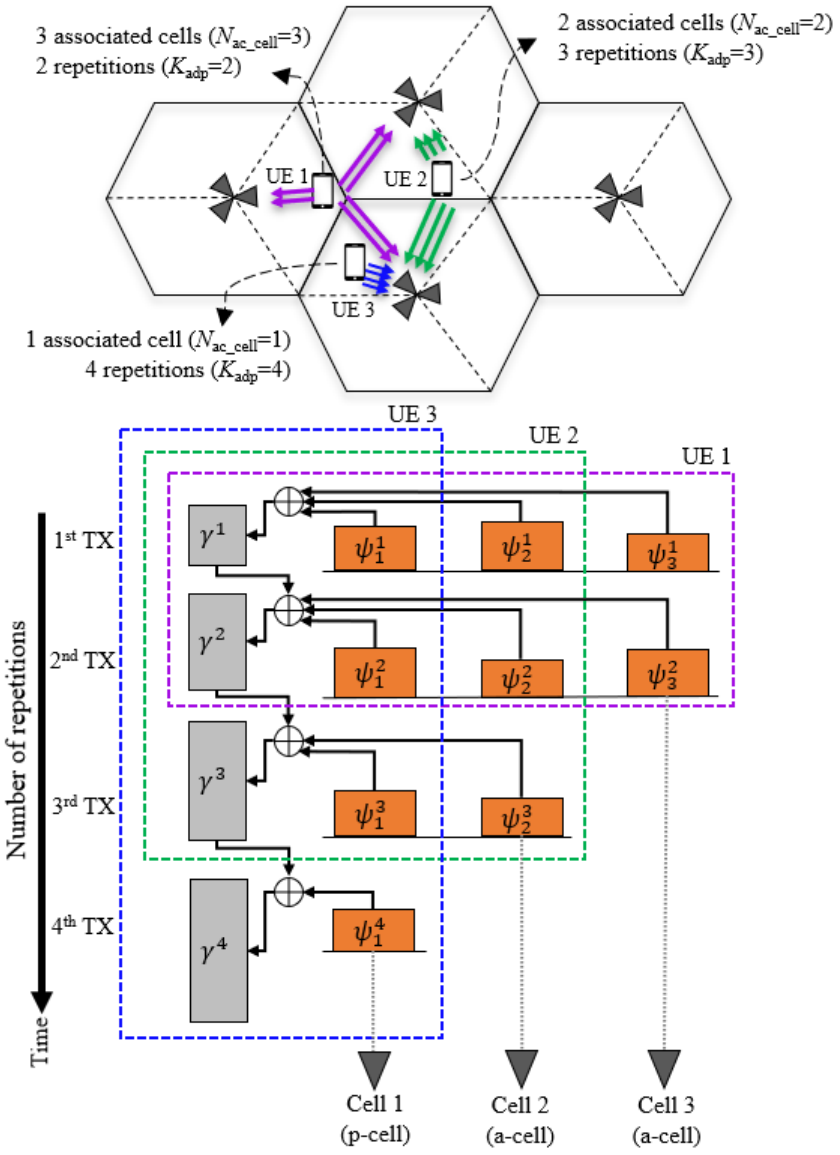

Figure 4.3: Proposed adaptive K-Repetition control scheme I.

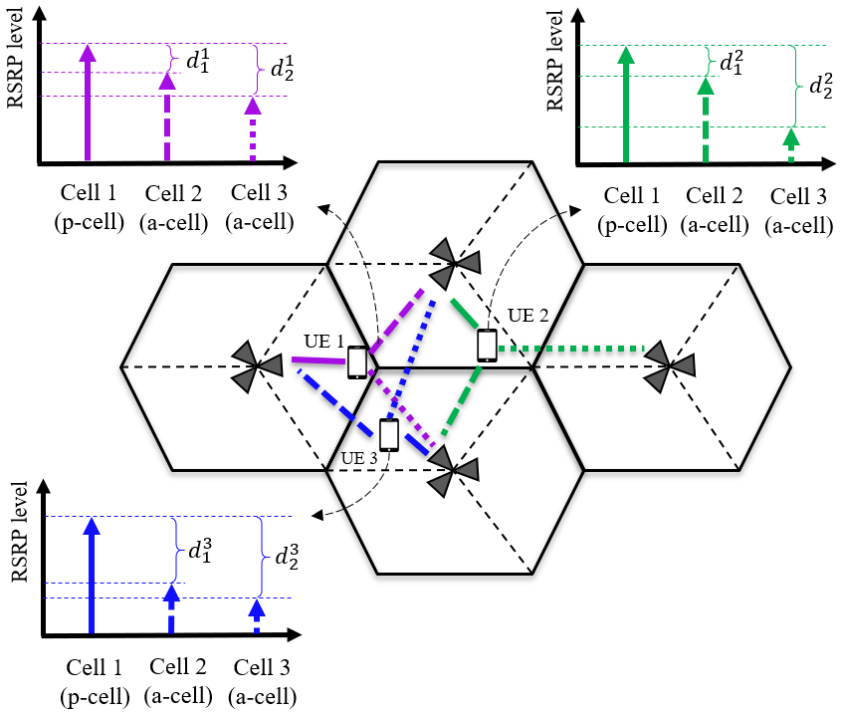

Figure 4.4: Associated cells for the proposed adaptive K-Repetition control scheme II.

Figure 4.4. The total variation d^i [dB] in RSRP levels for the i-th UE can be given as:

$$d^i = \sum_{u=1}^{N_{\text{ac\_cell}}-1} d_u^i \quad . \tag{4.3}$$

The adaptive K-Rep control scheme II configures two thresholds: the lower and upper ones, T_{low} and T_{up} for the total variation d^i in RSRP levels to adjust the number of repetitions K_{adp}. The lower threshold T_{low} indicates the boundary between 2 and 3 repetitions ($K_{\text{adp}} = 2$ and 3), whereas the upper one T_{up} specifies that between 3 and 4 repetitions ($K_{\text{adp}} = 3$ and 4). For instance, for the UE 1 with a total variation d^1 of 30 dB and the T_{low} and T_{up} of 20 dB and 70 dB respectively, the number of repetitions K_{adp} for the UE 1 is set to $K_{\text{adp}} = 3$. Therefore, the K_{adp} assigned to each UE in the proposed scheme II varies depending on the lower and upper thresholds, which would affect the overall system performance.

Figure 4.5 demonstrates the proposed adaptive K-Rep control scheme II that all UEs have the same $N_{\text{ac\_cell}}$ ($N_{\text{ac\_cell}} = 3$ in Figure 4.5), while the number of repetitions varies for the UEs depending on their location. The UE 1 with $N_{\text{ac\_cell}} = 3$ and $K_{\text{adp}} = 2$ obtains the combined SINR from 6 distinct signals, including 3 signals from 3 associated cells in the 1st repetition and 3 additional signals in the 2nd repetition. In contrast, for the UE 3 with $N_{\text{ac\_cell}} = 3$ and $K_{\text{adp}} = 4$, the combined SINR comes from 12 different signals, including 4 signals from 3 associated cells for each repetition of 4 repetitions.

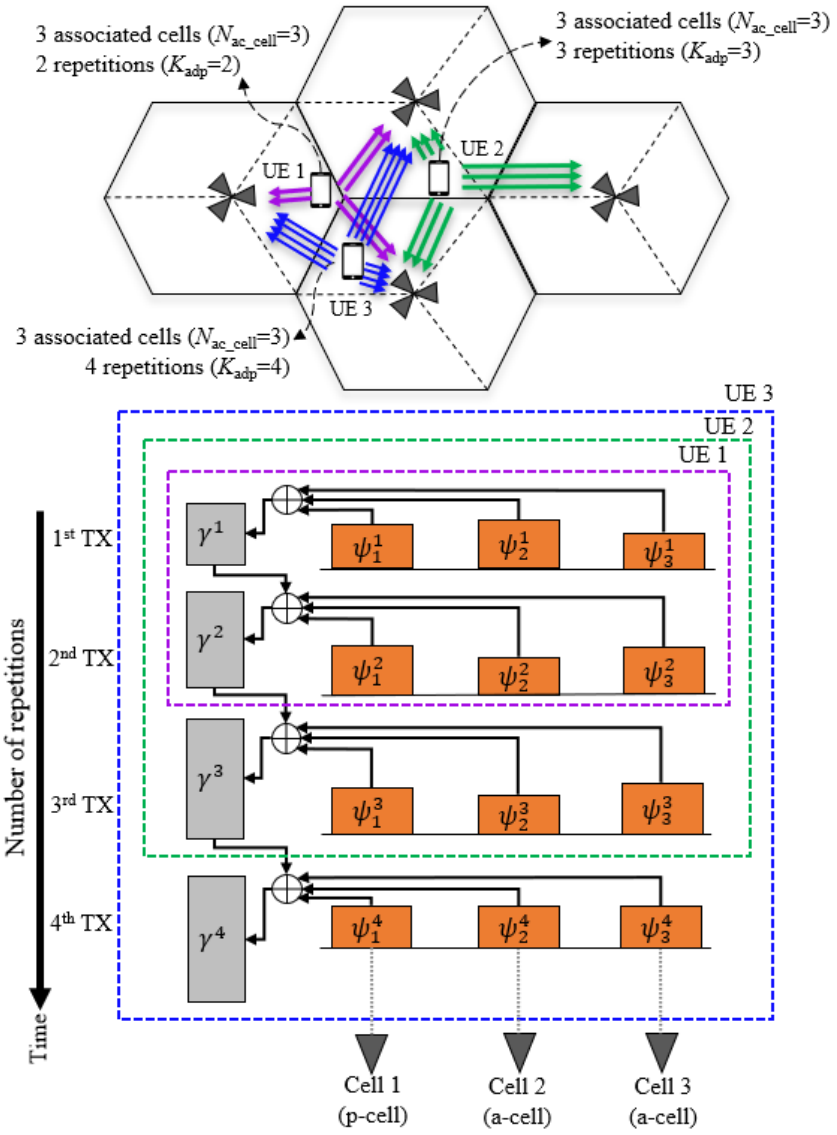

Figure 4.5: Proposed adaptive K-Repetition control scheme II.

The reduction in the average number of repetitions per packet achieved by the proposed adaptive K-Rep control schemes I and II contributes to a decrease in uplink transmission energy consumption, conserving battery resources for IoT URLLC UEs. Furthermore, the proposed scheme II would have larger potential to improve reliability when compared to the proposed scheme I due to the increased number of combined signals. Nevertheless, an increase in the number of combined signals leads to a rise in the processing load on the network side, which will be discussed in the performance evaluation section.

It is important to note that the exchange of control information will occur during the UE association phase. During this association phase, the p-cell provides a preliminary resource assignment, following which the p-cell communicates the specified number of repetitions to the assigned UE.

4.4 Evaluation Methodology

We employ computer simulation at the system level for performance evaluation. As shown in [35], the assumptions for the evaluation are consistent with the URLLC evaluation scenario for 5G NR. Table 4.2 summarizes the parameter settings used in the evaluation.

4.4.1 Network model

The network model includes 21 cells distributed across 7 sites, each with 3 sectors, under regular hexagonal urban macro (UMa) layout with the inter-site distance (ISD) of 500 [m], as shown in Figure 4.6.

The employment of optical fiber as a front-haul transport in C-RAN architecture for 5G NR networks is widely acknowledged to offer exceptionally low latency, typically within a few μs [73].

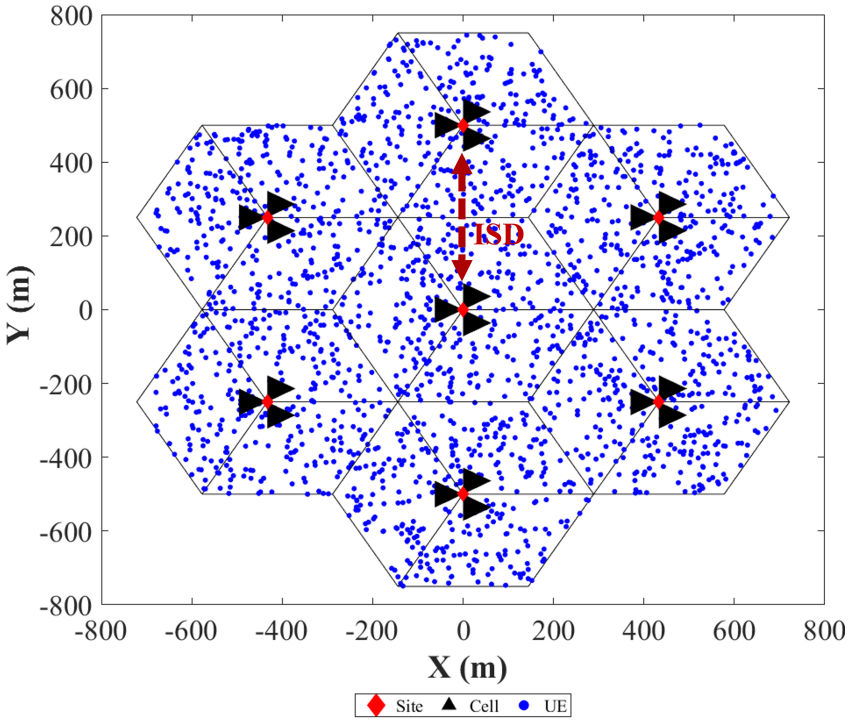

Figure 4.6: Network layout.

4.4.2 Communication channel model

The shared uplink channel contains 48 resource blocks (RBs) in 10 [MHz] bandwidth and operates at carrier frequency of 4 [GHz]. The shared channel is accessible for GF transmission in all subframes. Based on the 5G NR numerology [75], the sub-carrier

spacing (SCS) is 15 [kHz] with 12 sub-carriers per RB. A mini-slot contains 2 OFDM symbols, giving a transmission time interval (TTI) length t_{TTI} of 0.143 [ms].

For signal propagation in radio channel, the 3GPP 3D UMa model [35] is used as the basis for the path loss model. An independent fading coefficient is assumed between two consecutive transmission repetitions, following an exponential distribution, for Rayleigh fading fluctuation. Although the receiver at UEs generally employs some channel estimation technique under the fading environment, we do not consider any channel estimation because we evaluate overall system level performance rather than physical layer performance.

We employ chase combining (CC) [74] as the packet combining scheme at the BS, assuming perfect combining. Importantly, all schemes compared in our study employ the same packet combining. Thus, the choice of packet combining scheme does not significantly affect the performance comparison in our evaluation. Packet reception at the BS relies on the combined SINR γ_i^K of the data packet being received. For a successful packet reception, we employ the decision manner based on the packet error rate (PER) associated with the SINR of the received packet, assuming QPSK modulation under the successive interference cancellation (SIC).

4.4.3 Power control model

The radio channel is affected by path loss and Rayleigh fading. To compensate for the path loss, URLLC UEs employ fractional open-loop power control with a path loss compensation factor $\alpha = 0.8$ and a target received power $P_0 = -80$ [dBm] [39].

4.4.4 Traffic model

Each UE generates data packets that have the same duration as one TTI, and the packets arrive at each UE, following a Poisson process with an average arrival rate λ of 5 packets per second. The number of UEs N_{UE} is set in the range from 40 to 400 [/cell].

4.4.5 Latency model

We define the total latency of K-Rep process as t_K [ms], which is defined as:

$$t_K = K \cdot t_{\mathrm{tx}} + t_{\mathrm{align}} + t_{\mathrm{buf}} + t_{\mathrm{proc}} \quad , \tag{4.4}$$

where K is the number of repetitions, t_{tx} is the packet transmission time for one data packet, which is assumed t_{TTI}.

The frame alignment delay t_{align} is given as a uniformly distributed random variable ranging from 0 to t_{TTI}. The buffering delay t_{buf} at the UE with the preceding packet is different for each packet. Note that the UE transmits only a single data packet per TTI,

and any subsequent data packet transmission has to wait until the previous data packet has been transmitted with its K repetitions.

The processing time of the BS, denoted as t_{proc}, includes the time for signal transfer from the associated cells and the signal combining process. In order to simplify simulations at the system level, the time for transferring signals from each cell to the BBU via fiber front-haul transport is assumed to be negligible. Then, we assume that t_{proc} is equal to t_{TTI}.

4.4.6 Transmission energy consumption model

The transmission energy consumption E_{tx} [J/packet] per packet can be assumed as [47]:

$$E_{\text{tx}} = \frac{P_{\text{tx}} \cdot t_{\text{TTI}} \cdot K}{\eta} \quad , \tag{4.5}$$

where P_{tx} donates the transmit power of the UE and η denotes the efficiency of the transmit power amplifier.

4.4.7 Simulation methodology

To ensure statistically significant performance in the 10^{-5} quantile, the performance evaluation is conducted through Monte Carlo simulation by averaging over 10^7 packet transmissions.

Table 4.2: Simulation assumptions.

Parameters	Assumption
Network layout	Hexagonal grid with 21 cells distributed at 7 sites, 500 m inter-site distance (ISD)
UE distribution	Uniformly distributed outdoor
Carrier	4 GHz Carrier frequency
Bandwidth	10 MHz Bandwidth
PHY numerology	15 kHz sub-carrier spacing, 12 sub-carriers/RB, 2 OFDM symbols (mini-slot) per TTI
Uplink shared channel	48 RB
Channel model	3D UMa path loss [35], Rayleigh fading
Thermal noise density	-174 dBm/Hz
Power control	Open loop power control (OLPC) with $\alpha = 0.8$ and $P_0 = -80$ dBm
Traffic model	1 TTI packet duration with the size of 32 bytes, Poisson arrival with $\lambda = 5$ PPS per UE
Number of UEs	40-400 UEs per cell
Combining	Chase-combining (MRC)
Front-haul transport	Optical fiber [73]
Efficiency of TX power amplifier	$\eta = 0.8$ [47]

4.5 Evaluation Results

4.5.1 Performance evaluation of adaptive *K*-Repetition control scheme I

We compare the performance under site diversity reception of the proposed adaptive K-Rep control scheme I to that of the K-Rep scheme with a constant number of repetitions for all UEs employing the same number of associated cells $N_{\text{ac\_cell}}$ as the proposed adaptive K-Rep control scheme I, referred to as constant K-Rep scheme I. The performances are represented by the packet loss probability and the transmission energy consumption at the UE side.

The packet loss probability at latency of 1 ms is shown in Figure 4.7 for varying selection threshold T_{slct} for selecting assisting cells. Although the constant K-Rep scheme I with any repetitions continuously improves performance with the T_{slct}, primarily due to an increase in the number of associated cells $N_{\text{ac\_cell}}$, the proposed scheme I outperforms any constant K-Rep scheme for the T_{slct} below approximately 15 dB. Moreover, at $T_{\text{slct}} \approx$

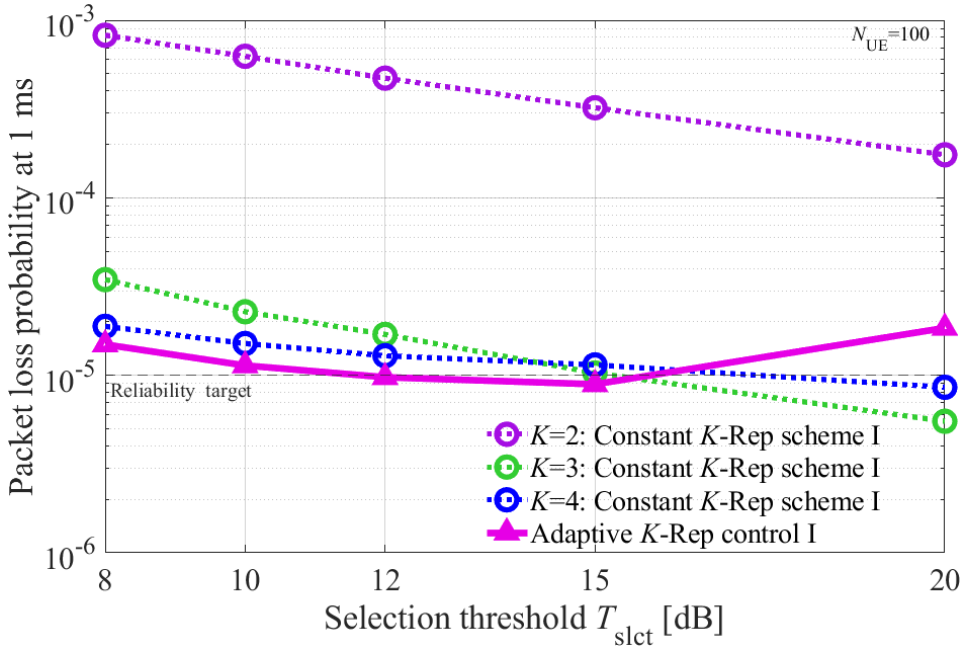

Figure 4.7: Packet loss probability at 1 ms for varying selection threshold T_{slct} in the proposed adaptive K-Rep control scheme I.

15 dB, the proposed scheme I achieves the lowest packet loss probability and can satisfy URLLC target for latency of 1 ms and 10^{-5} reliability.

Figure 4.8 depicts the transmission energy consumption E_{tx} per packet for the proposed scheme I and the constant K-Rep scheme I. The transmission energy consumption for each constant K-Rep scheme I ($K = 2$, $K = 3$, and $K = 4$) remains constant across all the T_{slct} due to the fixed number of repetitions for all UEs. Noticeably, our proposed scheme I significantly reduces transmission energy consumption for larger T_{slct} compared with the constant K-Rep scheme I for $K = 3$ and $K = 4$. This is because the larger T_{slct} causes an increase in $N_{\text{ac\_cell}}$ and a decrease in the number of repetitions K_{adp}, resulting in decreased energy consumption. Compared to the constant K-Rep scheme I for $K = 3$ and $K = 4$, the proposed scheme I with T_{slct} of 15 dB exhibits a decrease in energy consumption E_{tx} of 2.37 μJ/packet (from 8.38 to 6.01; E_{tx} ratio of the constant K-Rep scheme I to the proposed scheme I is 1.39) and 5.16 μJ/packet (from 11.17 to 6.01; E_{tx} ratio is 1.86), respectively. As a result, applying the proposed scheme I extends battery life by 1.39 and 1.86 times when compared to the constant K-Rep scheme I for $K = 3$ and $K = 4$, respectively.

Figure 4.9 presents the complementary cumulative distribution function (CCDF) of the latency for both the proposed adaptive K-Rep control scheme I and constant K-Rep scheme I, under the condition of $T_{\text{slct}} = 15$ dB. The result shows that only the proposed scheme I can satisfy the URLLC requirements.

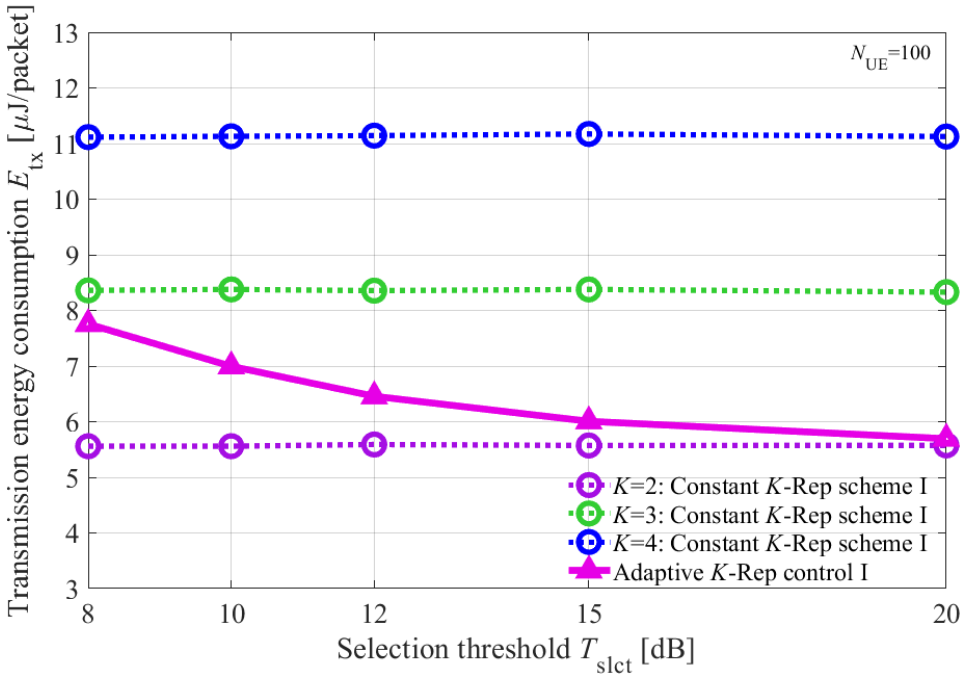

Figure 4.8: Transmission energy consumption for varying selection threshold T_{slct} in the proposed adaptive K-Rep control scheme I.

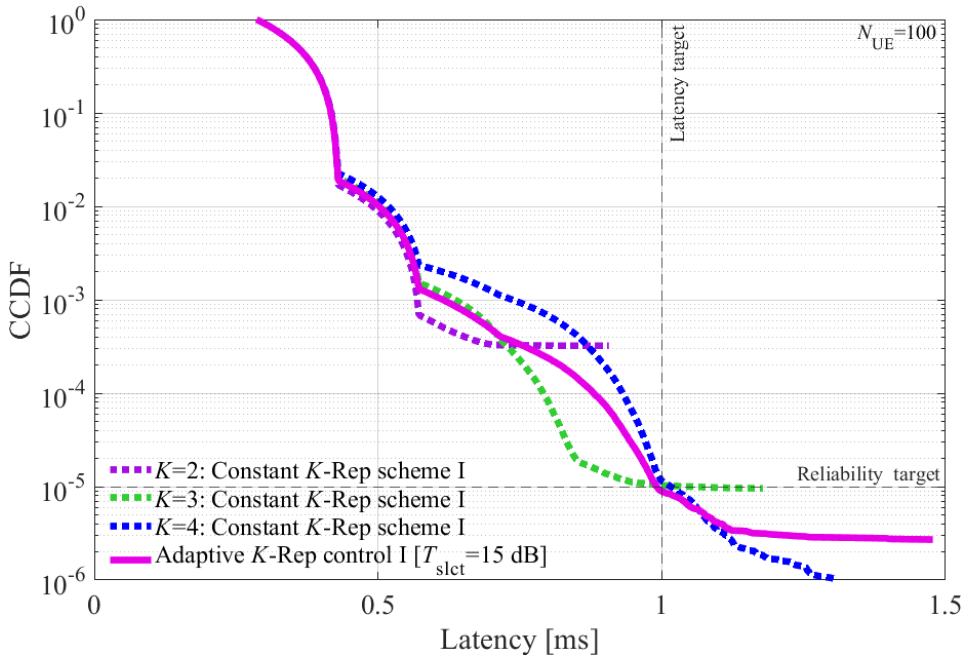

Figure 4.9: CCDF of latency for the proposed adaptive K-Rep control scheme I.

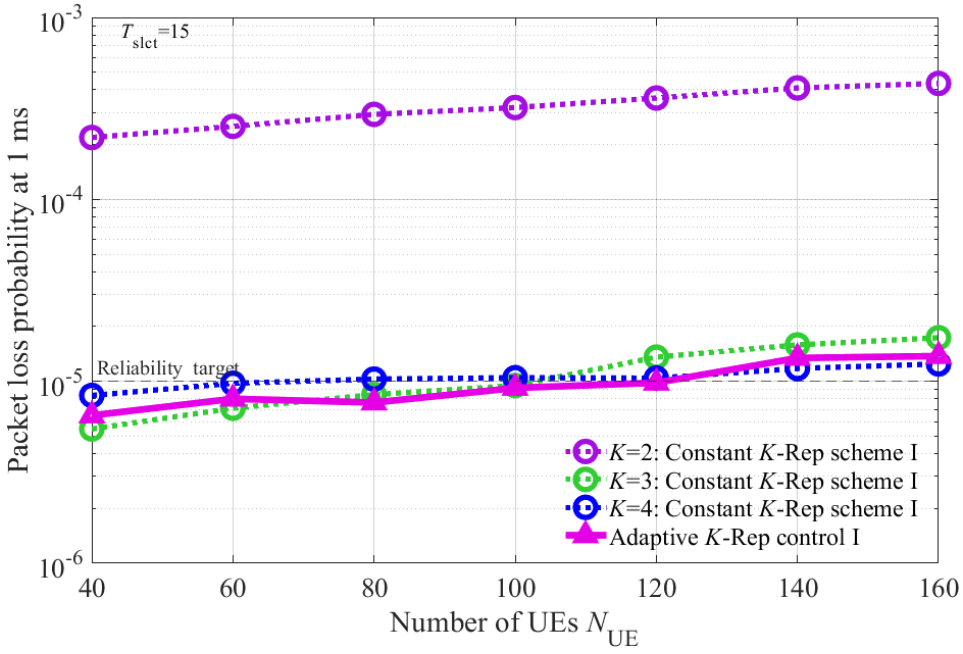

Figure 4.10: Packet loss probability at 1 ms for varying number of UEs N_{UE} in the proposed adaptive K-Rep control scheme I.

Figure 4.10 illustrates the packet loss probability at a latency of 1 ms for varying the number of UEs N_{UE}, under a selection threshold T_{slct} of 15 dB. Varying the number of UEs per cell, instead of the packet arrival rate, has a large impact on the congestion and interference levels within the network. We can observe how the system handles with increasing user density, which is a critical aspect of evaluating its performance. The results demonstrate that the proposed scheme I consistently achieves a packet loss probability of 10^{-5} for N_{UE} values up to approximately 120. Furthermore, although the constant K-Rep scheme I with $K = 3$ and $K = 4$ also meets URLLC targets for cases with low traffic loads (corresponding to smaller N_{UE}), the proposed adaptive K-Rep control scheme can extend the network capacity satisfying the URLLC requirements.

4.5.2 Performance evaluation of adaptive *K*-Repetition control scheme II

We present performance evaluation under site diversity reception for the proposed adaptive K-Rep control scheme II with the number of associated cells $N_{\mathrm{ac\_cell}}$ of 3, in comparison to both the proposed adaptive K-Rep control scheme I with the optimal T_{slct} of 15 dB and the constant K-Rep scheme with the same $N_{\mathrm{ac\_cell}}$ as the proposed scheme II, referred to as constant K-Rep scheme II. In the evaluation, the average number of combined signals N_{cbn} at the BS is also evaluated to assess the processing load at the network side. Since the N_{cbn} affects the processing load at the network side, it is important to consider the N_{cbn} to prevent network overload and ensure optimal performance.

Table 4.3: Total variation in RSRP levels d^i.

Percentage in CDF [%]	0	10	20	30	40	50	60	70	80	90	100
Total variation d^i [dB]	0.0	7.8	10.9	14.1	17.9	22.1	27.1	33.3	41.6	54.6	104.5

In order to determine the values for the lower and upper thresholds T_{low} and T_{up}, we obtain the cumulative distribution function (CDF) of the total variation d^i in RSRP levels for all UEs and then the value of d^i associated with every 10% point of the CDF, as presented in Table 4.3. During the performance evaluation, we show values of the lower and upper thresholds utilizing the percentage values specified in the aforementioned table.

Figure 4.11 illustrates the packet loss probability at latency of 1 ms for varying the lower and upper thresholds in the proposed scheme II. All the constant K-Rep scheme II and the proposed scheme I maintain a consistent packet loss probability throughout all regions as the thresholds T_{low} and T_{up} do not affect their performance. The proposed scheme I can achieve almost the same performance as the constant K-Rep scheme II with $K = 4$. The result indicates that for the proposed scheme II, most of the regions with varying lower and upper thresholds can meet the target requirements of 1 ms latency and reliability of 10^{-5}. Significantly, the proposed scheme II can optimize the packet loss probability for the lower threshold T_{low} of 20 and the upper one T_{up} of 100, and outperforms the constant K-Rep scheme II with $K = 3$, which exhibits the most superior performance.

Figure 4.12 shows the transmission energy consumption E_{tx} for varying lower and upper thresholds in the proposed scheme II. The result indicates that the proposed adaptive K-Rep control scheme II can reduce transmission energy consumption at almost all regions with varying lower and upper thresholds, compared to the constant K-Rep scheme II for $K = 3$ and $K = 4$. Furthermore, the reduction in energy consumption becomes greater for larger threshold settings. In addition, for the $T_{\text{low}} = 50$ and $T_{\text{up}} = 100$, the proposed scheme II demonstrates almost the same energy consumption while clearly providing a significant improvement in packet loss probability, compared with the proposed scheme I. The proposed scheme II can significantly decrease energy consumption at the optimal parameter setting for packet loss probability with T_{low} of 20 and T_{up} of 100 as shown in Figure 4.11. This improvement is particularly noticeable when compared to the constant K-Rep scheme with $K = 3$ and $K = 4$, with an improvement rate of 14.45% and 35.84%, respectively.

Figure 4.13 shows the average number of combined signals N_{cbn} at the BS for varying the lower and upper thresholds for the proposed scheme II. It can be observed that

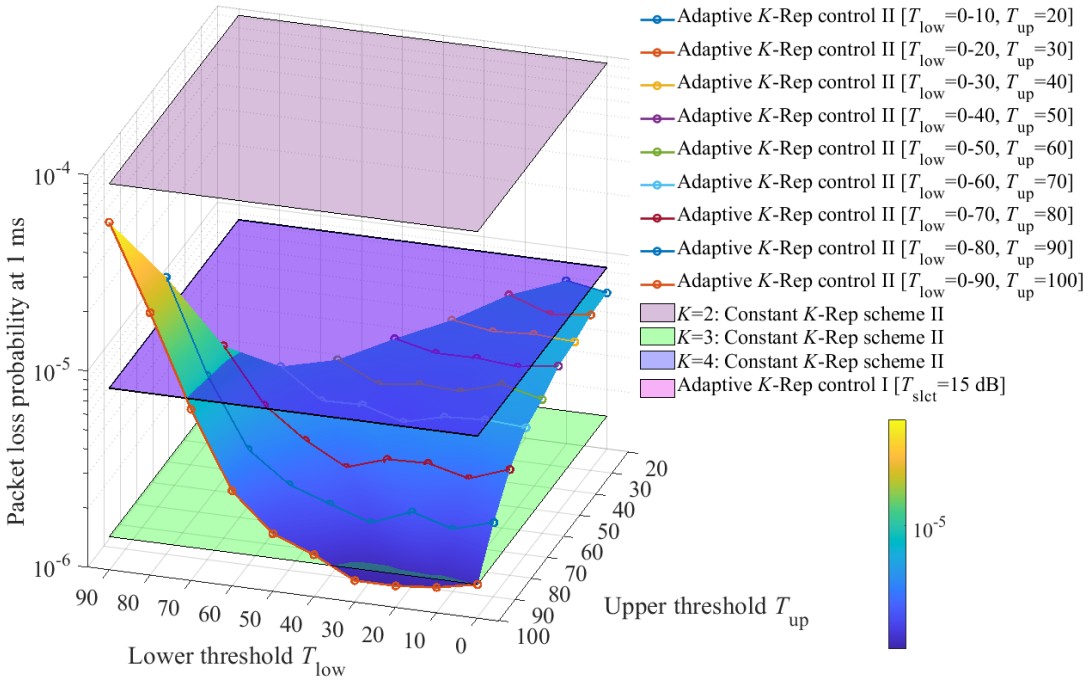

Figure 4.11: Packet loss probability at 1 ms for varying lower and upper thresholds in the proposed adaptive K-Rep control scheme II.

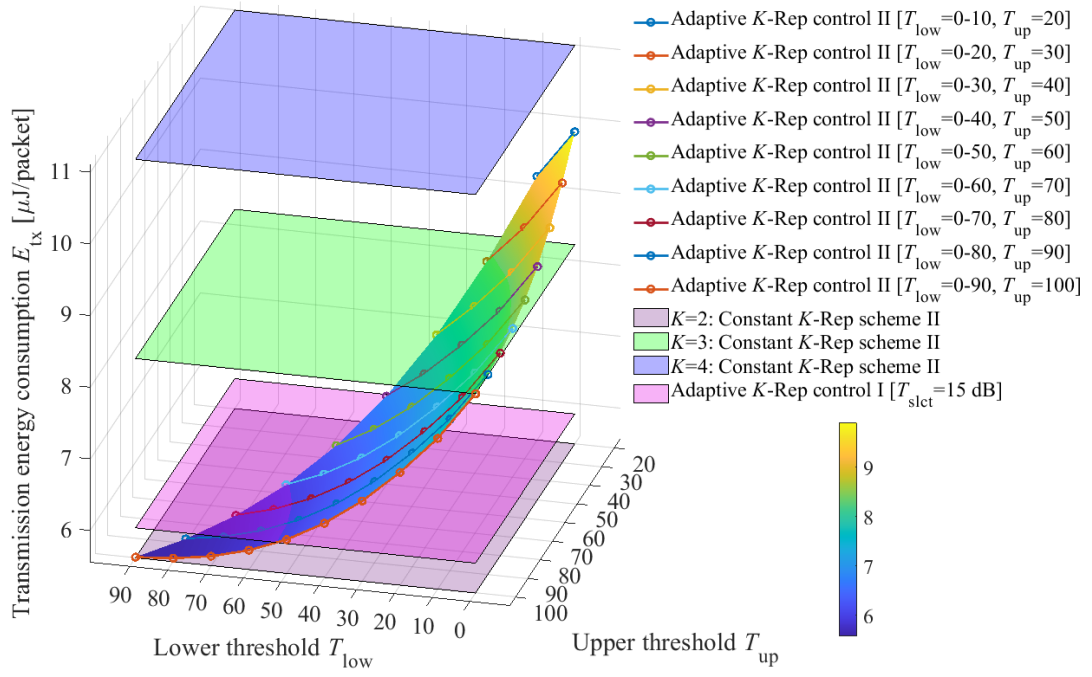

Figure 4.12: Transmission energy consumption for varying lower and upper thresholds in the proposed adaptive K-Rep control scheme II.

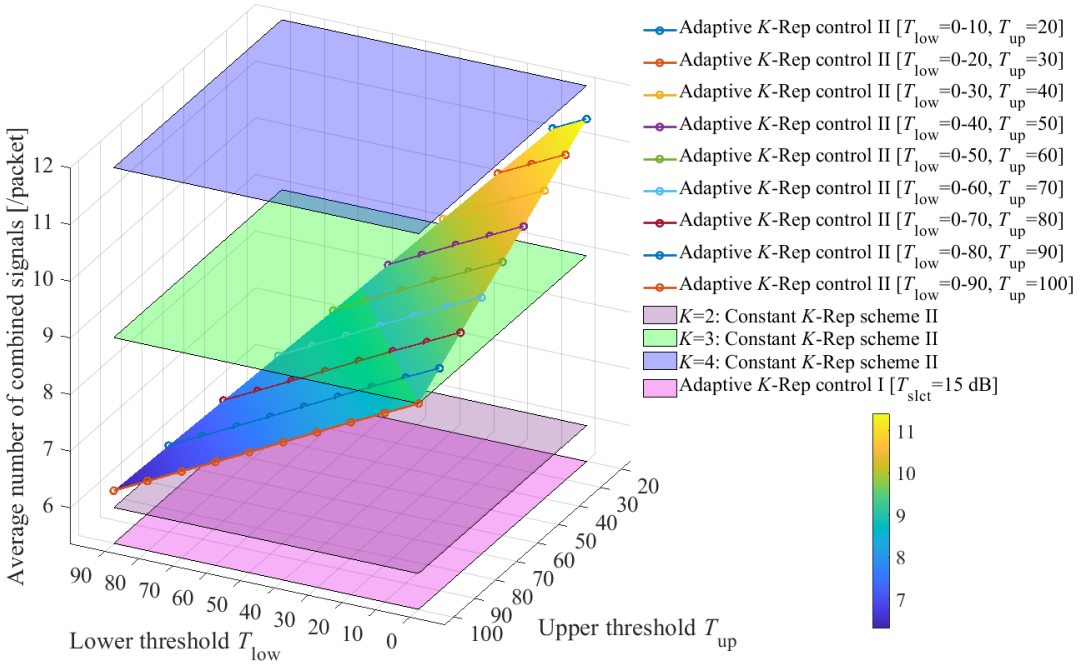

Figure 4.13: Average number of combined signals for varying lower and upper thresholds in the proposed adaptive K-Rep control scheme II.

the proposed scheme I requires the smallest number of combined signals as the average number of associated cells $N_{\text{ac\_cell}}$ is 2.29, unlike other schemes employing a fixed $N_{\text{ac\_cell}}$ of 3. For the lower and upper thresholds of 70 and 100, the proposed scheme II involves a higher number of combined signals, amounting to a 30% increase in the processing load at the network side while demonstrating almost the same packet loss probability (as shown in Figure 4.11) and reduced transmission energy consumption (from Figure 4.12), compared with the proposed scheme I.

Figure 4.14 illustrates CCDF of the latency for the proposed scheme II with the optimal threshold setting of $T_{\text{low}} = 20$ and $T_{\text{up}} = 100$ for packet loss probability. The result shows that the proposed scheme II outperforms other schemes in terms of reliability. We observe that the constant K-Rep scheme II with $K = 3$ almost approaches the same performance, however, it requires 3 repetitions for all the UEs, leading to higher energy consumption E_{tx} at UE side (from Figure 4.12) and larger number of combined signals at the network side (from Figure 4.13), compared with those in the proposed scheme II. At reliability of 10^{-5}, the proposed scheme remarkably improves the latency compared with the proposed scheme I and constant K-Rep scheme with $K = 4$ to 15.01% and 15.44%, respectively.

Figure 4.15 illustrates the packet loss probability at a latency of 1 ms for varying N_{UE}. This result is under the optimal threshold settings of $T_{\text{low}} = 20$ and $T_{\text{up}} = 100$ for the proposed scheme II, as shown in Figure 4.11. Under higher traffic conditions, the

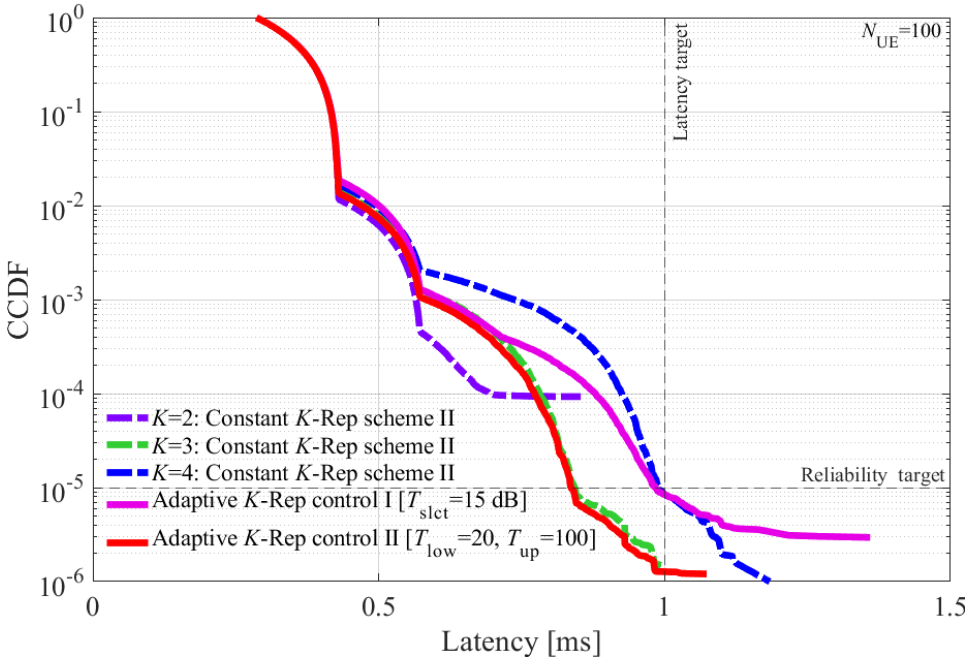

Figure 4.14: CCDF of latency for the proposed adaptive K-Rep control scheme II.

result indicates that the proposed scheme II achieves a packet loss probability of 10^{-5} for N_{UE} values up to around 350. Moreover, the constant K-Rep scheme II with $K = 3$ demonstrates comparable performance to the proposed scheme II. However, the constant K-Rep scheme II with $K = 3$ consumes a higher E_{tx} compared to the proposed scheme II. Additionally, the constant K-Rep scheme $K = 4$ meets URLLC targets for cases with only low traffic loads.

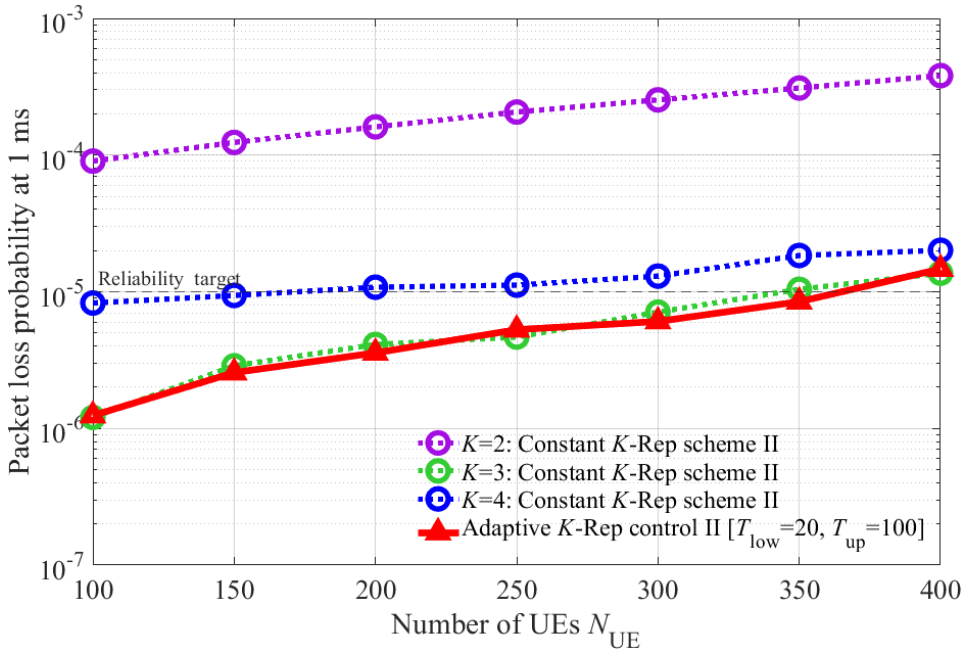

Figure 4.15: Packet loss probability at 1 ms for varying number of UEs N_{UE} in the proposed adaptive K-Rep control scheme II.

4.6 Conclusion

This chapter employs the site diversity reception to the K-Rep scheme for GF URLLC communications and proposes its two innovative adaptive K-Rep control schemes to improve signal quality and reduce the number of repetitions. The evaluation results demonstrate that the proposed adaptive K-Rep control schemes satisfy the URLLC requirements while reducing energy consumption. Compared to the conventional K-Rep schemes, the proposed schemes achieve a significant improvement in reliability and a reduction in transmission energy consumption, enhancing energy efficiency at IoT UE side.

In future work, we aim to develop an analytical model that provides the behavior and performance of the proposed system, validating its high reliability and low latency capabilities. This model will estimate optimal threshold values for system parameters, offering practical solutions by providing equations to determine suitable threshold values with significantly reducing computational complexity, compared with exhaustive search methods. Additionally, further exploration will be conducted to investigate the trade-off between reliability and processing load on the network side.

We have identified an issue that is increasing power consumption on the network side due to the combination of multiple signals. To address this issue, we need to conduct further investigation and make necessary adjustments.

Chapter 5

Conclusion

The 5G NR cellular network aims to provide eMBB with necessitating high data rates and URLLC services with low-latency and high-reliability transmissions. The rapidly increasing interest from various verticals for 5G NR network. Energy efficiency is one of the key performance indicators in 5G NR networks targeted to support diversified use cases. The integration of several technologies into 5G networks to meet diverse user needs will result in a complex network design, leading to increased energy consumption. Therefore, the significance of energy efficiency is most important.

One promising approach to address eMBB challenges involves the deployment of HetNets with MBSs and SBSs. While HetNets enhance coverage and support eMBB services, the dense implementation of SBSs within MBS coverage can increase power consumption, potentially reducing energy efficiency. Therefore, various techniques for reducing power consumption and enhancing energy efficiency in 5G NR cellular networks have been suggested. Despite the fact that these techniques can reduce power consumption and improve energy efficiency, they may lead to a degradation in system throughput when compared to the no-sleep control system.

To solve this issue, this thesis proposes an enhanced SBS sleep control algorithm based on energy efficiency. The proposed sleep control introduces a 2-phase control procedure and its second phase activates additional SBSs from the sleep SBSs to improve the energy efficiency while retaining the system throughput. Computer simulations demonstrate that this proposed scheme improves energy efficiency by 14.89% while maintaining almost the same system throughput of over 99% when compared with the no-sleep control system. Consequently, the proposed scheme can contribute to providing high capacity green HetNets for eMBB services in 5G NR cellular networks.

The 5G NR network also offers URLLC services with strict latency and reliability requirements. GF transmissions with K-Rep transmission have been introduced to meet URLLC requirements. Due to its repeated operation, the K-Rep scheme significantly increases the number of packet transmissions. Consequently, an excessive increase in packet transmissions causes severe interference at the receiving BS, resulting in degraded reliability. Moreover, the increase in packet transmissions on the K-Rep scheme results

in a significant increase in energy consumption, leading to the early depletion of the battery and a decrease in energy efficiency on the UE side.

To mitigate these challenges, this thesis proposes two adaptive K-Rep control schemes for GF URLLC communications, utilizing site diversity reception to enhance signal quality and reduce energy consumption. The evaluation results demonstrate that the proposed adaptive K-Rep control schemes satisfy the URLLC requirements while reducing energy consumption. Compared to the conventional K-Rep schemes, the proposed schemes achieve a significant improvement in reliability and a reduction in transmission energy consumption, enhancing energy efficiency at IoT UE side.

In summary, the proposed solutions in this thesis address energy efficiency concerns for eMBB services on the network side and URLLC services on the UE side within the dynamic environment of a 5G NR cellular network. Extensive computer simulation results at the system level demonstrate the effectiveness of these solutions in improving the energy efficiency of 5G NR networks.

Bibliography

[1] M. Series, "IMT Vision–Framework and Overall Objectives of the Future Development of IMT for 2020 and Beyond," *Recommendation ITU*, vol. 2083, no. 0, 2015.

[2] A. Gupta and R. K. Jha, "A Survey of 5G Network: Architecture and Emerging Technologies," *IEEE Access*, vol. 3, pp. 1206–1232, 2015.

[3] 3GPP TR 38.913, "Study on Scenarios and Requirements for Next Generation Access Technologies," Technical Report (TR), Mar. 2022.

[4] A. Dogra, R. K. Jha, and S. Jain, "A Survey on Beyond 5G Network With the Advent of 6G: Architecture and Emerging Technologies," *IEEE Access*, vol. 9, pp. 67 512–67 547, 2021.

[5] J. Malmodin and D. Lundén, "The Electricity Consumption and Operational Carbon Emissions of ICT Network Operators 2010-2015," Report from the KTH Centre for Sustainable Communications, 2018.

[6] Ericsson, "5G Estimated to Reach 1.5 Billion Subscriptions in 2024," Ericsson Mobility Report, 2018.

[7] J. Wu, Y. Zhang, M. Zukerman, and E. K.-N. Yung, "Energy-Efficient Base-Stations Sleep-Mode Techniques in Green Cellular Networks: A Survey," *IEEE Communications Surveys Tutorials*, vol. 17, no. 2, pp. 803–826, 2015.

[8] Z. Hasan, H. Boostanimehr, and V. K. Bhargava, "Green Cellular Networks: A Survey, Some Research Issues and Challenges," *IEEE Communications Surveys Tutorials*, vol. 13, no. 4, pp. 524–540, 2011.

[9] M. Arbabzadeh, G. M. Lewis, and G. A. Keoleian, "Green Principles for Responsible battery Management in Mobile Applications," *Journal of Energy Storage*, vol. 24, p. 100779, 2019.

[10] P. K. D. Pramanik, N. Sinhababu, B. Mukherjee, S. Padmanaban, A. Maity, B. K. Upadhyaya, J. B. Holm-Nielsen, and P. Choudhury, "Power Consumption Analysis, Measurement, Management, and Issues: A State-of-the-Art Review of Smartphone Battery and Energy Usage," *IEEE Access*, vol. 7, pp. 182 113–182 172, 2019.

[11] Y.-N. R. Li, M. Chen, J. Xu, L. Tian, and K. Huang, "Power Saving Techniques for 5G and Beyond," *IEEE Access*, vol. 8, pp. 108 675–108 690, 2020.

[12] A. Mughees, M. Tahir, M. A. Sheikh, and A. Ahad, "Towards Energy Efficient 5G Networks Using Machine Learning: Taxonomy, Research Challenges, and Future Research Directions," *IEEE Access*, vol. 8, pp. 187 498–187 522, 2020.

[13] E. Hossain and M. Hasan, "5G Cellular: Key Enabling Technologies and Research Challenges," *IEEE Instrumentation Measurement Magazine*, vol. 18, no. 3, pp. 11–21, 2015.

[14] Z. Yan, S. Chen, Y. Ou, and H. Liu, "Energy Efficiency Analysis of Cache-Enabled Two-Tier HetNets Under Different Spectrum Deployment Strategies," *IEEE Access*, vol. 5, pp. 6791–6800, 2017.

[15] 3GPP TS 38.214, "NR; Physical Layer Procedures for Data," Technical Specification (TS), Sep. 2022.

[16] Y. Liu, Y. Deng, M. Elkashlan, A. Nallanathan, and G. K. Karagiannidis, "Analyzing Grant-Free Access for URLLC Service," *IEEE Journal on Selected Areas in Communications*, vol. 39, no. 3, pp. 741–755, 2021.

[17] Y. S. Soh, T. Q. S. Quek, M. Kountouris, and H. Shin, "Energy Efficient Heterogeneous Cellular Networks," *IEEE Journal on Selected Areas in Communications*, vol. 31, no. 5, pp. 840–850, 2013.

[18] G. Auer, V. Giannini, C. Desset, I. Godor, P. Skillermark, M. Olsson, M. A. Imran, D. Sabella, M. J. Gonzalez, O. Blume, and A. Fehske, "How Much Energy is Needed to Run a Wireless Network?" *IEEE Wireless Communications*, vol. 18, no. 5, pp. 40–49, 2011.

[19] H. Fourati, R. Maaloul, L. Fourati, and M. Jmaiel, "An Efficient Energy-Saving Scheme Using Genetic Algorithm for 5G Heterogeneous Networks," *IEEE Systems Journal*, vol. 17, no. 1, pp. 589–600, 2023.

[20] M. S. A. Shuvo, M. A. R. Munna, S. Sarker, T. Adhikary, M. A. Razzaque, M. M. Hassan, G. Aloi, and G. Fortino, "Energy-efficient Scheduling of Small Cells in 5G: A Meta-Heuristic Approach," *Journal of Network and Computer Applications*, vol. 178, p. 102986, 2021.

[21] T. Maeno, K. Mori, K. Sanada, and H. Kobayaasi, "Evaluation of Energy Efficiency for various Handover Methods in Heterogeneous Cellular Networks with Sleep Control," in *6th International Symposium for Sustainability*, 2016, pp. 9–10.

[22] L. Falconetti, L. Hevizi, and I. Godor, "Sleep Mode Control for Low Power Nodes in Heterogeneous Networks," in *ISWCS 2013; The Tenth International Symposium on Wireless Communication Systems*, 2013, pp. 1–5.

[23] T. Jacobsen, R. Abreu, G. Berardinelli, K. Pedersen, P. Mogensen, I. Z. Kovacs, and T. K. Madsen, "System Level Analysis of Uplink Grant-Free Transmission for URLLC," in *2017 IEEE Globecom Workshops (GC Wkshps)*, 2017, pp. 1–6.

[24] M. Vaezi, A. Azari, S. R. Khosravirad, M. Shirvanimoghaddam, M. M. Azari, D. Chasaki, and P. Popovski, "Cellular, Wide-Area, and Non-Terrestrial IoT: A Survey on 5G Advances and the Road Toward 6G," *IEEE Communications Surveys Tutorials*, vol. 24, no. 2, pp. 1117–1174, 2022.

[25] 3GPP TR 45.820, "Cellular System Support for Ultra-Low Complexity and Low Throughput Internet of Things (CIoT)," Technical Report (TR), Sep. 2015.

[26] F. Ademaj, M. Taranetz, and M. Rupp, "3GPP 3D MIMO Channel Model: A Holistic Implementation Guideline for Open Source Simulation Tools," *EURASIP Journal on Wireless Communications and Networking*, vol. 2016, no. 1, pp. 1–14, 2016.

[27] A. F. M. Shahen Shah, "A Survey From 1G to 5G Including the Advent of 6G: Architectures, Multiple Access Techniques, and Emerging Technologies," in *2022 IEEE 12th Annual Computing and Communication Workshop and Conference (CCWC)*, 2022, pp. 1117–1123.

[28] S. Ahmadi, *5G NR: Architecture, Technology, Implementation, and Operation of 3GPP New Radio Standards*. Academic Press, 2019.

[29] A. Radwan, M. F. Domingues, and J. Rodriguez, "Mobile Caching-Enabled Small-Cells for Delay-Tolerant e-Health Apps," in *2017 IEEE International Conference on Communications Workshops (ICC Workshops)*, 2017, pp. 103–108.

[30] M. Agiwal, A. Roy, and N. Saxena, "Next Generation 5G Wireless Networks: A Comprehensive Survey," *IEEE Communications Surveys Tutorials*, vol. 18, no. 3, pp. 1617–1655, 2016.

[31] 3GPP TS 36.213, "Evolved Universal Terrestrial Radio Access (E-UTRA); Physical Layer Procedures," Technical Specification (TS), Mar. 2017.

[32] T. Jacobsen, R. Abreu, G. Berardinelli, K. Pedersen, I. Z. Kovács, and P. Mogensen, "Joint Resource Configuration and MCS Selection Scheme for Uplink Grant-Free URLLC," in *2018 IEEE Globecom Workshops (GC Wkshps)*, 2018, pp. 1–6.

[33] D. G. Brennan, "Linear Diversity Combining Techniques," *Proceedings of the IRE*, vol. 47, no. 6, pp. 1075–1102, 1959.

[34] 3GPP TR 38.901, "Study on Channel Model for Frequencies from 0.5 to 100 GHz," Technical Report (TR), Oct. 2019.

[35] 3GPP TR 38.802, "Study on New Radio Access Technology Physical Layer Aspects," Technical Report (TR), Mar. 2017.

[36] 3GPP TR 36.819, "Coordinated Multi-Point Operation for LTE Physical Layer Aspects," Technical Report (TR), Sep. 2013.

[37] C.-L. I, J. Huang, R. Duan, C. Cui, J. Jiang, and L. Li, "Recent Progress on C-RAN Centralization and Cloudification," *IEEE Access*, vol. 2, pp. 1030–1039, 2014.

[38] M. Chiang, P. Hande, T. Lan, C. W. Tan *et al.*, "Power Control in Wireless Cellular Networks," *Foundations and Trends® in Networking*, vol. 2, no. 4, pp. 381–533, 2008.

[39] R. Abreu, T. Jacobsen, G. Berardinelli, K. Pedersen, I. Z. Kovács, and P. Mogensen, "Power Control Optimization for Uplink Grant-Free URLLC," in *2018 IEEE Wireless Communications and Networking Conference (WCNC)*, 2018, pp. 1–6.

[40] C. Ubeda Castellanos, D. L. Villa, C. Rosa, K. I. Pedersen, F. D. Calabrese, P.-H. Michaelsen, and J. Michel, "Performance of Uplink Fractional Power Control in UTRAN LTE," in *VTC Spring 2008 - IEEE Vehicular Technology Conference*, 2008, pp. 2517–2521.

[41] S. Zhang, J. Gong, S. Zhou, and Z. Niu, "How Many Small Cells Can be Turned Off via Vertical Offloading Under a Separation Architecture?" *IEEE Transactions on Wireless Communications*, vol. 14, no. 10, pp. 5440–5453, 2015.

[42] S. Samarakoon, M. Bennis, W. Saad, and M. Latva-aho, "Opportunistic Sleep Mode Strategies in Wireless Small Cell Networks," in *2014 IEEE International Conference on Communications (ICC)*, 2014, pp. 2707–2712.

[43] I. Ashraf, F. Boccardi, and L. Ho, "SLEEP Mode Techniques for Small Cell Deployments," *IEEE Communications Magazine*, vol. 49, no. 8, pp. 72–79, 2011.

[44] M. A. Marsan, L. Chiaraviglio, D. Ciullo, and M. Meo, "Multiple daily base station switch-offs in cellular networks," in *2012 Fourth International Conference on Communications and Electronics (ICCE)*, 2012, pp. 245–250.

[45] X. Chen, J. Wu, Y. Cai, H. Zhang, and T. Chen, "Energy-Efficiency Oriented Traffic Offloading in Wireless Networks: A Brief Survey and a Learning Approach for Heterogeneous Cellular Networks," *IEEE Journal on Selected Areas in Communications*, vol. 33, no. 4, pp. 627–640, 2015.

[46] S. Ozaku, Y. Shimbo, H. Suganuma, and F. Maehara, "Adaptive Repetition Control Using Terminal Mobility for Uplink Grant-Free URLLC," in *2020 IEEE 91st Vehicular Technology Conference (VTC2020-Spring)*, 2020, pp. 1–5.

[47] Q. Song, C. She, and F.-C. Zheng, "Optimization of Repetition Scheme for URLLC with Diverse Reliability Requirements," in *2022 IEEE 95th Vehicular Technology Conference: (VTC2022-Spring)*, 2022, pp. 1–5.

[48] G. Forecast *et al.*, "Cisco Visual Networking Index: Global Mobile Data Traffic Forecast Update, 2017–2022," 2019.

[49] M. P. Mills, "The Cloud Begins with Coal: Big Data, Big Networks, Big Infrastructure, and Big Power," *Digital Power Group*, 2013.

[50] W. Van Heddeghem, S. Lambert, B. Lannoo, D. Colle, M. Pickavet, and P. Demeester, "Trends in Worldwide ICT Electricity Consumption from 2007 to 2012," *Computer Communications*, vol. 50, pp. 64–76, 2014.

[51] S.-F. Chou, T.-C. Chiu, Y.-J. Yu, and A.-C. Pang, "Mobile Small Cell Deployment for Next Generation Cellular Networks," in *2014 IEEE Global Communications Conference*, 2014, pp. 4852–4857.

[52] F. Salahdine, J. Opadere, Q. Liu, T. Han, N. Zhang, and S. Wu, "A Survey on Sleep Mode Techniques for Ultra-Dense Networks in 5G and Beyond," *Computer Networks*, vol. 201, p. 108567, 2021.

[53] Y. He, L. Tang, and Z. Zhou, "A Distance-Sensitive Distributed Repulsive Sleeping Strategy for Densely-Deployed Small Cells in Green Cities," in *2018 IEEE/CIC International Conference on Communications in China (ICCC Workshops)*, 2018, pp. 211–216.

[54] P. Phaiwitthayaphorn, K. Mori, H. Kobayashi, and P. Boonsrimuang, "Cell Throughput based Sleep Control Scheme for Heterogeneous Cellular Networks," *ECTI Transactions on Computer and Information Technology*, vol. 12, no. 1, pp. 26–33, 2018.

[55] S. Habibi, V. Solouk, and H. Kalbkhani, "Adaptive Energy-Efficient Small Cell Sleeping and Zooming in Heterogeneous Cellular Networks," *Telecommunication Systems*, vol. 77, no. 1, pp. 23–45, 2021.

[56] K. R. Krishnan and H. Luss, "Power Selection for Maximizing SINR in Femtocells for Specified SINR in Macrocell," in *2011 IEEE Wireless Communications and Networking Conference*, 2011, pp. 563–568.

[57] D. Tse and P. Viswanath, *Fundamentals of Wireless Communication*. Cambridge University Press, 2005.

[58] A. Israr, Q. Yang, W. Li, and A. Y. Zomaya, "Renewable Energy Powered Sustainable 5G Network Infrastructure: Opportunities, Challenges and Perspectives," *Journal of Network and Computer Applications*, vol. 175, p. 102910, 2021.

[59] Y. Chen, S. Zhang, and S. Xu, "Characterizing Energy Efficiency and Deployment Efficiency Relations for Green Architecture Design," in *2010 IEEE International Conference on Communications Workshops*, 2010, pp. 1–5.

[60] Y. Sagae, S. Sawamukai, Y. Ohwatari, K. Kiyoshima, K. Kanbara, and J. Takahashi, "5G Network," *NTT DOCOMO Technical Journal*, vol. 22, no. 2, pp. 23–39, 2020.

[61] J. Sachs, G. Wikstrom, T. Dudda, R. Baldemair, and K. Kittichokechai, "5G Radio Network Design for Ultra-Reliable Low-Latency Communication," *IEEE Network*, vol. 32, no. 2, pp. 24–31, 2018.

[62] 3GPP TR 38.824, "Study on Physical Layer Enhancements for NR Ultra-Reliable and Low Latency Case (URLLC)," Technical Report (TR), Mar. 2019.

[63] S. Ye, *Support of Ultra-reliable and Low-Latency Communications (URLLC) in NR*. Cham: Springer International Publishing, 2021, pp. 373–400.

[64] P. Popovski, Č. Stefanović, J. J. Nielsen, E. de Carvalho, M. Angjelichinoski, K. F. Trillingsgaard, and A.-S. Bana, "Wireless Access in Ultra-Reliable Low-Latency Communication (URLLC)," *IEEE Transactions on Communications*, vol. 67, no. 8, pp. 5783–5801, 2019.

[65] C. She, C. Sun, Z. Gu, Y. Li, C. Yang, H. V. Poor, and B. Vucetic, "A Tutorial on Ultrareliable and Low-Latency Communications in 6G: Integrating Domain Knowledge into Deep Learning," *Proceedings of the IEEE*, vol. 109, no. 3, pp. 204–246, 2021.

[66] M. Maier, M. Chowdhury, B. P. Rimal, and D. P. Van, "The Tactile Internet: Vision, Recent Progress, and Open Challenges," *IEEE Communications Magazine*, vol. 54, no. 5, pp. 138–145, 2016.

[67] A. Avranas, M. Kountouris, and P. Ciblat, "Energy-Latency Tradeoff in Ultra-Reliable Low-Latency Communication With Retransmissions," *IEEE Journal on Selected Areas in Communications*, vol. 36, no. 11, pp. 2475–2485, 2018.

[68] 3GPP TS 38.300, "NR; NR and NG-RAN Overall Description," Technical Specification (TS), Sep. 2022.

[69] N. H. Mahmood, R. Abreu, R. Böhnke, M. Schubert, G. Berardinelli, and T. H. Jacobsen, "Uplink Grant-Free Access Solutions for URLLC services in 5G New Radio," in *2019 16th International Symposium on Wireless Communication Systems (ISWCS)*, 2019, pp. 607–612.

[70] F. Jiang, B.-c. Wang, C.-y. Sun, Y. Liu, and X. Wang, "Resource Allocation and Dynamic Power Control for D2D Communication Underlaying Uplink Multi-Cell Networks," *Wireless Networks*, vol. 24, pp. 549–563, 2018.

[71] T. H. Jacobsen, R. Abreu, G. Berardinelli, K. I. Pedersen, I. Z. Kovács, and P. Mogensen, "Multi-Cell Reception for Uplink Grant-Free Ultra-Reliable Low-Latency Communications," *IEEE Access*, pp. 80 208–80 218, 2019.

[72] A. Dataesatu, K. Sanada, H. Hatano, K. Mori, and P. Boonsrimuang, "Adaptive K-Repetition Transmission Employing Site Diversity Reception for 5G NR Uplink Grant-Free URLLC," in *2023 IEEE 97th Vehicular Technology Conference (VTC2023-Spring)*, 2023, pp. 1–5.

[73] D. H. Hailu, B. G. Gebrehaweria, S. H. Kebede, G. G. Lema, and G. T. Tesfamariam, "Mobile Fronthaul Transport Options in C-RAN and Emerging Research Directions: A Comprehensive Study," *Optical Switching and Networking*, vol. 30, pp. 40–52, 2018.

[74] T. V. K. Chaitanya and E. G. Larsson, "Optimal Power Allocation for Hybrid ARQ with Chase Combining in i.i.d. Rayleigh Fading Channels," *IEEE Transactions on Communications*, vol. 61, no. 5, pp. 1835–1846, 2013.

[75] 3GPP TS 38.211, "NR; Physical Channels and Modulation," Technical Specification (TS), Sep. 2022.

Appendix A

Publication List

Journal Papers

(1) Arif Dataesatu, Kosuke Sanada, Hiroyuki Hatano, Kazuo Mori, Pisit Boonsrimuang, "Adaptive K-Repetition Transmission with Site Diversity Reception for Energy-Efficient Grant-Free URLLC in 5G NR," *IEICE transactions on communications*, vol. E107-B, no. 1, pp. 74–84, Jan. 2024.

(2) Arif Dataesatu, Kosuke Sanada, Hiroyuki Hatano, Kazuo Mori, Pisit Boonsrimuang, "System Performance Enhancement with Energy Efficiency Based Sleep Control for 5G Heterogeneous Cellular Networks," *International Journal of Intelligent Engineering and Systems*, vol. 15, no. 2, pp. 232–242, Apr. 2022.

International Conferences

(1) Arif Dataesatu, Kosuke Sanada, Hiroyuki Hatano, Kazuo Mori, and Pisit Boonsrimuang, "Adaptive K-Repetition Transmission Employing Site Diversity Reception for 5G NR Uplink Grant-Free URLLC," *in Proc. of 97th IEEE Vehicular Technology Conference* (VTC 2023 Spring), pp. 1-5, Italy, Jun. 2023.

(2) Arif Dataesatu, Pornpawit Boonsrimuang, Kazuo Mori, and Pisit Boonsrimuang, "Energy Efficiency Enhancement in 5G Heterogeneous Cellular Networks Using System Throughput Based Sleep Control Scheme," *in Proc. of 22nd International Conference on Advanced Communication Technology* (ICACT2020), pp. 549-553, Korea, Feb. 2020.

(3) Arif Dataesatu, Pornpawit Boonsrimuang, Kazuo Mori, and Pisit Boonsrimuang, "Comparative Analysis of Radio Propagation Models for LTE Network on The Sky Train," *in Proc. of 21st International Conference on Advanced Communication Technology* (ICACT2019), pp. 233-238, Korea, Feb. 2019.

(4) Pitchaya Boontra, Tanairat Mata, Arif Dataesatu, Kazuo Mori, and Pisit Boonsrimuang, "A PAPR Reduction for FBMC-OQAM Signals using ABC-OPTS Scheme," *in Proc. of 21st International Conference on Advanced Communication Technology* (ICACT2019), pp. 115-119, Korea, Feb. 2019.

Domestic Conferences

(1) Arif Dataesatu, Kosuke Sanada, Hiroyuki Hatano, Kazuo Mori, and Pisit Boonsrimuang, "Extended Adaptive Repetition Transmission under Site Diversity for 5G NR Uplink Grant-Free URLLC," *in Proc. of 13th International Symposium for Sustainability by Engineering (IS2EMU 2023)*, pp. 43-44, Sep. 2023.

(2) Arif Dataesatu, Kosuke Sanada, Hiroyuki Hatano, Kazuo Mori, and Pisit Boonsrimuang, "Adaptive K-Repetition Transmission with Site Diversity Reception for 5G NR Uplink Grant-Free URLLC," *IEICE Technical Report*, RCS2023-12, pp. 56-61, Apr. 2023.

(3) Arif Dataesatu, Kosuke Sanada, Hiroyuki Hatano, Kazuo Mori, and Pisit Boonsrimuang, "Adaptive Repetition Control with Site Diversity for 5G NR Uplink Grant-Free URLLC," *in Proc. of IEICE General Conference* 2023, no. B-5-65, pp. 310, Mar. 2023.

(4) Arif Dataesatu, Kosuke Sanada, Hiroyuki Hatano, Kazuo Mori, and Pisit Boonsrimuang, "System-Level Performance of Site Diversity Reception for K-Repetition Transmission in 5G NR Uplink Grant-Free URLLC," *in Proc. of 12th International Symposium for Sustainability by Engineering (IS2EMU 2022)*, pp. 3-4, Sep. 2022.

(5) Arif Dataesatu, Kosuke Sanada, Hiroyuki Hatano, Kazuo Mori, and Pisit Boonsrimuang, "System Performance Enhancement Using Sleep Control Scheme in 5G Heterogeneous Cellular Networks," *in Proc. of 11th International Symposium for Sustainability by Engineering (IS2EMU 2021)*, pp. 53-54, Sep. 2021.

Appendix B

Award

(1) 2023 Young Researcher's Encouragement Award from IEEE Vehicular Technology Conference (VTC 2023-spring), IEEE VTS Japan Chapter.